



T.R.

MUSTAFA KEMAL UNIVERSITY

GRADUATE SCHOOL OF NATURAL AND APPLIED SCIENCES

**ENHANCING DEEP EXTREME LEARNING MACHINES: NOVEL
MULTI-KERNEL AUTOENCODERS AND IMPLEMENTATION FOR
DETECTING THE CHRONIC OBSTRUCTIVE PULMONARY DISEASE**

GÖKHAN ALTAN

DEPARTMENT OF INFORMATICS

**In partial fulfillment of the requirements
for the Degree of Doctor of Philosophy**

HATAY

JANUARY, 2018



T.R.
MUSTAFA KEMAL UNIVERSITY
GRADUATE SCHOOL OF NATURAL AND APPLIED
SCIENCES

**ENHANCING DEEP EXTREME LEARNING MACHINES: NOVEL
MULTI-KERNEL AUTOENCODERS AND IMPLEMENTATION FOR
DETECTING THE CHRONIC OBSTRUCTIVE PULMONARY DISEASE**

GÖKHAN ALTAN
DEPARTMENT OF INFORMATICS

**In partial fulfillment of the requirements
for the Degree of Doctor of Philosophy**

HATAY
JANUARY, 2018

T.C.
MUSTAFA KEMAL ÜNİVERSİTESİ
FEN BİLİMLERİ ENSTİTÜSÜ

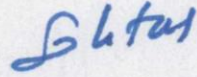
**ENHANCING DEEP EXTREME LEARNING MACHINES:
NOVEL MULTI-KERNEL AUTOENCODERS AND IMPLEMENTATION
FOR DETECTING CHRONIC OBSTRUCTIVE PULMONARY DISEASE**

Gökhan ALTAN


ENFORMATİK ANABİLİM DALI

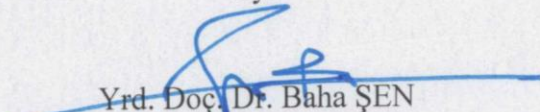
DOKTORA TEZİ


Yrd. Doç. Dr. Yakup KUTLU danışmanlığında hazırlanan bu tez 26/01/2018 tarihinde aşağıdaki jüri üyeleri tarafından **OYBİRLİĞİ** ile kabul edilmiştir.

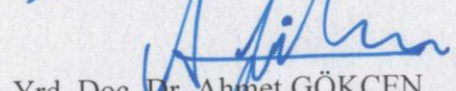


Prof. Dr. Halim Haldun GÖKTAŞ
Başkan


Prof. Dr. Fatih Vehbi ÇELEBİ
Üye


Yrd. Doç. Dr. Baha ŞEN
Üye


Yrd. Doç. Dr. Yakup KUTLU
Üye


Yrd. Doç. Dr. Ahmet GÖKÇEN
Üye

Kod No:

Prof. Dr. Erdal SERTKAYA
Enstitü Müdürü

Bu çalışma TÜBİTAK tarafından desteklenmiştir.

Proje No: 116E190

Not: Bu tezde kullanılan özgün ve başka kaynaktan yapılan bildirişlerin, çizelge, şekil ve fotoğrafların kaynak gösterilmeden kullanımı, 5846 sayılı Fikir ve Sanat Eserleri Kanunundaki hükümlere tabidir.

26.1.2018

DECLARATION

I hereby declare that all information in this thesis has been obtained and presented in accordance with ethical behaviour and academic rules. I also declare that this thesis is organised according to thesis preparation guide and all statements that do not belong to me are fully cited and responsibility of making digital format exactly same as master copy belongs to myself since any modification on thesis will be done by Council of Higher Education.

Gökhan ALTAN

ABSTRACT

ENHANCING DEEP EXTREME LEARNING MACHINES: NOVEL MULTI-KERNEL AUTOENCODERS AND IMPLEMENTATION FOR DETECTING THE CHRONIC OBSTRUCTIVE PULMONARY DISEASE

Despite the rapid development of medical diagnostic systems and treatment modalities contemporarily, the most commonly used diagnostic and examination tool is still the auscultation sounds for most commonly cardio-respiratory and respiratory diseases.

World Health Organization reports that respiratory diseases including Chronic Obstructive Pulmonary Disease (COPD) take the top places on the deadliest list. Taking into account of the limitations of diseases on social life, manpower deficit and the health budgets of the states and nations for these diseases, the early diagnosis and keeping under control in early stages is important steps for preventing disease reaching advanced levels.

One of the biggest deficiencies in the literature is the lack of a comprehensive and detailed respiratory disease database, which may be used as the focus for novel methods for computer-aided medical interfaces. This study comprises of a population of 77 subjects from different socioeconomic status and sexuality, aged between 38 and 68, consisting of 30 healthy subjects that have never smoked, and 47 patients with COPD (COPD0, COPD1, COPD2, COPD3, and COPD4) and asthma. RespiratoryDatabase@TR containing diagnostic aids such as auscultation recordings and multimedia data was created. RespiratoryDatabase@TR contains the 16-channels auscultation sounds including 4-channel heart sounds, 12-channels lung sound which were recorded synchronously left and right sides from anterior and posterior lung auscultation areas. It is a unique respiratory database with the features of acquiring patient specific multimedia data such as chest X-ray, pulmonary function test measurements, SGRQ-C questionnaire answers, lung and heart sounds, and enabling analysis on COPD levels.

Extreme Learning Machines (ELM) and Deep Learning are popular machine learning algorithms that enable rapid development of deep analyses in last decades. While the ELM has specifications of a single layer feedforward artificial neural network model, Deep Learning algorithms have the specifications of artificial neural network model that enables to optimize classifier parameters with supervised learning after applying pre-training with multilayer structure in unsupervised learning. In this thesis, Multi-kernel Deep ELM model is proposed, which can work with different decomposition kernels to realize the integrating the analysis capacity of Deep Learning and generalization performance of the ELM.

The auscultation sounds were analysed by using statistical features of the subbands extracted using the Hilbert-Huang Transform and Discrete Wavelet Transform and by using the quantization features of Second Order Difference Plots in three-dimensional space. Different classification models were developed on the basis of the COPD diagnosis and severity classification of the COPD and the performances were evaluated.

2018, 163 pages

Keywords: COPD, RespiratoryDatabase@TR, 3D-SODP, Deep Learning, Deep Extreme Learning Machines

ÖZET

DERİN AŞIRI ÖĞRENME MAKİNELERİNİN GELİŞTİRİLMESİ: YENİ ÇOK ÇEKİRDEKLİ AUTOENCODERLAR VE KRONİK OBSTRÜKTİF AKCİĞER HASTALIĞININ BELİRLENMESİNDE UYGULANMASI

Günümüzde hızla gelişmeyi sürdüren tıbbi teşhis sistemleri ve tedavi yöntemlerine rağmen, kardiyopulmoner ve en çok da solunum rahatsızlıkları için hala en yaygın kullanılan teşhis ve muayene aracı oskültasyon sesleridir.

Dünya Sağlık Örgütü, en ölümcül hastalıklar listesinde Kronik Obstrüktif Akciğer Rahatsızlığı (KOA) gibi solunum rahatsızlıklarının başları çektiğini duyurmuştur. Bu hastalıklar için ayrılan yüksek meblağlı sağlık bütçeleri, sosyal yaşamda meydana getirdiği kısıtlamalar ve işgücü açığı düşünüldüğünde, erken evrelerde tanı koyma ve kontrol altına alınması hastalığın ileri boyutlara ulaşmasını engellemeye önemli bir adımdır.

Literatürde en büyük eksiklerden biri Bilgisayar destekli medikal arayüzler için geliştirilecek yöntemlere temel olabilecek geniş ve detaylı solunum rahatsızlığı veritabanının bulunmamasıdır. Bu çalışma yaşları 38 ile 68 arasında değişen 30 sağlıklı, farklı evrelerdeki KOA (KOA0, KOA1, KOA2, KOA3, KOA4) ve Astım hastalarından oluşan 47 hastadan oluşan farklı sosyal-ekonomik düzeyden ve farklı cinsiyetten 77 kişilik bir popülasyonu kapsamaktadır. Kaydedilen oskültasyon sesleri ve multimedya verilerden oluşan tanı araçlarını içeren RespiratoryDatabase@TR oluşturulmuştur. RespiratoryDatabase@TR, ön ve arka oskültasyon bölgeleri olmak üzere 4 kanallı kalp, 12 kanallı akciğer odaklarını içeren 16 farklı kanaldan iki dijital stetoskopta sağ ve sol odaklardan eşzamanlı olarak kaydedilmiş oskültasyon seslerini içerir. Her hastaya özgü göğüs filmi, kalp ve akciğer sesleri, solunum fonksiyon testi ölçümleri, SGQR-C anketi cevapları gibi multimedya veri içermesi ve KOA seviyelerini analiz edebilmesine imkân sağlaması özellikleriyle eşsiz bir solunum veritabanıdır.

Aşırı Öğrenme Makineleri (AÖM) ve Derin Öğrenme son yıllarda derin analizleri hızlı biçimde gerçekleştirmeyi sağlayan popüler makine öğrenmesi algoritmalarıdır. AÖM ileri yönlü çalışan tek katmanlı yapay sinir ağı modeli olma özelliğine sahipken, Derin Öğrenme algoritmaları çok katmanlı yapısı ve denetimsiz öğrenmeyle ön eğitimden geçirilerek sonrasında sınıflandırıcı parametrelerinin optimize edilmesini sağlayan bir yapay sinir ağı modelidir. Bu tezde Derin öğrenmenin analiz kapasitesi ile AÖM genelleme başarımı ile hızını birleştirmeyi gerçekleştirecek farklı ayrıştırma yöntemleriyle çalışabilen çok çekirdekli Derin AÖM önerilmiştir.

Oskültasyon sesleri Hilbert-Huang Dönüşümü, Ayrık Dalgacık Dönüşümünden elde edilen alt bantların istatistiksel öznitelikleri ve 3 boyutlu uzayda İkinci derece fark haritalarının nicelemesiyle elde edilen öznitelikler kullanılarak analiz edilmiştir. KOA teşhisi ve KOA seviyelerinin belirlenmesi üzerine farklı modeller geliştirilmiş ve performansları hesaplanmıştır.

2018, 163 sayfa

Anahtar Kelimeler: KOA, RespiratoryDatabase@TR, 3D-SODP, Derin Öğrenme, Derin Aşırı Öğrenme Makinesi

ACKNOWLEDGMENTS

I would like to express my deepest gratitude to my thesis supervisor Asst. Prof. Dr. Yakup KUTLU for supporting me at every stage of my PhD, for piquing me about the advanced levels of Deep Learning, Extreme Learning Machines, novel signal processing with his guidance, and for his sincerely motivation.

The studies in the thesis are originated from TUBITAK-116E190 project outputs. I would like to express my thanks to Scientific and Technological Research Council of Turkish (TUBITAK) for providing fully support.

I specifically appreciate to members of my thesis monitoring committee, Assoc. Prof. Dr. Esen Yıldırım and Asst. Prof. Dr. Mustafa Yenid for sharing their experiences and for considerable guidance on novel approximations.

Thanks to Dr. Apdullah Yayık for his camaraderie and experience exchange on machine learning algorithms. I hope happiness is always with him and his beloved family.

Thanks to my colleagues and many friends for their hints at feeling me togetherness.

I know that being a parent and family is the most difficult and sacred duty of life. As the youngest individual in my family, I thank my family thousands of times for every second that they spend on me.

The biggest gratitude is for my lovely wife, Seda ALTAN, for her gentle patience when I spend most of my time on my PhD studies, and for unlimited confidence and support. I am truly thankful for having you in my life.

This thesis is dedicated to Turkish Science.

TABLE OF CONTENTS

ABSTRACT	I
ÖZET	II
ACKNOWLEDGMENTS	III
TABLE OF CONTENTS	IV
LIST OF FIGURES	VI
LIST OF TABLES	VIII
LIST OF SYMBOLS AND ABBREVIATIONS	X
1. INTRODUCTION	1
1.1. Motivation	1
1.2. The Scope of the Thesis	5
1.3. The Significance of the Thesis	7
1.4. The Thesis Organization	8
2. RELATED WORKS	10
2.1. Respiratory Sound Analysis	10
2.2. Respiratory Databases	16
2.3. Deep Learning and Deep Belief Networks	17
2.4. Extreme Learning Machines	19
3. MATERIAL AND METHODS	23
3.1. Introduction	23
3.2. Respiratory Sounds	23
3.2.1. Normal Respiratory Sounds	25
3.2.2. Abnormal Respiratory Sounds	26
3.3. Respiratory Diseases	33
3.3.1. Chronic Obstructive Pulmonary Disease	33
3.4. RespiratoryDatabase@TR	36
3.4.1. Pulmonary Function Test	41
3.4.2. Auscultation Scenario	43
3.4.3. Digitization of Auscultation Sounds	46
3.4.4. Sound Synchronizer	49
3.4.5. Sound Annotation	51
3.4.6. Significance of RespiratoryDatabase@TR	52
3.5. Feature Extraction	54
3.5.1. Hilbert-Huang Transform	55
3.5.2. Discrete Wavelet Transform	62
3.5.3. The Proposed 3D Second Order Difference Plot	66
3.5.4. Statistical Feature Extraction	70
3.6. Classification	73
3.6.1. Deep Learning	74
3.6.2. Extreme Learning Machines	81
3.6.3. The Proposed ELM Autoencoder Kernels	87
3.6.4. The Proposed Multi-kernel Deep ELM	90
3.7. Feature Selection	96

3.7.1.	Least-Square Method	98
3.7.2.	Sequential Forward Feature Selection	98
3.7.3.	Cross Validation.....	100
3.8.	Performance Measurements and Statistical Analysis	101
4.	RESEARCH FINDINGS AND RESULTS	103
4.1.	The Statistical Analysis of SGRQ-C.....	104
4.2.	Signal Length Impact	110
4.3.	The COPD Analysis.....	111
4.3.1.	Deep Belief Networks Results	112
4.3.2.	The Proposed Multi-kernel Deep ELM Results.....	114
4.4.	The COPD Severity Analysis.....	125
4.4.1.	Deep Belief Networks Results	127
4.4.2.	The Proposed Multi-kernel Deep ELM Results.....	128
4.5.	ELM Autoencoder Kernel Impact.....	130
4.6.	SODP Dimension Impact.....	135
5.	CONCLUSION AND DISCUSSION.....	138
	FUTURE WORK	141
	BIBLIOGRAPHY	142
	VITA	152
	APPENDIX 1	154
	APPENDIX 2	155
	APPENDIX 3	162

LIST OF FIGURES

Figure 1.1. The frequency ranges and names of the sounds	1
Figure 1.2. The shortened history of stethoscope	2
Figure 3.1. The anatomy of the lungs.	24
Figure 3.2. Normal vesicular lung sounds waveform.	25
Figure 3.3. Crackles sounds waveform	27
Figure 3.4. Rhonchi sounds waveform	28
Figure 3.5. Wheezes sounds waveform.....	29
Figure 3.6. Stridor sounds waveform.....	30
Figure 3.7. Squawk sounds waveform	31
Figure 3.8. The airways and alveoli patterns of lungs of healthy and COPD subjects	34
Figure 3.10. The model of RespiratoryDatabase@TR.....	39
Figure 3.11. Pulmonary Function Test Scenario (COSMED, 2018)	41
Figure 3.12. Pulmonary Function Test Curves belong to a COPD patient	42
Figure 3.13. Lung auscultation areas on (a) anterior side and (b) posterior side.....	43
Figure 3.14. Lung Auscultation Scenarios for Posterior Side.....	44
Figure 3.15. Lung Auscultation Scenarios for Anterior Side	45
Figure 3.16. Heart auscultation areas.....	45
Figure 3.17. Heart auscultation Scenarios	46
Figure 3.18. Littmann 3200 Digital Stethoscope	47
Figure 3.19. Patient specific listening and detailing module of the CMI	49
Figure 3.20. Sounds synchronization Module of the CMI.....	50
Figure 3.21. Auscultation Sounds Annotation Module of the CMI.....	51
Figure 3.22. EMD process on a random part of lung sound	56
Figure 3.23. Extracted IMFs and the original lung signal	59
Figure 3.24. Hilbert Spectral Analysis of lung sound.....	61
Figure 3.25. Discrete Wavelet Transform Coefficients with sym2 wavelet in 6 levels.....	64
Figure 3.26. Discrete Wavelet Decomposition at Level 3	65
Figure 3.27. Elliptical Distribution of lung sound using SODP	67
Figure 3.28. The dispersion of the proposed 3D-SODP	68
Figure 3.29. The octant regions of the proposed 3D-SODP	70
Figure 3.30. The Deep Learning model which is based on Convolutional Neural Network on image analysis.....	76
Figure 3.31. The Deep Belief Network structure.....	77
Figure 3.32. The presentation of RBM training in the DBN	78
Figure 3.33. The Deep Belief Network training	79
Figure 3.34. The structure of Single Layer Feedforward network based Extreme Learning Machines.....	83
Figure 3.35. The ELM Autoencoder model	88
Figure 3.36. Deep ELM Mode	95
Figure 3.37. The proposed Multi-kernel Deep ELM Model.....	97
Figure 3.38. The SFFS algorithm.....	99
Figure 3.39. Class distribution of COPD severity.....	102

Figure 4.1. 3D-SODP of lung sounds from random subjects with COPD0 and COPD4 .. 126

Figure 4.2. Highly responsible spaces using Cuboid polyhedrons-based 3D-SODP
quantization for separation of lung sounds from different COPD severities 129

Figure 4.3. The sensitivity and specificity rates of COPD severities using Deep ELM
model with proposed ELM autoencoder kernels 133

Figure 4.4. Comparison of the SODP and 3D-SODP quantization focusing on cuboid and
chaos segmentation on lung sounds from a random COPD patient 136



LIST OF TABLES

Table 3.1. Abnormal respiratory sounds and possible diseases with the lung sound types	32
Table 3.2. The COPD severities and symptoms according to level	35
Table 3.3. Distribution of diseases according to sexuality	48
Table 3.4. The comparison of the transformations	66
Table 3.5. Confusion Matrix for n classes.	101
Table 4.1. ANOVA Statistical Analysis of the SGRQ-C Questions	105
Table 4.2. (Continued) ANOVA Statistical Analysis of the SGRQ-C Questions	106
Table 4.3. Levene's Test and T-test Statistical Analysis of the SGRQ-C Questions	107
Table 4.4. (Continued) Levene's Test and T-test Statistical Analysis of the SGRQ-C Questions	108
Table 4.5. (Continued) Levene's Test and T-test Statistical Analysis of the SGRQ-C Questions	109
Table 4.6. The classification overall accuracy (%) of the proposed LU based Deep ELM model for various signal lengths on COPD severity classification	111
Table 4.7. The classification performances (%) of the DBN model for COPD diagnosis on each wavelet	113
Table 4.8. The classification performances (%) of the DBN model for COPD diagnosis on each HHT-based feature set	114
Table 4.9. The classification performances (%) of the Deep ELM model with traditional ELM Autoencoder kernel for COPD diagnosis on each wavelet	115
Table 4.10. The classification performances (%) of the Deep ELM model with traditional ELM Autoencoder kernel for COPD diagnosis on each HHT-based feature set	116
Table 4.11. The classification performances (%) of the Deep ELM model with LU decomposition based ELM Autoencoder kernel for COPD diagnosis on each wavelet	117
Table 4.12. The classification performances (%) of the Deep ELM model with LU decomposition based ELM Autoencoder kernel for COPD diagnosis on each HHT-based feature set	118
Table 4.13. The classification performances (%) of the Deep ELM model with Hessenberg decomposition based ELM Autoencoder kernel for COPD diagnosis on each wavelet	119
Table 4.14. The classification performances (%) of the Deep ELM model with Hessenberg decomposition based ELM Autoencoder kernel for COPD diagnosis on each HHT-based feature set	120
Table 4.15. The best classification performances (%) of the proposed multi-kernel Deep ELM and DBN models for COPD classification using proposed and traditional ELM autoencoder kernels on HHT features	121

Table 4.16. The best classification performances (%) of the proposed multi-kernel Deep ELM and DBN models for COPD classification using proposed and traditional ELM autoencoder kernels on DWT features	121
Table 4.17. The contingency table and detailed misclassified COPD severities for the best performance using the Deep ELM with traditional ELM autoencoder kernel with HHT features for COPD classification	123
Table 4.18. The contingency table and detailed misclassified COPD severities for the best performance using the proposed Deep ELM with LU decomposition based ELM autoencoder kernel with HHT features for COPD classification	124
Table 4.19. The contingency table and detailed misclassified COPD severities for the best performance using the proposed multi-kernel Deep ELM with Hessenberg decomposition with HHT features for COPD classification	125
Table 4.20. The classification performances (%) of the DBN model for COPD severity classification on each quantization models	127
Table 4.21. The classification performances (%) of the Deep ELM model for COPD severity classification on each quantization models	128
Table 4.22. Contingency table for COPD severity classification using the Deep ELM with the proposed LU decomposition based ELM autoencoder	131
Table 4.23. Sensitivity and specificity rates (%) for each COPD severities using the Deep ELM with the proposed LU decomposition based ELM autoencoder contingency table	131
Table 4.24. Contingency table for COPD severity classification using the Deep ELM with the proposed Hessenberg decomposition based ELM autoencoder	132
Table 4.25. Sensitivity and specificity rates (%) for each COPD severities using the Deep ELM with the proposed Hessenberg decomposition based ELM autoencoder contingency table	132
Table 4.26. The classification performances (%) of the Deep ELM and DBN models for COPD severity classification using proposed and traditional ELM autoencoder kernels	134
Table 4.27. Comparison of the best classification performances (%) of the proposed multi-kernel Deep ELM, traditional ELM autoencoder and DBN model for COPD severity classification using 3D-SODP and SODP quantization	137

LIST OF SYMBOLS AND ABBREVIATIONS

LIST OF SYMBOLS

x_i	: i^{th} input sample of ELM
t_i	: i^{th} desired output sample of ELM
m	: Hidden layer neuron number of ELM
h_{ik}	: Output of hidden layer of ELM
$g(\cdot)$: Activation function of ELM
$\hat{y}(t)$: Hilbert Transform
b_k	: Bias vector of ELM
w	: Output weight matrix of ELM
o	: Output sample of ELM
C_n	: n^{th} candidate IMF
r_n	: n^{th} residual signal
PV	: Cauchy's principle value integral
$H(\omega, t)$: Hilbert Spectrum
\Re	: Real part of the solution
ϕ, ψ	: Wavelet functions
δ	: Quantization function of 3D-SODP
μ_n	: n^{th} moment
η	: Learning rate
$E[\cdot]$: Estimation of the average over the probability distribution
σ	: Sigmoid Function
β^n	: The output weights of n^{th} hidden layer

ABBREVIATIONS

3D	:Three Dimensional
3D-SODP	:Three Dimensional Second Order Difference Plot

ALS	:Amyotrophic lateral sclerosis
ANFIS	:Adaptive-Network Based Fuzzy Inference Systems
ANN	:Artificial Neural Networks
ASAP	:Analyse de Sons Auscultatoires et Pathologiques
ANOVA	:Analysis of Variance
CATS	:Competition on Artificial Time Series
CMI	:Computer-assisted Medical Interface
CNN	:Convolutional Neural Networks
CORSA	:Computerized Respiratory Sound Analysis
COPD	:Chronic Obstructive Pulmonary Disease
COPD0	:Under COPD Risk
COPD1	:Mild Level COPD
COPD2	:Moderate Level COPD
COPD3	:Severe Level COPD
COPD4	:Very Severe Level COPD
CT	:Computer Tomography
CWT	:Continues Wavelet Transform
DBN	:Deep Belief Networks
DWT	:Discrete Wavelet Transform
ECG	:Electrocardiography
EEG	:Electroencephalography
ELM	:Extreme learning machine
EMD	:Empirical Mode Decomposition
FEV	:Forced expiratory volume
FEV/FVC	:Tiffeneau-Pinelli index
FN	:False Negative
FP	:False Positive
FVC	:Forced vital capacity
GMM	:Gaussian Mixture Model
GPU	:Graphical Processing Unit

Hess-ELM	:Hessenberg decomposition based extreme learning machine
HHT	:Hilbert-Huang Transform
HILSA	:Heart intestine and lung sound analysis
HMM	:Hidden Markov Model
HT	:Hilbert Transform
IMF	:Intrinsic Mode Functions
ISAAC	:International Society for Augmentative and Alternative Communication
k -NN	: k -Nearest Neighbour
Lu-ELM	:Lower upper triangularization based extreme learning machine
MARS	:Marburg Respiratory Sounds
MANOVA	:Multivariate analysis of variance
MFCC	:Mel-frequency cepstral coefficients
MNIST	:Modified National Institute of Standards and Technology
PCA	:Principle Component Analysis
PFT	:Pulmonary Function Test
PSD	:Power Spectral Density
R.A.L.E	:Respiratory Acoustics Laboratory Environment
RBF	:Radial Basis Function
RBM	:Restricted Boltzmann Machines
SFFS	:Sequential Forward Feature Selection
SGRQ-C	:St George's Respiratory Questionnaire – COPD
SLFN	:Single Layer Feed forward Neural Network
SODP	:Second Order Difference Plot
STFT	:Short-time Fourier Transform
SVM	:Support Vector Machines
TN	:True Negative
TP	:True Positive
WA-SEN	:Weighted average of Sensitivity
WA-SPE	:Weighted average of Specificity

1. INTRODUCTION

1.1. Motivation

Sound occurs as a result of the vibrations with different frequencies and decimals sent by the objects in the environment. It is a signal transmitted by the help of any interaction multiplying the objects in the environment. Depending on states of matter, madden type, different permeability and vibration characteristics, and the power, sound can sustain its continuity. The human ear has the ability to hear sonic sounds at a range of 20-20000 Hz and 0-140 db. It is a very difficult and demanding process that can be perceived by the human ear in the peripheral sound, when voices are present at low severity. The frequency ranges of the sounds are depicted in Figure 1.1.

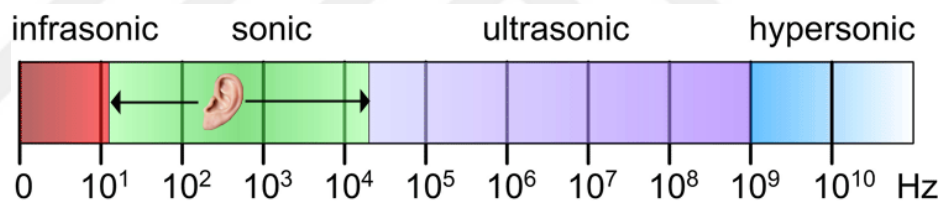


Figure 1.1. The frequency ranges and names of the sounds

Especially hearing adventitious sounds and making assessments on the inner body sounds are vital in various disciplines. The stethoscope which is the symbol of the medical profession is the most common tool to overcome hearing adventitious and low level sounds in medicine. In the first half of the 1800s, diagnosis was an empirical method and all diseases had a stable single symptom. While the physicians have placed their ear directly on the patient to observe inner body sounds, for diagnosing on the patients and the physical examination, French physician Rene Laennec was a steady believer to revise the examination method using diagnostic tools. In 1816, Laennec invented himself a monaural instrument with funnel shape of wooden parts to hear durable body sounds such as heart and lungs and named it as stethoscope. The word stethoscope is a compound word of two Greek words “stethos” which means chest and “skopein” that means exploring. In the

following years, the stethoscope turned into binaural functionality, the diaphragm, and the bell shape in design, rubber tubing and more developing specifications for obtaining more clear sound auscultation. The stethoscopes that have the ability to isolate the inner body sounds from the stethoscope by around 80% of ambient sounds were produced by dint of the ever-evolving materials. But, stethoscopes still continue to use the same working principle except electronic capabilities. The evolution of stethoscopes is depicted in Figure 1.2.

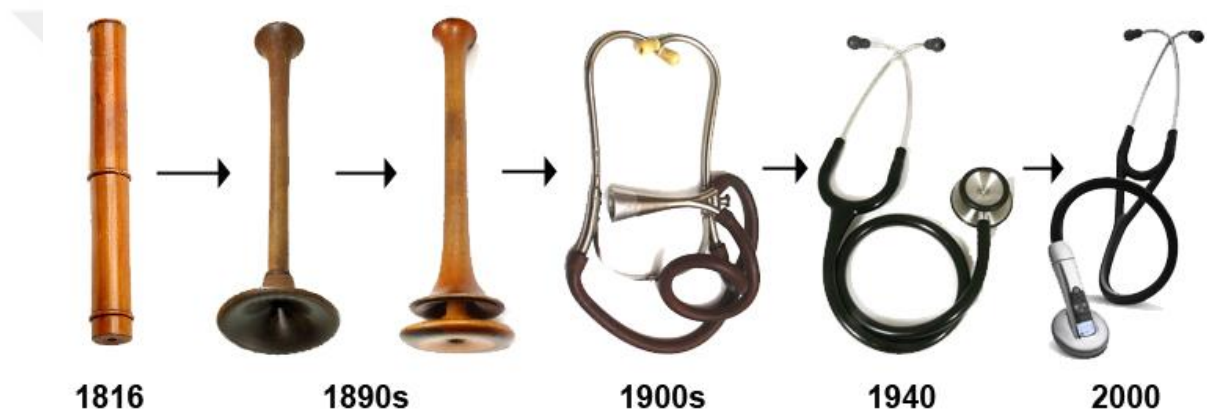


Figure 1.2. The shortened history of stethoscope

Over past 15 years, telemedicine applications have begun to be transformed physical examination and clinic results into online accessible subject-based models that can store chest X-ray, Electrocardiography (ECG), clinical results, lung sounds, heart sounds, and more by become a current issue in medicine.

It is possible to check and control treatment facilities on patients in telemedicine using individual communication panels and physician directed examinations and questions without unnecessarily staying in the same clinic. The response of the patient to treatment in time, accessing patient clinical history, the positive and negative reactions of medicine to treatment for improvements, the monitoring and controlling capabilities on chronic diseases can be performed in the light of the stored clinical data and biomedical signals. Biomedical signals recorded from the patients can be analysed for the diagnosis of cardiovascular, pulmonary and cardio-pulmonary diseases and keeping track of the treatment processes.

Treatment and diagnosis processes can be performed at any time with stored recordings; in the meanwhile online real-time physical examination models are still being developed. ECG, Electroencephalography (EEG), lung and heart sounds should be digitized in order to perform computerized online analysis of the diseases.

The use of digital stethoscopes is the simplest way for recording auscultation sounds on the assessment of pulmonary, cardiovascular diseases. The newly developed digital stethoscopes can record the auscultation sounds to internal memory, as well as they can interact Human-Computer interfaces using various serial communication methods to transfer the auscultation sounds to the digitized media with instant respiratory sound recording. The digital stethoscopes have ability to overcome low levels of inner body sounds using electronically amplification circuits. The amplified low level sound allows physicians to hear and interpret adventitious auscultation sounds. Generic electronic stethoscopes which allow to set frequency ranges, to record into internal memory, to perform simple signal processing algorithms for filtering and visualization of auscultated sounds, and to interact with real time telemedicine applications are being developed rapidly and robustly by various manufacturers.

Auscultation is the most common diagnostic tool which enables hearing sounds within body such as heart sound, lung sounds, blood vessel, and gastrointestinal sounds using a stethoscope. The developments on digital stethoscopes provided hearing the internal organs in more detail and helping to increase more accurate and steady treatment processes (Melbye, 2001). The aim of the auscultation is to isolate the internal sounds as noiseless as possible from the environmental sounds and is to transfer unequivocal auscultation sounds to the physician in the clinical settings. One of the most important advantages of auscultation is that it allows the different regions of the same organ to compare and assessing functionality.

During the evaluation of organs, auscultation tones from various regions are often used to determine the status and severity of diseases. Although it has not been established with a precise standardization for appropriate auscultation conditions, it can be performed by the use of the stethoscope in direct contact with the patient, and the soft and quality materials to help an easy and clear audition in a place where the normal temperature of the

room is kept constant, the patient can feel comfortable, it is isolated from the environmental sounds and well lighted.

The auscultation needs the anatomical knowledge and specialization skills for medical personnel. The age, gender, weight, sickness, skin thickness, posture and specific inconvenience of the patients are the conditions that may affect the level and clarity of the auscultation sounds. In addition to aforementioned auscultation conditions, the auscultation areas determined by CORSA can be accepted as specific directions for hearing the relevant organs. While the auscultation procedure is achieved by hearing the stomach area in the lying position for gastrointestinal sounds, heart sounds and lung sounds can be heard more clearly from the back and chest area in sitting position. First, auscultation is performed while the patient is in a comfortable position. If no sound is heard, the auscultation area must be changed. Sound may be difficult to hear due to skin thicknesses and texture specifications of skin. In this case, a fixed auscultation sound is tried to get by the way of pressing on the diaphragm part of the stethoscope. When auscultation sound is received clearly, the diaphragm must be kept immobile and not to be moved. In case of movement in consequence of the physician's diaphragm touch and contact between skin surface and the diaphragm, auscultation is heard noisy and may be deteriorated its characteristic. Considering noise in the digitization of auscultation sounds, it causes misclassification in the diagnosis systems that utilize machine learning algorithms.

When studies on biomedical signal processing are reviewed, most of them especially focused on lung and heart sounds among auscultation sounds by identifying and detecting the abnormal lung sounds, and a variety of diagnosis models of cardiac, pulmonary and cardiopulmonary diseases. Heart sound is a diagnostic procedure that is still not abandoned by specialist cardiologists for definitive diagnoses and comparisons of murmurs, even if it is a clinical procedure that is not much preferred after widespread use of the ECG. On the other hand, lung sound is a discipline that has rapidly increasing significance in recent decades and has begun to research intensely due to respiratory diseases on the list of World's the deadliest. This thesis focuses on a computerized analysis of the cardiovascular and pulmonary diseases that are leading to the first places in the world's deadliest disease list using lung sounds and heart sounds.

The auscultation of respiratory sounds is an effective and inexpensive method for detecting pulmonary abnormalities. Pathological variations in the characteristic lung sounds can have significant information about the disorders in the lungs and heart. The clinicians may encounter different interpretations about pathological variations during the evaluation process of the diseases. The factors that cause different interpretations are the experience in the province, the hearing ability, auscultation environment and method, the patients based cases, and the patterns come in different forms such as wheezing, crackles, murmur and more. Therefore, the standardization of the auscultation methods is one of the most important steps to eliminate these factors for the diagnosis and assessment of the respiratory diseases. The computer assisted diagnosis tools and methods are an easy and effective way in a standardized method to detect the pathological variations in the respiratory sounds. There is a close relationship between the auscultated lung sounds and pulmonary diseases (Kandaswamy et al., 2004).

1.2. The Scope of the Thesis

Pattern Recognition is a process stack that includes data acquiring, pre-processing, feature extraction, feature dimensionality reduction, classification or clustering and validation, sequentially. Although each of these stages is important ring in the chain which assists the next procedure and entire process, the first procedure, data acquiring, is of great importance in terms of the accurate functioning of subsequent processes.

In this thesis, a unique respiratory database, RespiratoryDatabase@TR, was created. RespiratoryDatabase@TR has a great importance in the development of new approaches considering the deficiency of computer-assisted analysis of respiratory diseases. It is comprised of chest X-rays for medical image processing , pulmonary function test measurements, SGRQ-C questionnaire answers, lung and heart sounds for digital signal processing approaches. A graphical interface is designed for RespiratoryDatabase@TR for pre-processing, segmentation, labelling, annotation and synchronization of the auscultation sounds. It enables analysis on respiratory diseases including the data from the subjects

with the Chronic Obstructive Pulmonary Disease (COPD), asthma, the COPD levels, healthy people.

Thesis focuses on auscultation sounds analyses to diagnose asthma, and the COPD. The diagnosis of COPD severities is necessarily for keeping under control the diseases before reaching advanced levels. The COPD is an incurable disease and treatment process provides only consists of stabilizing the current level. Therefore, early diagnosis of the COPD severities, especially in mild, moderate, and under risk severities is a pioneer procedure for both medicine science and engineering science. While the COPD affects the people aged between 35 and older, the other widespread chronic disease, asthma, is encountered with both children and adults. In addition to the analysis of the COPD, the analysis of the auscultation sounds with asthma was evaluated in the thesis.

The Hilbert-Huang Transform (HHT) and the Discrete Wavelet Transform (DWT) are in the most efficient digital signal processing approaches with the capability of extracting time-frequency-energy characteristics of non-stationary signals. These transformations were applied to the lung sounds and the signal characteristics were decomposed. The obtained subbands and the Intrinsic Mode functions (IMF) at the different frequency ranges were examined by extracting statistical features. In contrast with statistical analysis with transform estimations, quantization features were counted using the proposed three-dimensional Second Order Difference Plot (SODP) analyses.

A novel extension of traditional Extreme Learning Machines (ELM) with multi-layer model is proposed. Deep ELM models have capabilities of assessing deepest levels for the input data. Integration of novel approaches namely the Hessenberg decomposition approach based ELM, lower upper decomposition based ELM, and traditional kernel ELM were proposed as a classification model. The proposed multi kernel Deep ELM model has Deep Learning specification with detailed analyses, and ELM specifications with fast learning and generalization performance. Performances of proposed methods are compared with Deep Belief Networks (DBN), multi-layer Artificial Neural Networks (ANN). These classifiers were applied to dataset including statistical features and quantization features to diagnose the COPD, asthma, and COPD levels. The classification performances were measured using sensitivity, precision, specificity, overall accuracy.

In this thesis efficiency of digitized auscultation sounds focusing lung and heart sections were analysed using 16-channel synchronously acquiring scenarios by two digital stethoscopes. In pre-processing part, to reveal synchronized auscultation sounds, coughing peaks were overlapped for left and right sides on the auscultation sounds. The data points before the coughing peak were removed from the overlapped sounds. The inspiration was caught after 1s and auscultation sounds were segmented into a 15s data.

1.3. The Significance of the Thesis

This thesis aims to analyse auscultation sounds for diagnosing respiratory diseases including the COPD, and asthma. The significant part of the thesis is severity classification of the COPD to early diagnosis of the COPD and to prevent reaching advance levels.

Although there are some limited and inaccessible lung sounds databases based on respiratory sounds in the literature, there is no specific and extensive auscultation database directed to a specific disease. A comprehensive database creation is priority requirement for particularly COPD disease, which is becoming widespread with an accelerating increase, and other chronic respiratory disorders. The first step of the thesis is acquiring data from the healthy subjects and the patients with respiratory diseases, especially with the COPD. The patient population is comprised of patients from various levels of the COPD (COPD0, COPD1, COPD2, COPD3, and COPD4), asthmatic patients and healthy subjects. The acquired multimedia database is named as RespiratoryDatabase@TR. It is a unique respiratory database with including modular computer-assisted medical interface (CMI); 16-channel auscultation sounds from heart and lungs, chest X-rays, pulmonary function test measurements, and SGRQ-C questionnaire answers. The database enables developing computerized analysis approaches and diagnosis models for pulmonary, cardiac, and cardiopulmonary diseases.

In contrast with the complexity of the transformation methods, simple mathematical operations such as mapping and the quantization of the signals may provide fast and significant characteristics for non-linear and non-stationary signals. The plotting based segmentations and regional segmentations enable extracting distinguishing quality features.

The proposed SODP algorithm has ability to quantize octant-based features in three-dimensional space according to the sign parameters of the points.

The ELM autoencoder is an unsupervised technique which outperforms deep analysis with ELM flexibility for machine learning algorithms. The traditional ELM autoencoder defines the output weights and hidden layer neurons with singular value decomposition model by setting feature matrix as both input and output of the structure. In addition to singular value decomposition, the Hessenberg decomposition, and Lower upper (LU) decomposition are proposed as adaptable ELM autoencoder kernels.

Deep Learning has best-in-class performance with feature engineering. Deep learning systems can detect and generate more detailed complex presentations of input data. The ELM has accurate generalization performances with short training times. The integration of the Deep Learning and ELM approaches fixes with the high performed, fast classifications with Deep ELM. An improvement learning capacity of the ELM using multilayer ELM and various decomposition methods kernels is modelled. A multi-kernel Deep ELM modal is evaluated for deep analyses, complex presentation in autoencoder algorithms. The proposed two novel ELM auto encoders; Hessenberg decomposition based ELM autoencoder kernel, Lower upper decomposition based autoencoder kernel are adapted to Deep ELM model as kernels with a multi-kernel optimization optionality.

Empirical and statistical effects of digitized auscultation sounds are experimented using 16-channel for different respiratory diseases using multi-kernel Deep ELM model.

1.4. The Thesis Organization

This thesis consists of six chapters. Chapter 1 describes the deficiencies respiratory diseases and machine learning applications and explains the incentive information and the aims of the thesis in general terms. Chapter 2 issues about previous studies on computerized analysis of respiratory diseases, the COPD severity classification disciplines, specifications of lung sounds, and recent Deep Learning and ELM models and compares each other disciplines in terms of efficiency and variability with related studies. Chapter 3 is committed for formulation of mathematical statistical substructure of decomposition and

kernel setting for classification models. Hilbert-Huang Transform, Discrete Wavelet Transform, Three-dimensional Second Order Difference Plot (3D-SODP) quantization, statistical feature extraction, and feature dimensionality reduction, Deep Learning, ELM kernels and Deep ELM are subjected particularly. Besides, experimental setup and database collection steps are provided. In Chapter 4, the structure of experimental model, experiential results, and classification performance measurements of proposed model are given. Finally, Chapter 5 covers assessments on the results and grants discussions on the proposed classifiers and feature quantization methods, contributions of the thesis and revolution approaches for future works.

2. RELATED WORKS

In this chapter respiratory sounds analysis, the COPD, respiratory databases, Deep Learning, DBN, ELM and Deep ELM research fields and related works are reviewed in four subsections.

2.1. Respiratory Sound Analysis

Pathological parts on the lung sounds can be detected and classified using frequency characteristics and musical characteristics (Parkhi and Pawar, 2011). Systems that enable automatic detection of wheezing sounds by analysing frequency and time domain on auscultation sounds recorded with various types of sensors and microphones from various types of obstructive respiratory diseases have been established. Meanwhile there are analysing studies, recommended methods and models in literature for diagnosis of the COPD and asthma, which are common respiratory diseases, the studies directly based on proposing the detection and identification of abnormal lung sounds such as crackles, wheeze sounds from various respiratory diseases by analysing the frequency bands.

Jane et al. (2004) performed 6th level of Autoregressive Model and calculated power spectral density (PSD) and peak frequency on lung sounds. The 49 of lung sounds were acquired with a sampling frequency of 5000 Hz for 120s during instinctive breathing. They analysed the distinction of cycling and suggested a cycle measurement alternative to the PFT measurements for detecting the patients with high obstruction.

Hossain et al. (2004) applied Hilbert transform, fast Fourier transform and linear regression analysis for analysing the lung sounds at frequency domain. The lung sounds were recorded from 22 of patient in group I, II, and III with a sampling frequency of 10240 Hz for 60s (10s breath holding). They extracted mean amplitude, mean flow, and mean power features and investigated the correlation between mean power and flow rate meaningful for the diagnosis of asthmatic patients.

Wisniewski et al. (2010) utilized Tager energy operator, short-time Fourier transform (STFT), and separated the lung sounds in frequency bands using wavelet decomposition

with Daubechies 6th order. The kurtosis, Shannon entropy, Renyi entropy, sample entropy features were extracted from decomposed wavelets. 246 lung sounds including wheeze and normal lung sounds from healthy subjects, subjects with asthmatic, the COPD. They suggested controlling chronic lung diseases using mobile and wearable devices instead of tracking risk factors.

Ulukaya et al. (2016) proposed a rational expansion wavelet transformation which has a tuneable capability using Q factor in discrete wavelet transform. They extracted wavelets in new form using proposed transformation for 3 levels on lung sounds from 20 subjects with a sampling frequency of 9600 Hz for 15s. They analysed asthma disease and detected of wheeze sounds, crackle sounds and normal lung sounds using computed statistical features from decomposed wavelets. The statistical features are fed into k -NN, SVM with RBF kernel classifiers. The pathological lung sounds and normal lung sounds were classified with average accuracy rates of 95.17%, 93.17%, 94.33%, 93.33%, and 86.67% for energy entropy, standard deviation, minimum, and kurtosis, respectively using the SVM classifier.

Kandaswamy et al. (2004) proposed an approach for classifying six types of lung sounds such as normal, wheeze, crackle, squawk, stridor, and rhonchus using Wavelet transform. They performed discrete wavelet transform based wavelet shrinkage denoising in the pre-processing stage and decomposed subbands using 7th level wavelet transform. The mean, average power, standard deviation, and the ratio of absolute mean features for Coif4, sym10, db12, db8 subbands were extracted and fed into ANN classifier model. Daubechies wavelet of order 8 was noticed as the responsive subbands. They achieved an average classification rate of 92.00%.

Charleston et al. (2011) estimated multichannel lung sounds to separate normal lung sounds and pathological lung sounds from interstitial lung disorders. They applied the univariate autoregressive and the multivariate autoregressive models to 25 channels of lung sounds from 27 subjects (8 of non-smoker healthy subjects) with a sampling frequency of 10000 Hz for 15s. The lung sounds were digitally filtered at a range from 75 to 2000Hz for reducing environmental, muscle and other inner body sounds. The PSD, the eigenvalues of the covariance matrix, and univariate autoregressive, multivariate autoregressive

coefficients were extracted from multichannel lung sounds and fed into ANN model. They evaluated aggregable classification performances with accuracy rates of 75% and 93% for healthy subjects and patients, respectively.

Mastorocostas (2006) applied wavelet transform filter in the pre-processing stage for the lung sounds and designed a fuzzy rule-based classification model for three types of stationary and non-stationary lung sounds. They achieved detecting accuracies of 93.90%, 98.18%, and 100% for fine crackles, coarse crackles and squawks, respectively.

Kumar (2007) proposed a fuzzy expert system to assess the auscultation sounds such as lung sounds and heart sounds for diagnosing pulmonary and heart state using raw sounds. He called the model as HILSA kit. The rule-based fuzzy model classified the disorders in the lung with a classification performance of 47.6%.

The biggest deficiency of computerized analysis of the auscultation sounds is mixed the inner body sounds from different organs. Leontios et al. (1998) utilized a wavelet based stationary and non-stationary filtering technique to separate heart sounds from lung sounds. The lung sounds that were tested in the analysis are recorded with a sampling rate of 2500 Hz for 30s. He denoted the accuracy of the reducing technique as an easy and fast model.

Tocchetto et al. (2014) studied on the classification of three types (normal, crackles and wheezes) of 92 lung sounds which were recorded with a sampling frequency of 44100 Hz for 3s including one of respiratory cycle duration. They performed a downsampling by 4 and 8th order Chebyshev filtering to reduce noises in the pre-processing stage. They applied 5th level wavelet packet transform with Sym10, DB5, Coif2 subbands and extracted statistical features from wavelet coefficients. The extracted features are fed into ANN classifier model. The maximum classification performance of 99.26% is achieved using hyperbolic tangent sigmoid activation function.

Riella et al. (2009) improved an unusual approach to analyse the lung sounds. They plotted spectrogram of the lung sounds using STFT and obtained a spectral projection of the spectrogram distribution using 9x9 Laplacian filters. The diversity of the filter is counted and the obtained varieties are used as the inputs of the ANN model. The ANN model was achieved an accuracy rate of 92.86% for the detection of non-wheeze and wheeze sounds.

Mondal et al. (2014) implemented lung sound classification to assess lung status. They utilized morphological complexity of the 30 lung sounds with a sampling frequency of 8000 Hz. The lung sounds were collected from various respiratory diseases such as asthma, the COPD, Interstitial lung diseases. The higher order statistical features such as kurtosis, skewness, lacunarity, and sample entropy were calculated and fed into ELM and SVM classifiers. The classifier models reached a classification performance of 92.86% and 91.50% for ELM and SVM, respectively.

Bahoura et al. (2004) proposed a GMM classification model which differentiates normal lung sounds and wheeze sounds. The lung sounds from 24 subjects (12 normal lung sounds) were digitized at 6000 Hz. They defined the 8th order Gaussian Mixture Model (GMM) as a powerful statistical method for lung sounds and extracted Mel-frequency cepstral coefficients (MFCC) from subbands and Cepstral parameters as the features. They tested the obtained feature set with the proposed GMM model with ANN and Vector Quantization classifiers and achieved a classification accuracy of 77.85%, 75.19%, and 83.72% for ANN, Vector Quantization, and GMM, respectively. Palaniappan et al. (2014) also used MFCCs to differentiate the pathological lung sounds and healthy lung sounds. The 68 of lung sounds (17 healthy lung sounds) were digitized at sampling rate of 10000 Hz and applied 8th order Butterworth filter, 1st order Butterworth filter and low-pass filtered at 2.5 kHz in the pre-processing stage. 13 of MFCCs were extracted as features and were tested with SVM and k-NN classification algorithms. The designed model implemented a comparison on accuracies of 92.19% and 98.26% for SVM and *k*-NN respectively.

Uysal et al. (2014) aimed at the classifying healthy and pathological lung sound. They utilized 34 of lung sounds (14 healthy lung sounds) with a sampling frequency of 11025 Hz in the computerized analysis of sounds. The lung sounds were denoised using 4th level Butterworth high pass filter and cut-off frequency at a range of 30-150 Hz in the pre-processing stage and were decomposed into wavelet coefficients using 7th order wavelet transform with Daubechies 7 subbands. The mean power, variance, standard deviation and absolute average value were counted for each subband and fed into the ANN classifier

model. An average accuracy rate of 97.16% is reached using gradient descent backpropagation algorithm.

Yamashita et al. (2011) studied on identifying the lung sounds of pulmonary emphysema and healthy lung sounds. They utilized Hidden Markov Models (HMM) and bigram models for extracting meaningful acoustic characteristics of the pathological lung sounds. They arranged two-stage discrimination by using two likelihood predefined threshold using three states of HMM and PSD. 151 of lung sounds (39 healthy lung sounds) including inspiration and expiration processes with a sampling rate of 10000Hz. They were resulted statistical analysis with a prosperous classification rate of 88.7% in the experiments.

Newandee et al. (2003) studied on the severity classification of the COPD. They assessed on the combination of cardiac state and clinical data as significant discrimination features. HRV measurements, blood pressure, respiration measurements, respiration spectra and the cross-spectral amounts were analysed with the Principal Component Analysis (PCA) and cluster analysis. They separated the COPD patients and healthy subjects with a classification accuracy of 99% and also the COPD severity classification was performed with an accuracy rate of 88%. Işık et al. (2015) also utilized clinical parameters such as age, sexuality, haemoglobin, haematocrit, FEV, FVC, diabetes mellitus, hyper tension, state of coronary artery disease, polycythaemias, and oxygen deficiency to perform severity classification of the COPD. The clinical parameters were collected from 507 subjects including severe COPD, very severe COPD, moderate severe and mild severe. They fed the clinical parameters as the input of the ANN and achieved a classification accuracy rate of 99%.

Naves et al. (2016) proposed a detailed multistage classification model on respiratory sounds. Their database consists of 36 lung sounds with a sampling rate of 8 kHz. Higher-order statistics such as second-, third- and fourth-order cumulants were calculated and Fisher's discriminant ratio algorithm was used to reduce feature dimensionality. In the first stage they differentiated the Vesicular, wheeze and crackle sounds using k -NN algorithm. In the second stage the model determined classification of monophonic and polyphonic types of wheezes, fine and coarse types of crackles with Bayes classifiers. The multistage

classification model has reached seriatim accuracy rates of 98.1% and 94.6% for training and validation.

Morillo et al. (2013) focused on the discrimination of the subjects with COPD and pneumonia. The lung sounds from 58 patients (33 COPD) were utilized in the analysis. The PSD, mean frequency, median frequency, spectral crest factor, Shannon entropy, Rényi entropy, Tsallis entropy, second-order moment, skewness, kurtosis, and relative power were calculated as the features. The integration of the PCA and probabilistic ANN was estimated with classification performances of 72%, 81.8%, and 77.6% for sensitivity, specificity, and accuracy, respectively. They discussed on the efficiency of diagnosing close diseases in modest ways with non-linear determination boundaries.

Amaral et al. (2010) designed an automatic diagnostic model using spirometry measurements such as FEV, FVC, and FEV/FVC during forced oscillation, and clinical parameters such as age, weight, height, intercept resident, resonance frequency. The features are collected from 15 COPD patients and 15 non-smoker subjects. The clinical features were fed into ANN classifier and statistically analysed using Mann-Whitney U test. The COPD patients were recognized with a higher classification performance of 90% for sensitivity, specificity, and accuracy.

Hosseini et al. (2011) referred to diagnosing the COPD using image processing techniques on three-dimensional Computer Tomography (CT) images. They segmented lung parts from the CT images and used parenchyma variation and morphological erosion on the left and right lungs. They performed a segmentation and identification using Bayesian classifier with a classification accuracy of 77% for both left and right lung. Cheplygina et al. (2014) processed on CT images from 100 of COPD patients and 100 healthy subjects. Representation of CT images with 50 Region of interest features, diversity density were utilized in various instance learning algorithms. The highest classification accuracy rate of 77.60% was achieved with SVM method.

Ying et al. (2016) utilized 361 features such as self-administered questionnaire answers, clinical history, and questionnaires on the COPD symptoms, physical examination variability, spirometry measurements and genetic epidemiology of 10300 subjects. The features were fed into the deep learning classification algorithm. The DBN estimated the

COPD severity with a classification accuracy of 97.2%. They suggested overcoming performance evaluation problem by integrating the DBN and Fisher score feature selection algorithm.

2.2. Respiratory Databases

In the literature, it is seen that the databases used in the computer-aided analysis of lung sounds are specific to the study, have not an open access. There are three of pioneer respiratory sounds databases based on available studies. Unfortunately, except for R.A.L.E. respiratory, the databases are not (commercially or otherwise) available. The databases may have problems in characterizing interrelated diseases in consequence of the they do not focus on specific diseases, do not share the definite diagnosis of the patients and other diagnostic tools. A database on COPD and severities of the COPD was not encountered. The inability to access specific databases, including respiratory diseases with high amount of mortality, prevents innovations and researches on computer-aided analysing discipline. An open access auscultation sound database is a big necessity to test the methods to be developed on respiratory diseases.

The additional audio recordings are available to educate the recognition of respiratory sounds in various diseases which are far from being diagnosed in the books that are fundamental sources for medical students (Kraman, 1993; Tilikian and Conover, 1993; Lehrer, 1993; Mangiore, 2000). Some studies in the literature analyse the lung sounds obtained from these books. The lack of lung sounds constitutes a situation that low validity, specificity and precision for crowded populations. Using a combination of the additional multimedia from the books also creates a handicap in terms of comparison. The determination of the processes for the disease is being negatively affected, this is because the environment in which a standard auscultation process is not currently guide-lined, the recording devices have different specifications, and the auscultation areas are not particular.

R.A.L.E.® (Respiratory Acoustics Laboratory Environment) repository designed for students and educators, doctors, nurses to have an idea on auscultation sounds. It provides 50 recordings of respiratory sounds which were digitized at 10 kHz from healthy subjects

and patients with respiratory disease including all age groups using the physical examinations recommended by the American Thoracic Society and the American College of Chest Physicians. It is available in several versions with commercial-use (RALE, 2005; Bahoura and Pelletier, 2004).

Marburg Respiratory Sounds (MARS) database consists of chest X-rays, clinical interviews, clinical test amounts, the Pulmonary Function Test (PFT) measurements for many disorders using typical clinical procedures with a CMI. It conforms the CORSA standards. The MARS has more than 5000 of lung sounds from 50 patients with bronchial asthma, 40 with the COPD, 5 with lung fibrosis, 45 patients with pneumonia and 250 healthy subjects (Gross et al., 2003).

Computerized respiratory sound analysis (CORSA) is a project which is held by the European Respiratory Society for 10 years in Belgium, Britain, Finland, France, Germany Italy and the Netherlands. The basic aim of the CORSA is standardization of the auscultation process, building guidelines for the physicians in physical examination and allowing computer-aided analysis of lung sounds. It consists of 364 of lung sounds such as snoring, stridor, cough, wheeze, crackle, and other sounds with a sampling rate of 10 kHz (Sovijärvi et al., 2000).

2.3. Deep Learning and Deep Belief Networks

Altan et al. (2016) proposed an arrhythmia classification model using R peak centred complete ECG waveform and additional Second order difference plot features as the input of the model. The median filter was applied to the ECG waveform to eliminate the noises. They discriminated 5 types of arrhythmia with a high accuracy rate of 96.10%, sensitivity rate of 95.33%, and selectivity rate of 95.68% by multi-stage DBN classifier.

Altan et al. (2016) analysed EEG for the slow cortical potential in stroke patients using the negativity and positivity trials according to electrical activity changes in the EEG. The stroke is a disease that limits life and activities also vital necessities. The brain computer interfaces have ability to overcome the limits for stroke patients. They extracted time-frequency-power features using HHT and calculated the higher order statistical

features. The statistical features were fed into the DBN classifier. They reached the remarkable classification performance rates of 90.30%, 96.58%, and 91.15%, for sensitivity, selectivity, and accuracy, respectively.

Altan et al. (2017) acquainted an ECG-based coronary artery disease diagnostic model. They acquired the frequency characteristic information of segmented 15s short-term ECG using the HHT. The statistical features were calculated to create the feature set. They iterated both the DBN and ANN classifier models with the same number of layer, and neuron size. They achieved the highest classification performances of 98.05%, 98.88%, and 96.02% for accuracy, specificity, and sensitivity, sequentially using the DBN.

Kutlu et al. (2017) performed a fish recognition using the morphological features from fish images. They marked the specific landmarks on the fish images and the distance metric of the landmarks to each other. The morphological features were fed into the DBN classifier model with two hidden layers. The recognition performance of 97.61%, 99.55% and 99.12% were achieved for accuracy, specificity and sensitivity sequentially.

Abdel-Zaher and Eldeib (2016) proposed a breast cancer diagnosis model using clinical features including clump thickness, uniformity of cell size, and uniformity of cell shape, marginal adhesion, single epithelial cell size, bare nuclei, bland chromatin, normal nucleoli, and mitoses amounts as the features from 683 samples. They experienced various backpropagation algorithms in the supervised stage of the ANN and the DBN classifier and achieved spectacular performance rates of 99.68%, 100%, and 99.47% for accuracy, sensitivity, and specificity using the DBN model. They proved that the DBN model has higher breast cancer classification performances than ANN with the same structure of model.

Shen et al (2015) compared the efficiency of the DBN and the ANN on forecasting exchange. They deal forecasting amounts among 1976-2004 years from various states. The root mean square error, mean absolute error, mean absolute percentage error, direction accuracy, Pearson correlation coefficient, variance were calculated from forecasting tests to evaluate the performance. They applied Conjugate gradient algorithm to accelerate learning procedure in the supervised stage for both two classifier. The DBN classifier outperforms ANN classifier with the same model considering all the five performance measurements.

Also, Kuremoto et al. (2013) analysed time series forecasting on CATS benchmark data and achieved less mean absolute error amount using the DBN than the ANN model.

Tamilselvan et al. (2013) recommended a health diagnosis model using the DBN classifier. They iterated the proposed model against SVM, and ANN classifiers on iris dataset, wine dataset, Wisconsin breast cancer diagnosis dataset and Escherichia coli dataset. They reached separation accuracy rates of 100%, 100%, 97.18%, and 98.39 for iris dataset, wine dataset, Wisconsin breast cancer diagnosis dataset and Escherichia coli dataset on training, sequentially. The results also demonstrated the highest efficiency of the DBN on benchmark dataset by reaching 90.99% classification accuracy.

Bezak et al. (2014) generated a robotic grasping simulation with advance specifications. Especially, the object orientation and recognition approaches were based on Deep Learning algorithms. They optimized CNN model and the DBN model for grasping parameters, object location and the hand positioning for simulation parameters.

Drotar et al. (2015) assayed the efficiency on reducing dimensionality of dataset and iterated various hybrid classifiers to test the conditions on Parkinson disease. They contrast t-test, Bhattacharyya distance, ANOVA and entropy, tree-based ensemble, least absolute shrinkage and selection operator, minimum redundancy maximum relevance algorithms in integration with SVM, DBN, Random forest classifiers. They proved that the feature selection algorithms increased the classification performance and the highest accurate hybrid classifier-feature selecting model is handled with DBN and statistical feature selection algorithms.

2.4. Extreme Learning Machines

Wang et al., (2011) suggested an approximation to state the input weights and biases in deterministic ways on behalf of randomized stating by conventional ELM column and row rankings. They called the ELM kernel as Effective ELM. Therefore, preventing the learning deficiency was overcome by linear calculation and was turned into more stable and fast ELM kernel. The efficiency of the Effective ELM model was structured on radial basis function activation function.

Zong and Huang (2013) proposed Weighted ELM to overcome imbalanced data problems in training processes. Traditional ELM needs same size of features for each instance in the training processes. The Weighted ELM offers weighting the features taking into account the effect of the feature for training errors as a feature selection algorithm. The less responsible feature weights were converged to zero among training dataset.

Kutlu et al. (2017) proposed a cognitive activity classifier model which is based on arithmetic tasks and text reading on EEG. They extracted time-domain features and regional feature from difference plots with various levels. The features fed into the traditional ELM kernel and Lower-upper triangularization method based ELM (Lu-ELM). The Lu-ELM kernel has reached higher classification performances than traditional ELM kernel.

Zong and Huang (2011) introduced ELM model for face recognition. They utilized active appearance model including shape, texture and appearance features and the holistic-based features on four popular face databases and applied various feature dimensionality reduction algorithms on the feature set to detect significant feature. They compared the ELM model with the SVM classifier performance and pointed out the performance of the ELM classifier was more accurate than the SVM.

Mohammed et al. (2011) also proposed the face recognition models using ELM classifier. They applied Curvelet Transform to the face images and extracted multi resolution information. They offered a novel bidirectional two dimensional PCA for decreasing the feature size for a stable generalization and fast ELM realization. They achieved spectacular recognition performances up to 100%.

Kim et al. (2009) experienced the ELM model on separation of six types of arrhythmias using ECG. The morphological features were extracted by PCA. They contrasted the classification performances concerning various popular machine learning algorithms. They achieved performance rates of 98.00%, 97.95%, and 98.72% for average sensitivity, average specificity, and average accuracy using ELM classifier.

Kutlu et al. (2015) introduced visual multimedia related reactions of the EEG signals for disabled people with stroke, ALS and other myopathy disorders. They utilized quantization methods on plots of P300 waveforms as the input of the ELM classifier with

QR Decomposition kernel. The proposed model achieved almost 100% classification accuracy in milliseconds.

Kumar et al. (2017) predicted wave heights using ocean wave situation data. They handled past wave characteristics from gulf stations of three oceanic cities during 2011-2015 years to train and to test the classifier which is based on ensemble ELM. They experienced the ANN, traditional ELM and ensemble ELM, and achieved minimum root mean square error value of 0.1881 for ensemble ELM.

Wang et al. (2017) proposed an online speller system using EEG signals. They utilized 12 channels P300 waveforms from eight subjects to perform prediction of the digit among 40 characters. They selected sequential ELM and SVM classifiers and denoted the efficiency of the ELM over the SVM with its simple mathematical model. The ELM classification model reached an average accuracy of 97.35% in a remarkable time.

Xie et al. (2016) performed a diagnosis model of breast cancer using the segmentation, position and enhancement properties of the tumor on mammography images. They eliminate the states expect the tumor segment and extracted eleven of mass features, seven of background features, and eight of boundary features from the regional segmentation. They examined SVM and ELM classifiers and achieved classification best performance rates of 96.29%, 94.32%, and 96.02% for sensitivity, specificity, and accuracy.

In last decade, the ELM has become more popular with advanced kernels and the ELM approaches, and machine learning tricks. Deep analysis of the patterns and signals are evaluated using the Deep Learning models. Although, Deep Learning provides generating layer by layer presentations of the input feature sets with various depths in different dimensional spaces, the training time is still a handicap for realizable models even if the parallel computing and the GPU usage becomes widespread. Due to increase training time, the Deep ELM models are experimented with various kernels and models.

Kasun et al. (2013) are the pioneer researchers for constructing the Deep ELM model with multilayer structure with Autoencoder integration. They experienced the Deep ELM model on MNIST dataset by feeding pixel based features and compared the classification performance and training time with DBN, traditional ELM, and common Deep learning

autoencoder models. They attained the highest testing accuracy rate of 99.03% in 444s for Deep ELM model among the Deep Learning approaches and ELM model.

Tang et al. (2016) proposed a multilayer ELM model as a Deep Learning approach. They calculated the input weights and biases using unsupervised ELM sparse autoencoder algorithm and afterwards a supervised ELM model to optimize the output weights for the multilayer input weights. They pointed out the importance of the sparsity parameter for different datasets and achieved higher classification and generalization performance than traditional single layer ELM model for big data and time series.

Guo et al. (2017) performed time series evaluation on forecasting. They utilized similarity based functions including Euclidean model to obtain the segmented time series. The prediction model on forecasting time series are derived using Deep ELM model which is the multilayer ELM model with traditional ELM kernel. They reached the best generalization performance with the Deep ELM model among ANN, SVM, ANFIS, ELM and Deep ELM classifiers.

Sun et al. (2017) presented an ELM Autoencoder based model, generalized ELM Autoencoder, which has same parameter optimization steps with the Deep ELM. They tested the proposed Deep ELM model on real world datasets and interpreted the efficiency of the Deep Learning approaches including DBN sparse autoencoder and Deep ELM model. They denoted the generalized ELM Autoencoder as the most powerful generalization algorithm.

Ding et al. (2015) assayed on Deep ELM modal using EEG data, Ionosphere, and diabetes datasets. They denoted the difference between multilayer ELM and Deep ELM models with the use of kernel tricks. They achieved high classification accuracies in training testing stages for both three datasets with minimalist training times.

3. MATERIAL AND METHODS

3.1. Introduction

The pattern recognition processes are comprised of data acquiring, pre-processing, classification and performance achievement steps. The elaborate information about auscultation sounds, auscultation scenarios, respiratory diseases, signal processing techniques, quantization methods, statistical feature extraction, classification algorithms with novel kernels and structure, performance metrics are described in this section.

3.2. Respiratory Sounds

Respiratory sounds are also called breath sounds and lung sounds. The lungs are the respiratory organs that are more or less in the form of pyramids on the left and right side of the heart in the chest cavity. The volume of your lungs varies according to age, personality, and sex. The lungs come into existence from the tracheobronchial distribution with tree form branching. At the ends of these branches, pulmonary lobules were separated into air vents (acinus) resembling grape bunches. The air vents are also divided into air bladder. The lung lobes are stacked on top of each other irregularly. The air bladders at the ends of the lobes are called bronchi. The bronchioles open up to non-uniform spaces. A lot of channels with a length of 3 mm long and a width of 40 micron are emerged from the bronchioles. The walls of the ducts are indented and the number of bronchioles is about 750 million. The walls of the alveoli are made of simple layer epithelium. The capillary vessels around alveoli enable gas exchange during inspiration and exhalation. The anatomy of the lungs is seen in Figure 3.1.

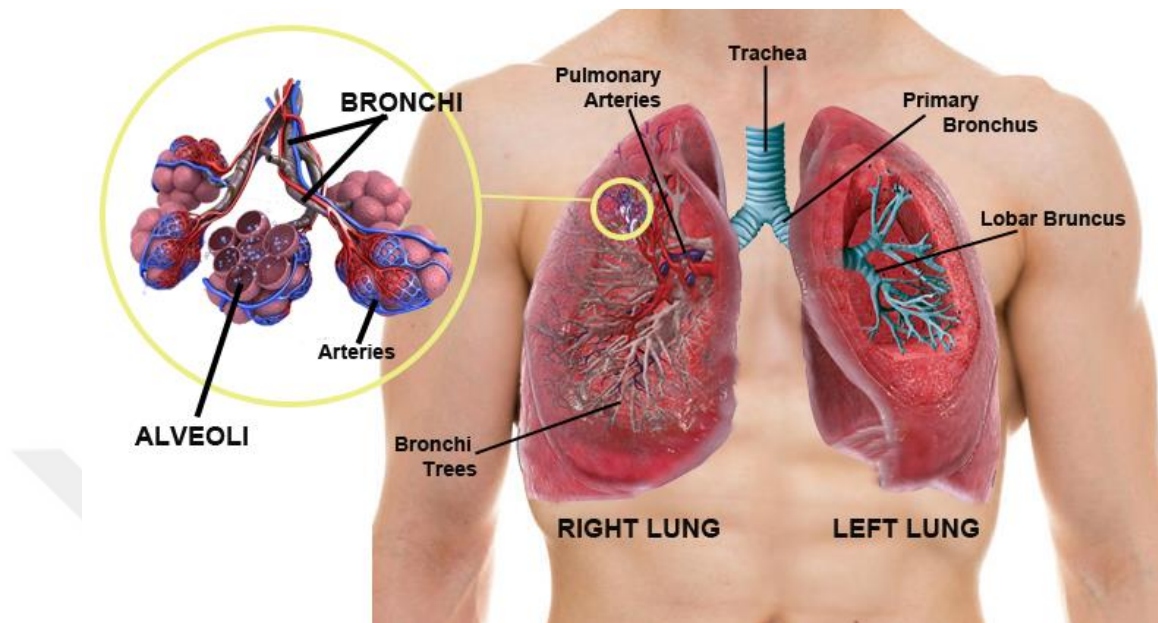


Figure 3.1. The anatomy of the lungs.

Lung sounds are used to assess air entry to the lung and to assess obstruction to airways. Lung sounds occurs due to the circulation of the air flow during inspiration and exhalation. While the patient breathes normally with mouth open, the upper, middle and lower lung fields are auscultated posteriorly from back, and anteriorly from chest. During the auscultation of lungs, first a quiet respiration with at least one complete respiratory cycle that includes both inspiration and exhalation. Deep breathing is preferable for preventing inaudible auscultation. In the diagnosis and physical examination processes, the length of inspiration and expiration, time among inspiration-expiration, and the intensity of pitch on the respiratory sounds are utilized to assess the pulmonary diseases. In the final step, the presence or absence of adventitious sounds on the lung sounds is detected for severity identification of the diseases. The detection of normal and abnormal respiratory sounds has been evaluated as chest auscultation considering anatomical or functional status of the lungs (Sovijärvi et al., 2000). The density and intensity of the lung sounds characterize the abnormalities and the type during the auscultation. The clinicians decide if the airways of the lungs are completely obstructed or narrowed by comparing the auscultation sounds from the right and left lobes and the back and chest areas of the

patients. The characteristics of auscultation sound from the different lobes and the areas usually have distinctive textures on the same patient (McGee, 2012).

3.2.1. Normal Respiratory Sounds

It is a type of sound that indicates the healthy individual has no pathological abnormality and respiratory disease. It is divided into two types according to the auscultated region, bronchial and vesicular. Bronchial sounds are heard over tracheobronchial distribution with the specifications of higher pitches, an equality of durations and a pause between inspiration and expiration. Vesicular sounds are heard over lung tissue with the specifications of lower pitches, longer duration of inspiration, and a steady inspiration and expiration with no intervals. Waveform and spectrogram of normal vesicular lung sound are depicted in Figure 3.2. Normal lung sounds are the sound waveforms that can be heard at frequencies between 100-1000Hz.

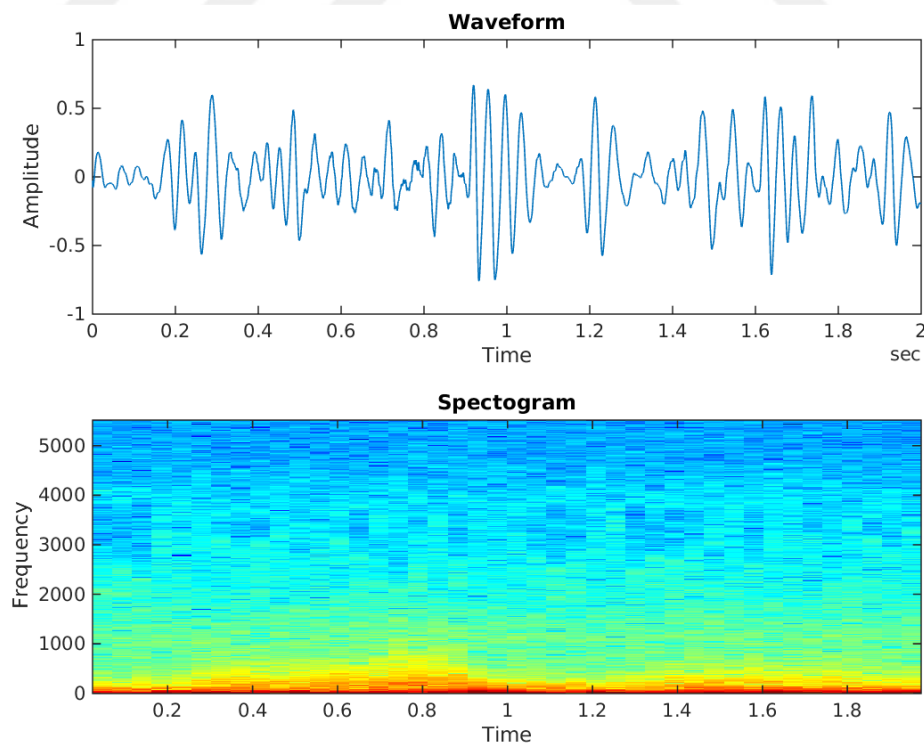


Figure 3.2. Normal vesicular lung sounds waveform.

3.2.2. Abnormal Respiratory Sounds

It is a pathological sound that occurs as a result of obstructions, inflammations, restrictive cases, consolidation, cavitation, losing the flexibility, and pleural effusion with complete atelectasis of lung. Intensity of breath sounds is a healthy indication of ventilation in the lung airways. If an asymmetry in intensity during the breathing is detected, the abnormal lungs sounds are marked in the decreased intensity on the side of atelectasis.

3.2.2.1. Crackles

This type sounds are continuous irritation or short intermittent abnormal sounds that are non-musical in nature. The crackles are also known as crepitation, or rales. The crackles are formed by strong vibrations of the bronchi which cause as a result of the pressure change when the airways in the lungs are suddenly opened during the inspiration (Loudon and Murphy, 1984; Vyshedskiy et al., 2009). The inspiration results with passing air through shortly and in small quantities by a slight forcing or the traction power, and recloses when the pressure is equalized (Vannuccini et al., 2000). Thus, a sudden explosive sound is produced with little air passage each time. Crackle is frequently observed in the respiratory and cardiac (cardio-respiratory) disorders (Sovijärvi et al., 2000). The crackles can also be characterized as fine, medium, and coarse crackles depending on the time. The duration is about 20ms and is seen in the wide frequency band (Sovijärvi et al., 2000). The waveform and spectrogram of the crackle is seen in Figure 3.3.

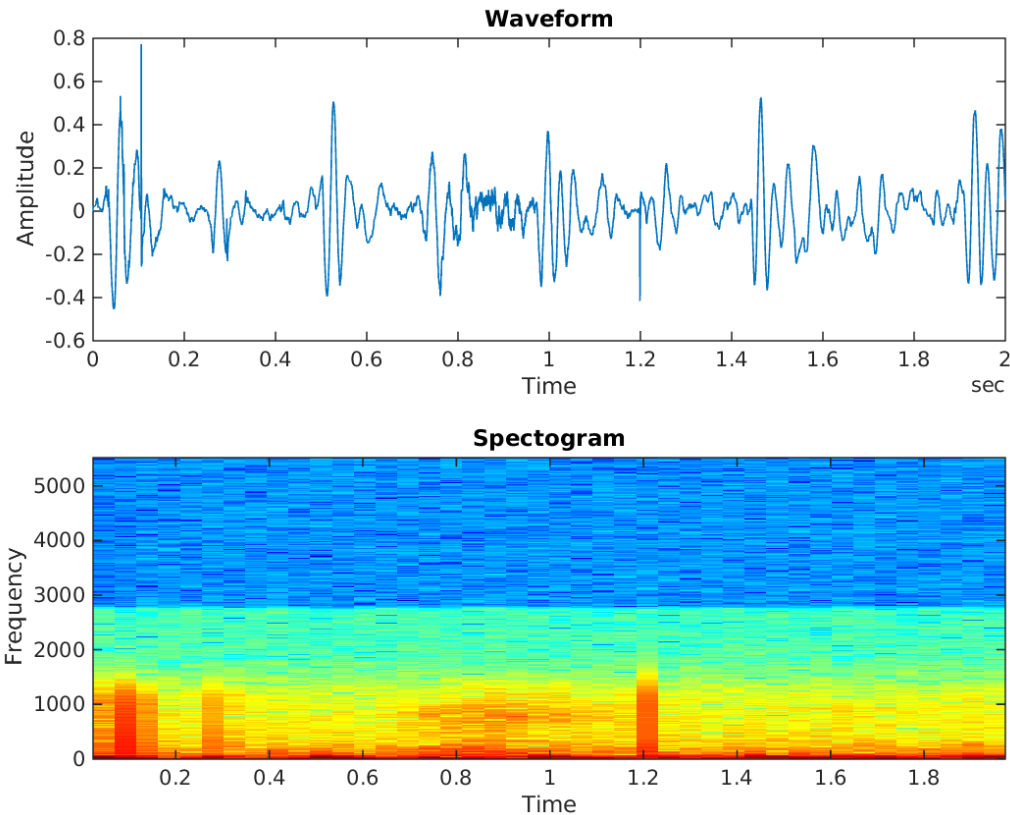


Figure 3.3. Crackles sounds waveform

3.2.2.2. Rhonchi

It is caused by the narrow airways in the lungs. The path between small airways that moves away from each other during the airflow is turned into vibrations and a single musical sound is heard. Although the sound frequency varies depending on the structure of the vibrating solid scleroma, it is generally digitized at lower than 200 Hz (Lehrer, 1984). If the scleroma of the airways is large and flexible, the frequency is low (sonor), if the scleroma is thin and rigid, the frequency is high (synaptic) (Melbye, 2001). It may occur during inspiration and/or expiration. Rhonchi are noisy, coarse, low frequency breathing sounds resembling snoring voice originating from obstructed bronchi due to mucus accumulation. The waveform and spectrogram of the rhonchi is seen in Figure 3.4.

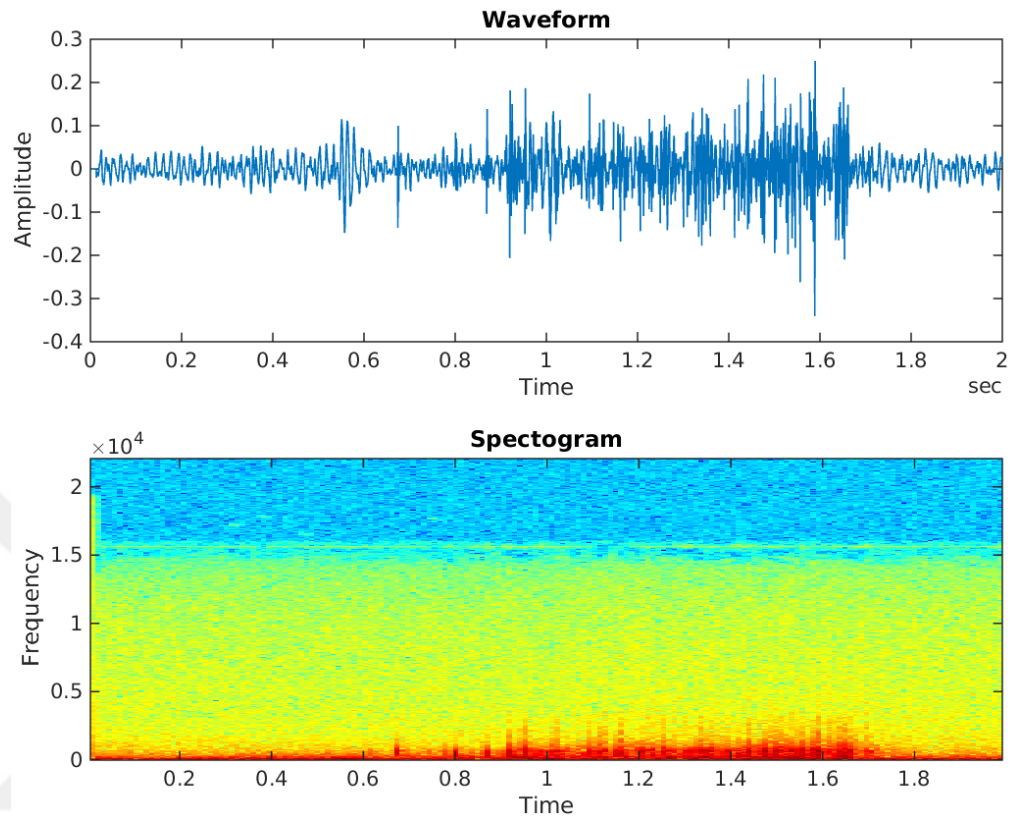


Figure 3.4. Rhonchi sounds waveform

3.2.2.3. Wheeze

Wheeze and rhonchi are very similar auscultation sounds to each other. In most study, it is named as low pitched rhonchi. The most significant characteristic that separates wheeze from the rhonchi is to have whistling wheezes (Loudon and Murphy, 1984). The wheezes are continuous sounds in both inspiratory and expiratory. That type breathing sounds occur when the air passes through from partially occluded airways is airborne. Whistled wheezes are heard during the auscultation of the patients with heavy breathing difficulties and respiratory types that produce high-pitched tone due to narrowing of the small airways pending the expiration. Wheezes have musical clarity (Vannuccini et al., 2000). These respiratory sounds are usually the types of wheezing that are encountered in the asthma patients. Whistling wheezes are respiratory sounds caused by asthma, congestive heart failure, chronic bronchitis and COPD disorders. The duration of the

wheezing is more than 100 milliseconds and has higher frequencies than 400Hz. The waveform and spectrogram of the wheeze is seen in Figure 3.5.

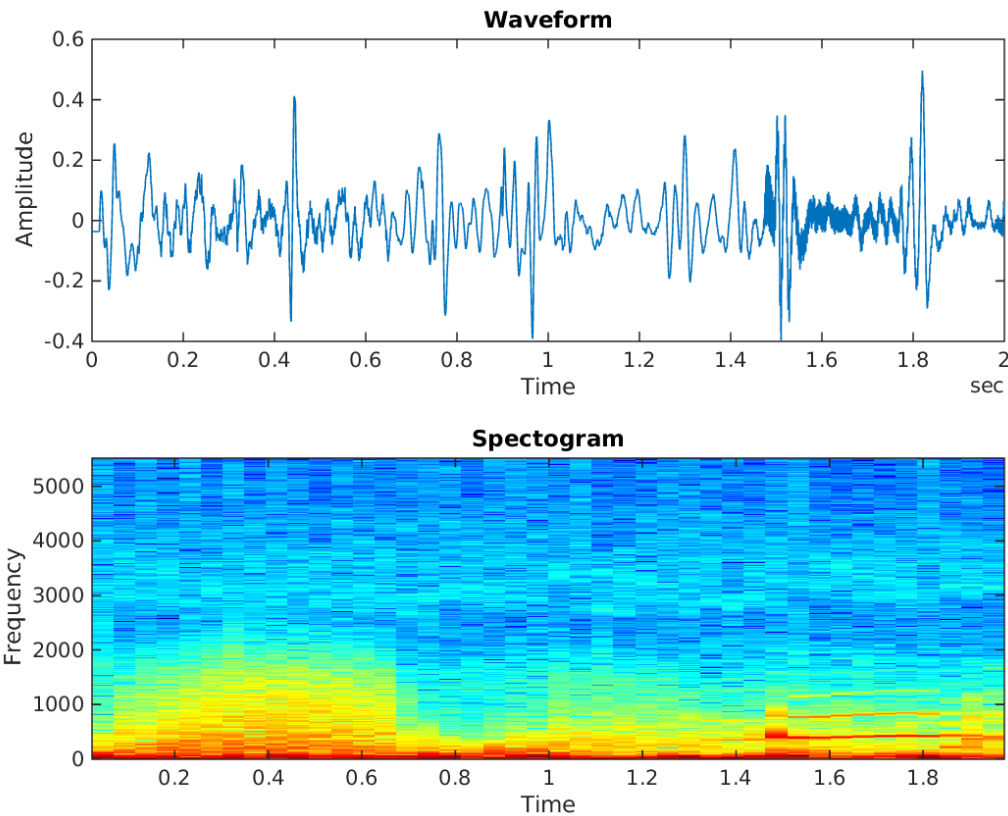


Figure 3.5. Wheezes sounds waveform

3.2.2.4. Stridor

Stridor is a loud, high-pitched abnormal respiratory sound. Stridor is known as creaking or grating noise, too. Its tonal characteristics are extremely musical. It is a wheezing that tends to be formed from the trachea or larynx demanding on morphological or dynamic obstructions in the air flow at very high levels. It is a type of intermediate lung sounds that can be characterized in frequency spectra over 1000 Hz (Loudon and Murphy, 1984; McGee, 2012). The waveform and spectrogram of the stridor is seen in Figure 3.6.

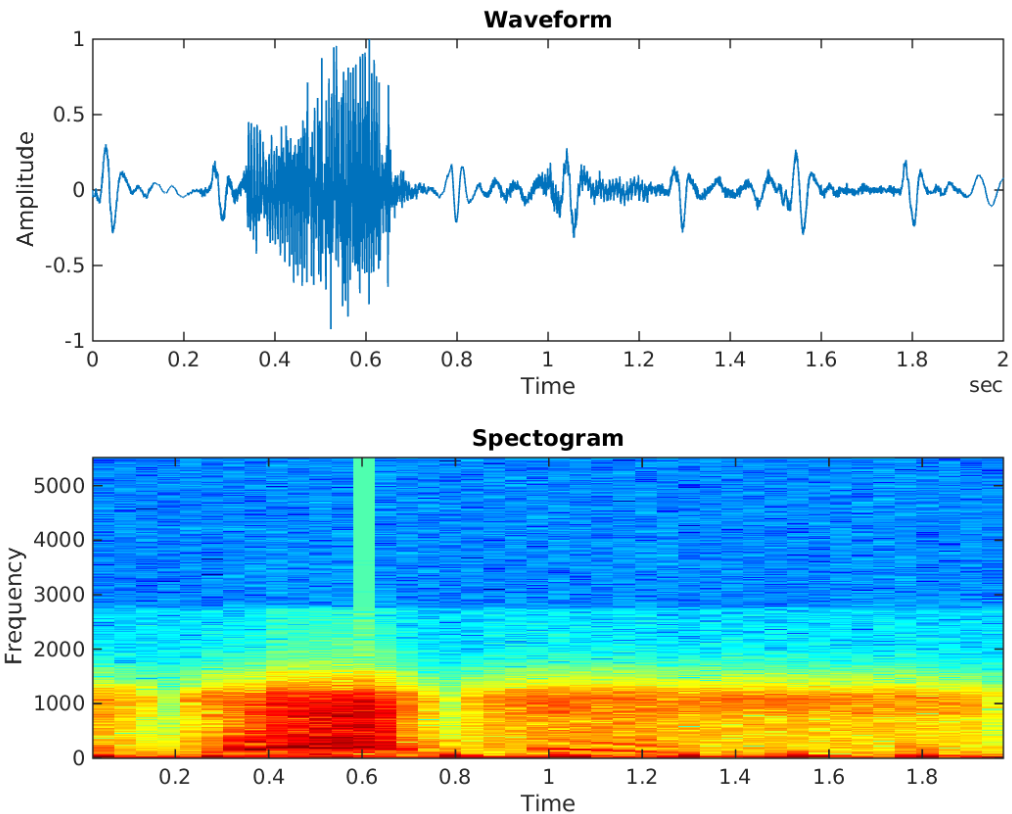


Figure 3.6. Stridor sounds waveform

3.2.2.5. Squawks

It is short breathing wheezing that occurs as a result of limiting lung diseases such as inflammation and fibrosis. Squawks are heard during the rales and sometimes at the beginning of the rale sounds. Its duration rarely exceeds 400 milliseconds and a frequency between 200 and 800Hz. It takes form as the vibrations that occur as a result of sudden pressure changes in small airways, such as crackles (Pasterkamp et al., 1997). Such breath sounds can be considered as a combination of crackle lung sounds and wheeze lung sounds (Kraman, 1993). The waveform and spectrogram of the squawks is seen in Figure 3.7.

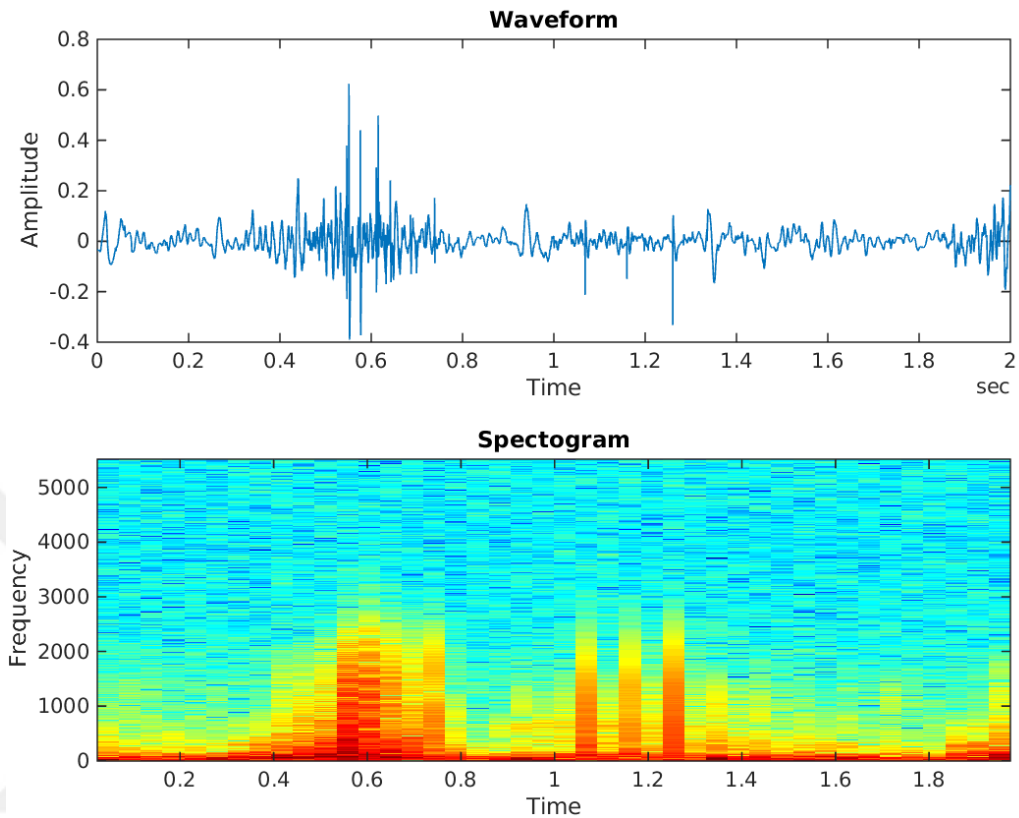


Figure 3.7. Squawk sounds waveform

All abnormal lung sounds are used in the diagnosis and control of different pulmonary and cardiac diseases as shown in Table 3.1. The fact that detecting and successfully classification process of the abnormal lung sounds, reducing the diagnosis time to minimum and early starting for the treatment have undeniable importance.

Respiratory sounds may have different acoustic characteristics depending on the health status of the patient, the position of the patient during the auscultation procedure, the environmental insulation, the respiratory flow, respiratory rate and the physical condition. In the light of these characteristics, certain standardizations were defined for the recording of the auscultation of respiratory sounds. In view of the fact that studies recorded the respiratory sounds with some standards to prevent the involutions in respiratory databases, most of them based on the CORSA (Sovijärvi et al., 2000) and ASAP (Reichert et al., 2009) standardizations during the recording process of the auscultation. Currently, pulmonary disorders take the first places in the list of most deadly diseases in the world.

Lowering the living standards of the people, millions of people losing their lives demanding to respiratory diseases are indications of the need for faithful, convenient and usable researches and productions in the fields of clinical support systems and decision support systems to diagnose respiratory and cardio-respiratory diseases. The first step in achieving this aim is the development of computer-assisted breath sounds analysis techniques and the implementation of a rapid and general diagnosis and treatment systems by applying it to different populations.

Table 3.1. Abnormal respiratory sounds and possible diseases with the lung sound types

Abnormal Lung Sound	Possible Diagnosis
Crackles	Alveolitis, pulmonary fibrosis, pneumonia, asbestosis, chronic bronchitis, bronchiectasis, congestive heart failure
Wheezes	Obstructive pulmonary disorders (e.g. asthma), cystic fibrosis
Stridor	Laryngitis, anatomical hypothesis, laryngeal disturbances, phono phobia, airway inflammation, tumors, tracheal narrowing
Squawks	Allergic inflammation, pulmonary fibrosis, interstitial fibrosis
Rhonchi	Tumors, pneumonia, chronic obstructive pulmonary disorders (COPD)

In the respiratory systems, there is a wide range of normal and abnormal respiratory sounds with typical characteristics for pathological changes in the waveforms or respiratory diseases. The analysing ability of the acoustic patterns in respiratory sounds will improve the learning of pathological and physiological findings about pulmonary disorders. Advancing the analysing methods and productions of medical devices for clinical evaluation will take advantage in the diagnosis and early diagnosis of respiratory diseases and will minimize the dependence on Chest and heart diseases specialists. Because of the requirements in respiratory diseases and the integration of the machine learning, data mining and signal processing and respiratory sounds is a wide profession that will be worked frequently for years.

3.3. Respiratory Diseases

Epidemiology is a science that examines on aspects affecting human life. The epidemiology is a Greek words association of the epi (about), demios (humanity) and logia (science). Therefore, it is accepted as a principle that focuses on the distribution, spreading of the diseases in human society and the factors affecting the distributions. The aims of epidemiology are recognizing and explaining disease aetiologies and their reasons, and taking necessary preventive and therapeutic precautions to ensure the control and eradication of diseases in the human society (Gülesen, 2003).

3.3.1. Chronic Obstructive Pulmonary Disease

The information obtained from epidemiological studies on the COPD has helped to understand the disease more clearly and to identify risk factors. In this regard, Fletcher and Peto (1977) performed an initiator study by monitoring 792 patients aged between 30 and 59 years for eight years. It was reported that smokers had a rapid decreasing in FEV1 measurement in the course of the monitoring process, and the subjects had clinically significant airway stiffness.

In the past, uncertainties in the definition of the COPD have strengthened the assessment of prevalence morbidity and mortality of the disease. The estimations of the COPD frequency, asymmetric criteria that may lead to misclassification of airway obstruction during the PFT, variability of bronchodilators taken before or after evaluation of spirometry quality have usually resulted in misleading measurements and evaluations (Vogelmeier et al., 2017).

Despite all these confounding factors, there is a general consensus that the COPD morbidity and mortality have increased over the past 30 years (WHO, 2016). The most important reason for the increase in COPD frequency and the widespread deaths is likely to be the smoking epidemic in the community and the elderly patient's population (Sonia, 2008). Air pollution causing from biomass fuel use, not just smoking, has been identified as a risk factor for the frequency of the COPD (GOLD, 2016).

In recent years, the COPD is regarded as a preventable, controlled disease. It is a consequence of the limitation on the progressive airflow and the obstruction and destruction of mainly small airways. The airways and alveoli of the healthy and COPD subjects are demonstrated in Figure 3.8. Early diagnosis of the disease, quitting of smoking in early severity and removal of other risk factors are also effective in preventing the progression of the disease. The COPD, which negatively affects the quality of life during periods of exacerbations, can be directed to the stabilized course through appropriate treatment methods. The PFT alone is not considered adequate for the COPD severity assessment and diagnosis of the COPD due to other inflammatory conditions that the patient may have (Sharon, 2011). Due to the complexity of determining airway obstruction, the COPD remains a misdiagnosed or undiagnosed condition in many countries (Kaya et al., 2010).

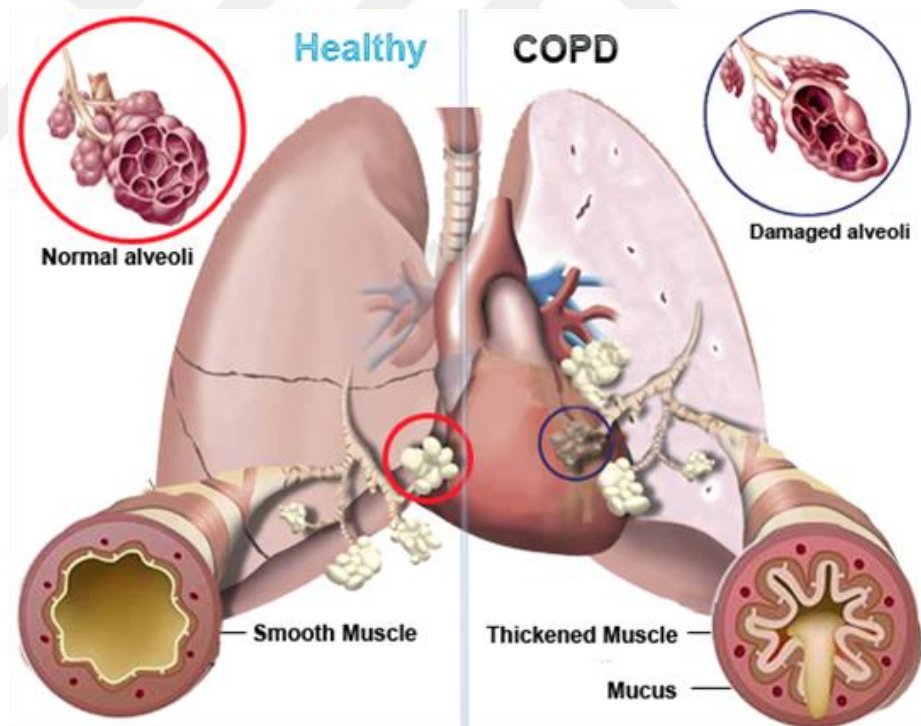


Figure 3.8. The airways and alveoli patterns of lungs of healthy and COPD subjects

The researchers have utilized extreme smoking, living in rural areas, over aging, lower body mass indexes, lung problems in childhood, socioeconomic conditions,

hereditary disorders, working in occupations exposed to smoke, organic and inorganic dust, exposing to environmental influences as the risk factors. It was determined that the risk of the COPD progression in smokers is 30x higher than non-smokers (Kaya et al., 2010).

Respiratory disorders exposed during infancy can lead to low function of the lungs in adulthood. In healthy individuals, FEV1 measurement increases until adolescence, stabilizes between 12-35 years (plateau period), and decreases after 35 years. The individuals with high risk factors of the COPD has associated with an inadequate FEV1 increasing in childhood, low levels in the adolescent period with symptoms such as an early onset of FEV1 decreasing in the plateau period, and accelerated decreasing of FEV1 measurements in adulthood (Günen et al., 2008).

The COPD has five severities according to air capacity and functionality of the lungs during the PFT. The FEV, FVC measurements and the symptoms are utilized to determine the severities. The severity of COPD and symptoms for each level according to standardized measurements are described in (Roisin, 2016) and are come at Table 3.2.

Table 3.2. The COPD severities and symptoms according to level

Severity	Symptoms
COPD0: Under Risk	*PFT normal *Chronic symptoms (a bad or persistent cough, sputum)
COPD1: Mild Level	*FEV1/FVC < %70 *FEV1 \geq %80 *Have/not have chronic symptoms
COPD2: Moderate Level	*FEV1/FVC < %70 * %50 < FEV1 < %80 * Have/not have chronic symptoms
COPD3: Severe Level	* FEV1/FVC < %70 * %30 < FEV1 < %50 * Have/not have chronic symptoms
COPD4: Very Severe Level	* FEV1/FVC < %70 * FEV1 < %30 or FEV1 < %50 * Chronic respiratory failure

3.4. RespiratoryDatabase@TR

RespiratoryDatabase@TR is a multimedia respiratory database that consists of digitized auscultation sounds, chest X-rays, questionnaire answers, PFT measurements (Altan et al., 2017). A computer-assisted medical interface is frequently selected analysis method with the developments on the technology and biomedicine. The CMI enables handling clinical assessments, constructing clinical tests and test results, analysing the clinical results, and recounting detailed characteristics for clinical expertise. Additively to its accomplishments, the developments on the CMI has concentrated upon composing large patient cloud by accessing the patients' data and diagnostic information of chronic and genetic disorders without using temporary laboratory tests, spending much time, repeatable physical examinations. The CMI has safety measures ability to reach clinical history of patients such as permanent medicine, X-rays, ECG, and the auscultation sounds to help in the assessments of the patients direct for the physicians. The patients take an opportunity to be controlled by various physicians for various disorders at the same time. The CMI enables interaction between physicians and the patient using personal computer, medical instrument, software, or complex diagnostic devices. Contemporarily, the udbredt of the CMI does not limit the physicians, also allows receiving opinions from other specialists, saving diagnosis time, early starting to treatment and controlling of the diseases using mobile sensors on smart phones, and also wearable devices on anywhere.

Meanwhile clinical data have been used as high accurate of tracking devices using nanotechnology health sensors, various disciplines such as biomedicine and medical still need expert specialists. Intensive researches in medical departments should be advanced for reducing the dependence to specialists throughout diagnosis and treatment processes of the diseases. The assessing capacity on auscultation sounds demands on designating significant characteristics that cannot be expressed by patient-self applying. The variety of the auscultation areas, anatomy knowledge of inner body, and physical specifications, and posterior auscultation of lung sounds avoids self-auscultation. Especially, lung and heart auscultation demands specialists, expert personnel or specific wearable devices.

The budget which is reserved medicine has the vast majority position in the prevention and treatment of the diseases. The treatment methods concentrated on the pharmaceutical studies between 1980 and 2000; diagnostic models, prevention approaches, wearable monitoring systems were studied between 2000 and 2015. Fast and accurate developments of health technology generated a steady fact that many approaches shaped innovations for health contemporarily. In the next years, disciplines for advancing wearable health tracking technologies, telemedicine platforms, mobile capability platforms and patient monitoring will take a large place in the early diagnosis, controlling and treatment processes. The big data and cloud ideas on diseases have the biggest and favourite sharing in the transfer of biomedical signals that will be stored for various diseases.

The most consequential point of the health policy is providing healthy society, obviating the diseases, early diagnosing genetic disorders and keeping the disorders under control. Pulmonary diseases are met as a result of environmental factors such as air pollution, smoking, genetic factors, old age, sex, infections, seasonal change, and occupational cases. The most common respiratory diseases are asthma, bronchitis, COPD, lower respiratory tract infections. Some respiratory diseases have actuality with symptoms of the end-stage attacks, infections, seasonal outcome and treatable characteristic, but some are genetic disorders which are not curable and just can be kept under control in the existent severity (Troosters et al, 2005). Considering the recent researches in 2016, lower respiratory tract infection such as bronchitis, pneumonia is the most dangerous pulmonary disease with 3.2 million deaths and an incident of 291 million occurrences. The COPD takes the second place with 3.19 million death and incident of 174.5 million occurrences (GBD, 2016). The high prevalent ranges of the respiratory diseases indicate the necessity for research on controlling the diagnosis and classification models. Although most of the respiratory diseases also treat lower respiratory tract infections are curable and preventable diseases, on contrary no cure has yet been invented for the COPD. The COPD is only preventable and controllable in a severity. That is why early diagnosis of the COPD and early severity identification has great importance for preventing death incidents from respiratory diseases. The COPD is encountered with the people who are over 35 years old, are/were smokers, live in polluted environments. Thereupon the COPD, the lung loses its

elasticity, thickening of the texture and inflammation in the airways is seen. The symptoms of the COPD demand on the severity, but usually increasing level of short breathing, frequently coughing crises, losing self-care skills and wheezing (Decramer et al, 2012). It comes by advanced severities of both the asthmatic and bronchitis symptoms. Therefore, the COPD is not described by a single symptom and has 5 severities (COPD0, COPD1, COPD2, COPD3, and COPD4) for the diagnosis and treatment processes. Analysing the various respiratory tests, effort breathing tests, pulmonary function test, X-rays, clinical examinations, and other symptoms is all-important for enabling the diagnosis of respiratory diseases without assessments of the patient's self-management skills (Troosters et al., 2005). After posterior and anterior auscultation by pulmonary specialists, the SGRQ-C questionnaire, PFT, chest X-ray, and different assays helps to assessments of impacts in the definitive severity controlling of the COPD. The novel signal analysing models on auscultation sounds are great necessities to ensure the steady, split and deterministic recognition regardless of the clinical processes. The scheme of data acquisition process for the RespiratoryDatabase@TR is seen in Figure 3.10.

The deficiencies of computerized analysis on respiratory diseases are accessing respiratory databases and criterion standards during auscultation. The identification of the robust types and detection of the various abnormalities on the biomedical signals are possible with open-access databases such ECG databases that consist of labelled heart diseases, cardiac abnormalities; specific EEG databases that are recorded for analysis of neurological diseases and human-computer interfaces; image databases that focus on the dermatological diseases, texture and pattern abnormalities. But the respiratory sounds databases are in commercial use and are based on wheezing detection and limited number of respiratory diseases. This is an impediment for increasing analysing capability of the CMI for upgrading diagnosis and assessment methods on respiratory and cardiopulmonary diseases. Adequate severity of researches and databases on respiratory sounds are not enough for shedding the respiratory diseases from the deadliest lists and increasing capability of newly developed and effective diagnosis models. Taking into consideration to research deficiencies and limitations of the respiratory databases, acquisition of a

respiratory database that consists of the most deadly diseases such as the COPD and detailed severities of the COPD is required to improve signal processing approaches.

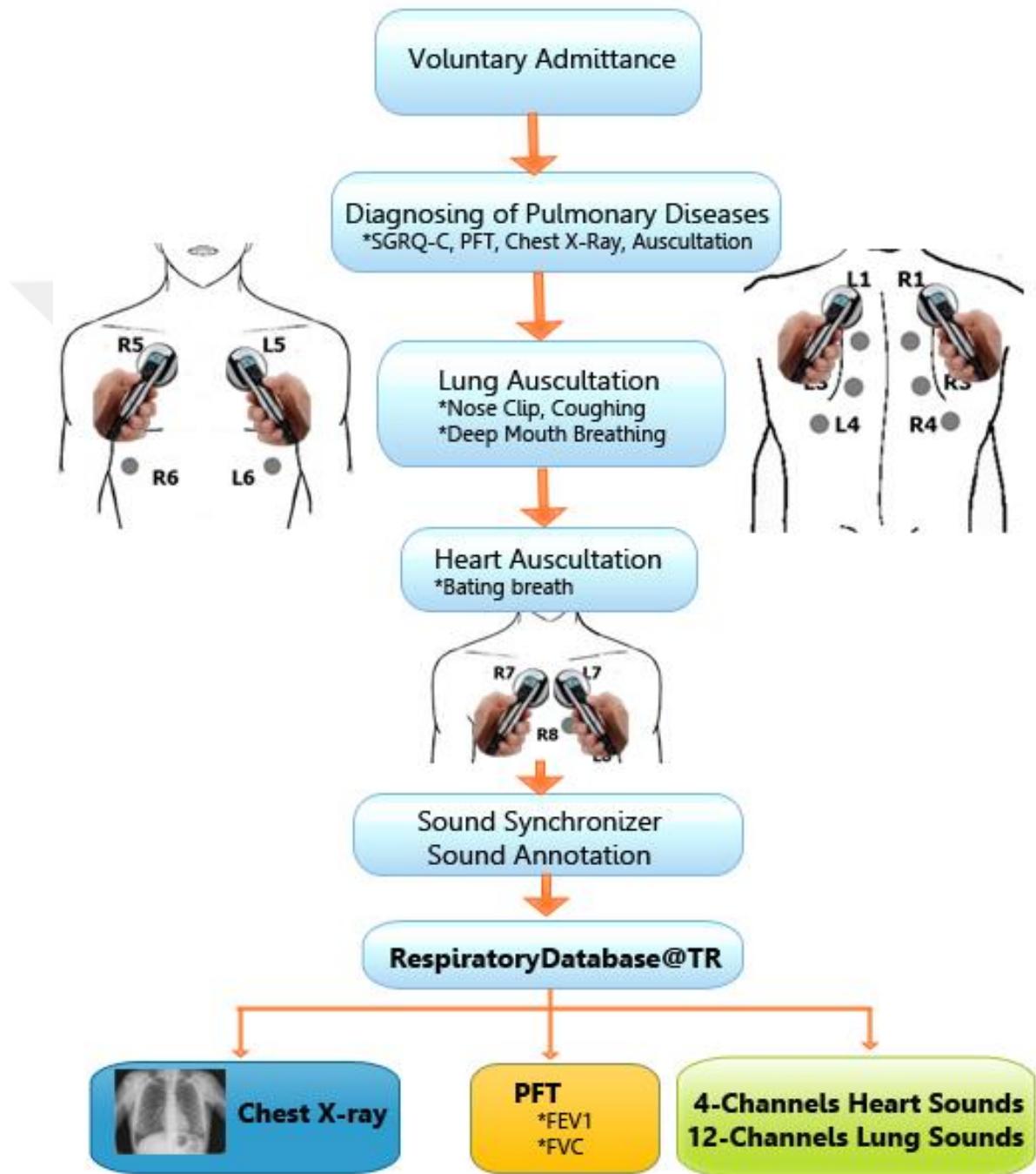


Figure 3.9. The model of RespiratoryDatabase@TR

Collecting a respiratory database is an important inception for composing health care systems, debugging effective and functional graphical user interfaces, tagging specific abnormalities types such as crackle and wheezing, particularization of auscultation sounds and imaging informs, the visualization of hard to hear adventitious sounds with ease of use. Since therefore, the clinical history of patients ensured by various clinical tests can be made ready to analyse in an accessible platform, the pursuance of further monitoring and advancing the severities will be huge pension facility for specialists.

People have a unique metabolisms and as a consequence of unique reactions to treatment processes. This case results with a big variety of durational times for treatments, actions, indications and treatments for patients. Even respiratory disease has variable symptoms according to subjects. A respiratory database with auscultation sounds affects positively the treatment process. Detecting the abnormalities in early stages without expert skills and specialists is possible for CMI. The lung sounds, detected abnormalities, classified wheezing, crackles throughout breathing attacks, clinical assessments, PFT measures, and chest X-rays will gain edge for clinicians and pulmonologist specialists during the patient specific monitoring, early managing of treatments. The aforementioned advantages gain a significant quality in the durational differences, evolutionary capability on the treatment and computerized diagnosis of the chronic diseases. Such a CMI system, which can be accessed online, saves time in clinical examinations for different pulmonologist specialists, as well as, it reduces national economic savings on medicine found by preventing multiplied necessity of X-rays, clinical analysis, PFT, and more. Regardless of the fact that X-rays are low-dose electromagnetic radiation, people can be affected by this dose of radiation when it is applied sequentially. The CMI systems with respiratory multimedia database may prevent harmful effects for human health.

The designed CMI provides a detailed controlling facility for assessing the aspect of obstructions, fluid accumulation, and constrictions in the airways for the respiratory diseases. The chest X-rays also enables to comment on heart vessels such as embolism on the grounds of including heart in the frame for cardiovascular and cardiopulmonary diseases.

3.4.1. Pulmonary Function Test

A PFT is an easy, economical way to criterion the airing capacity and functionality of the lungs using spirometers. When applying the PFT, the air volume in inspiration is measured by the air flow rate, afterwards the airflow rate in the expiration during breathing process. The measured airflow rates are the most common variables in diagnosis of severity, keeping track of disease complexion, and assessing treatment effects (Vaz Fragoso et al., 2010). Air capacity during the inspiration and expiration is amounted at rest; the measurements are utilized to find similarities and differences between healthy and diseased people among the similar ranges of physical trait and sex for assessment of the lung function.



Figure 3.10. Pulmonary Function Test Scenario (COSMED, 2018)

When the lungs reached full capacity, FEV1 (Forced expiratory volume) is the maximum air volume in expiration for the first 1 second. The amount of air volume discharged in inspiration during forced expiratory skills is called as FVC (Forced Vital Capacity). FEV1, FVC, and FEV1/FVC (Tiffeneau-Pinelli index) measurements for respiratory are vital values in diagnosis, severity classification and assessment processes of

the pulmonary disorders (Salvi and Barnes, 2009; Vaz Fragoso et al., 2010). The PFT measurements and the functionality curves are depicted in Figure 3.11.

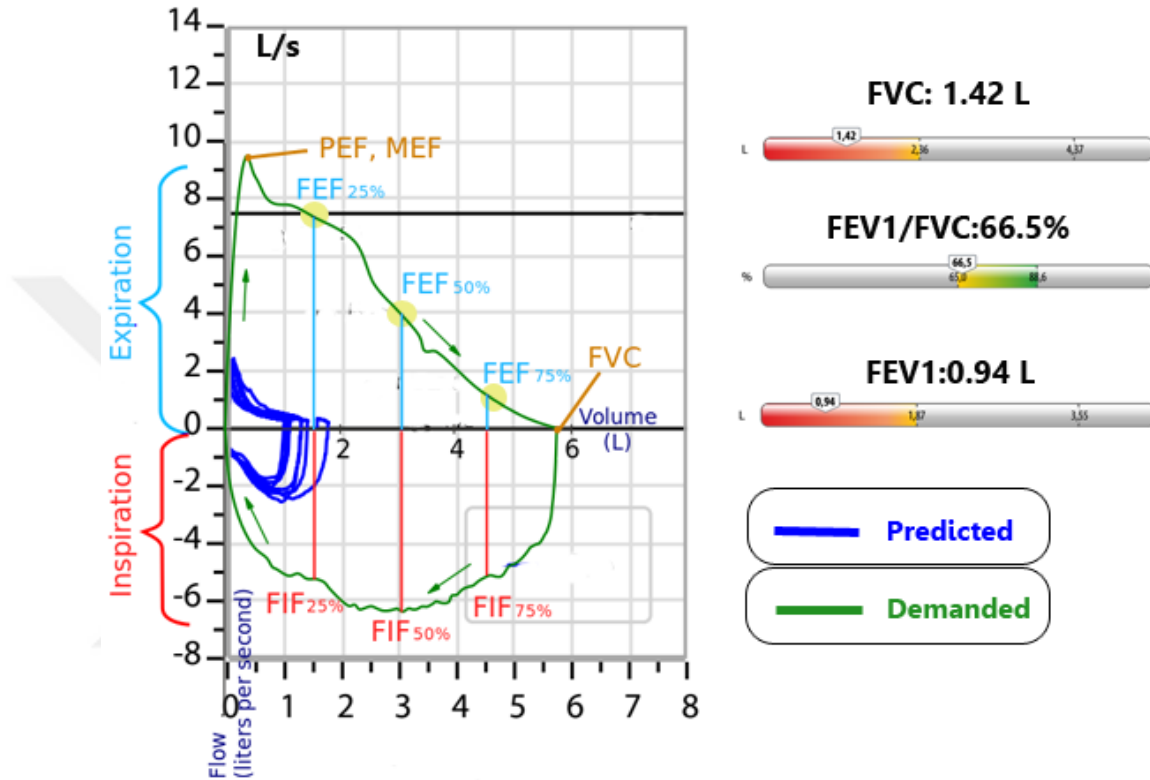


Figure 3.11. Pulmonary Function Test Curves belong to a COPD patient

The subjects were instructed about how they must breathe in and out and inflate procedure before applying the PFT. No bronchodilator medicine was received. The volunteer was forced to perform breathing by mouth by the help of closing the nose with a nasal plug during the PFT as seen in Figure 3.12. The mouthpieces for the PFT tool are used once and then discarded for every patient to isolate infectious diseases. Attach importance to maintaining the lips closed for measuring accurate PFT. The subjects were asked for force, deep breathing in and out for at least 5 seconds. The pick points of the routine are marked as PFT measurements. The achieved PFT measurements can be attached and input to the designed CMI using the PFT module.

3.4.2. Auscultation Scenario

The auscultation is still effective and cannot be abandoned method for the clinicians to diagnose cardio-pulmonary disorders. In recent years, deeply reliable systems are needed in the management of robust and painstaking diagnosis for disorders. The assessment difficulties on the adventitious lung sounds have increased the importance of using the computer-aided analysis methods. Analysis of the respiratory sounds helps the clinicians and specialists make objective, stable, reliable and detailed diagnosing with the integration of digital signal processing algorithms and the machine learning algorithms. Despite the continuous technological incomes in respiratory diseases, the must-have diagnostic tool is stethoscope that still works with primitive principles. In spite of the fact that chest auscultation areas are established protocols by CORSA (Celli et al., 2004; Sovijärvi, 2000), different areas may be auscultated if the physicians estimate it necessary.

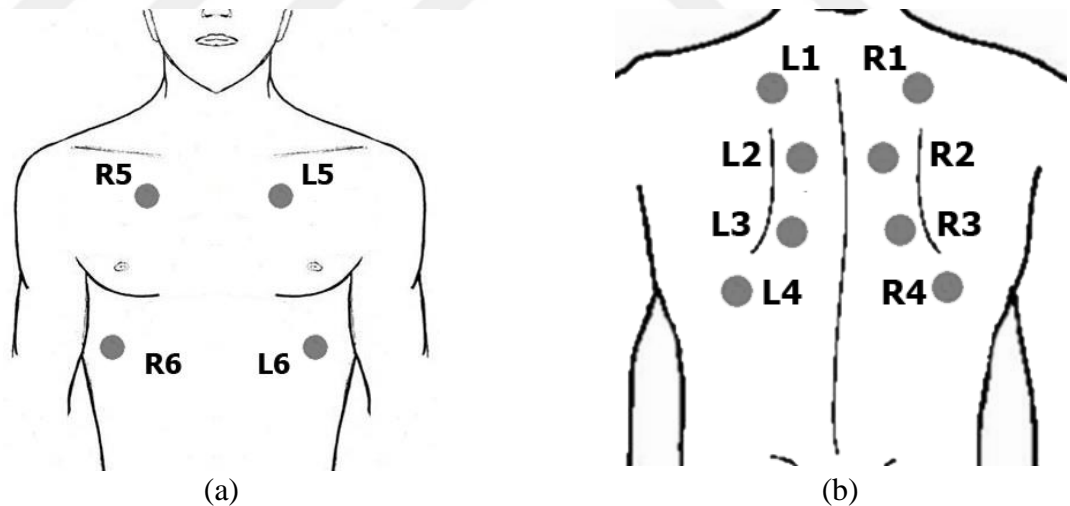


Figure 3.12. Lung auscultation areas on (a) anterior side and (b) posterior side

The thoracic areas such as left and right upper lung (L1, R1), left and right middle lung (L2, R2), left and right lower lung (L3, R3), and left and right costophrenic angle lung (L5, R5) for posterior side; left and right lower lung (L5, R5), and left and right lower lung (L6, R6) for anterior side of the patients. The lung auscultation areas which are labelled as (L) for left side and (R) for right side are indicated in Figure 3.13.

An auscultation room is divided from the clinic in the Hospital for isolating from external sounds, and is heated to adjust temperature, well lighted for making the patient feel comfortable in privacy. The subjects were in seated position when necessary auscultation sounds were recording. The aforementioned auscultation points with same identification number on left and right chest areas were auscultated utilizing two digital stethoscopes by pulmonologist specialist, synchronously (seen in Figure 3.14 and 3.15). The pulmonologist requested subjects not to speak, just deep breathing for 20s to avoid artificial sounds and noise on auscultation sounds. When the auscultation recording was begun, the subject was requested to cough once in the first 5s of auscultation, and deeply breathing from mouth in continuation until the pulmonologist finished auscultation.

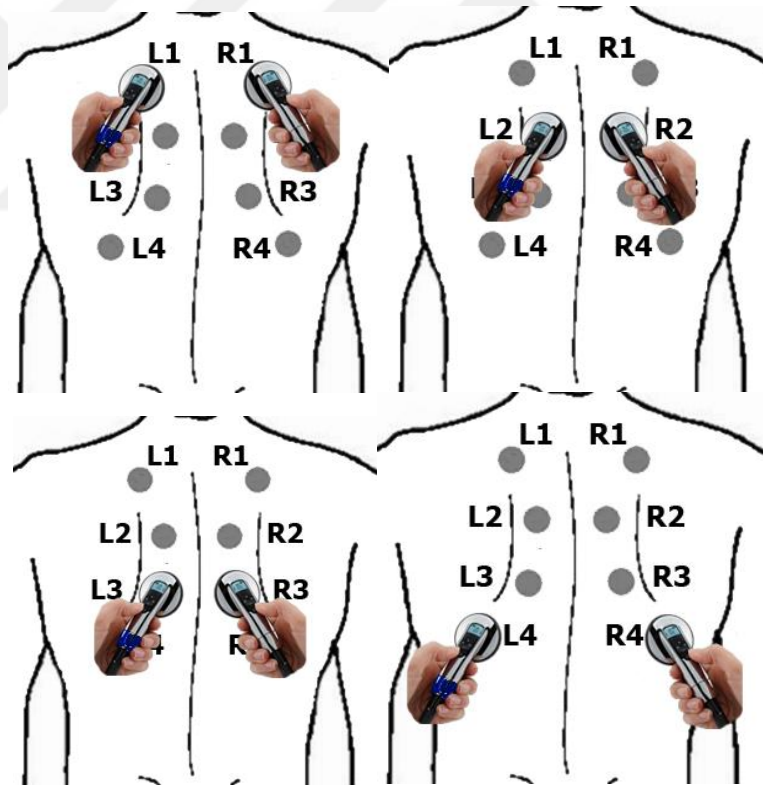


Figure 3.13. Lung Auscultation Scenarios for Posterior Side

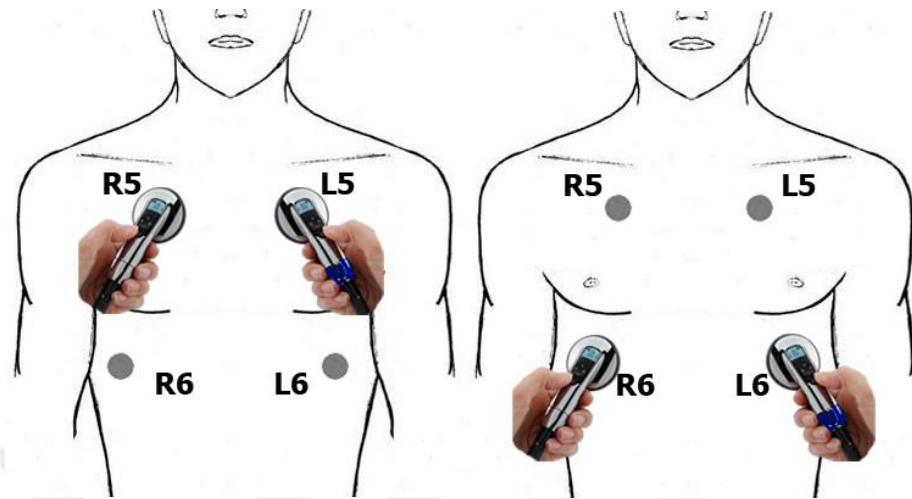


Figure 3.14. Lung Auscultation Scenarios for Anterior Side

Heart auscultation sounds were recorded from four areas: aortic (R7), pulmonic (L7), tricuspid (R8), and mitral (L8). The cardiac auscultation areas are indicated in Figure 3.16.

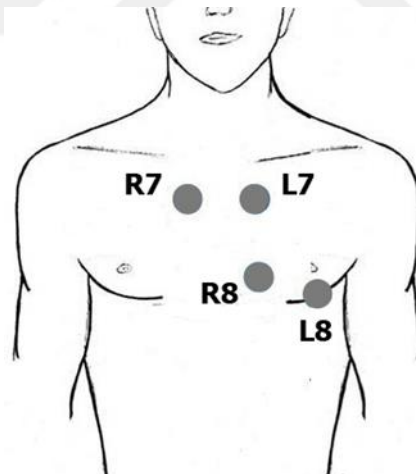


Figure 3.15. Heart auscultation areas

The inspiration and the expiration during heart auscultation gives a rise to failure on heart sounds with mix-up in breath sounds and to inaudibility because of increasing size of enlargement in the rib cage. Hence, the pulmonologist specialist asked the subjects coughing in the first 5s for the synchronization of the left and right cardiac areas, when the auscultation recording was started. The heart auscultation process is seen in Figure 3.17.

The subjects were requested bating breath to avert mix-ups and noise on the heart auscultation recordings.

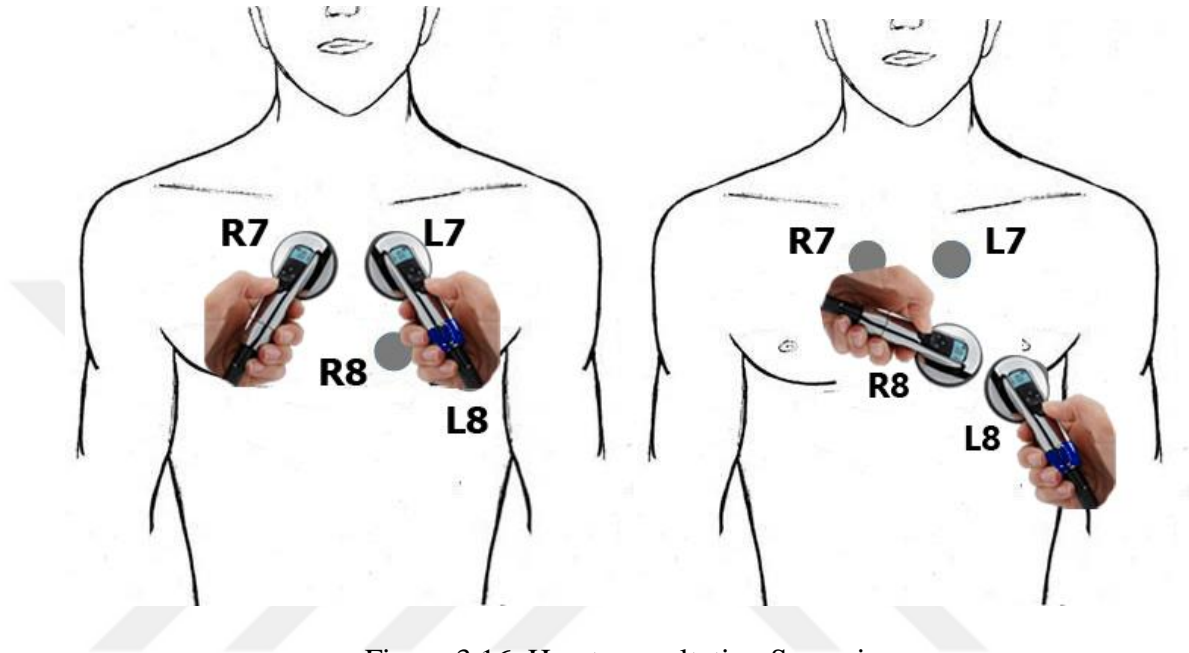


Figure 3.16. Heart auscultation Scenarios

The coughing in first 5s composes peaks in the auscultation sounds. The maximum peak was handled as the starting data point of the auscultation sounds to synchronize the parallel recordings from right and left digital stethoscopes. The recording was started over if auscultation recordings did not meet the requirements of the auscultation scenario. The designed CMI provides listening of recordings, point-based control, synchronization of two parallel records and visualization of the lung and heart sounds using a waveform plot.

3.4.3. Digitization of Auscultation Sounds

The various sensor based medical tools such as Piezoelectric microphone (Himeshima et al., 2012; Homs-Corbera et al., 2004; Matsutake et al., 2015; Umeki et al., 2015), LS-60 microphone (Waitman et al., 2000), electronic stethoscope (Dokur, 2009; Himeshima et al., 2012; Matsutake et al., 2015; Nakamura et al., 2016; Umeki et al., 2015) have been utilized in the computerization of the auscultation sounds. It is an obligation to

use sensitive microphones to hear and record short term and choked adventitious auscultation sounds such as crackles, wheezes and murmurs. The Littmann 3200 Electronic Stethoscopes were selected as the recording and auscultation tool in this thesis (Figure 3.18). The selected electronic stethoscope implements an average noise reduction of 75% (-12dB) with eliminating the external sounds and nearby organ sounds. It provides a filtering technology for three frequencies ranges (Bell, Diaphragm, and Extended) for adventitious auscultation sounds. The device can transfer data to the host via real time mode on serial communication protocol Bluetooth. It also has internal memory for storing 15 sounds and can transfer bulk auscultation sounds into host with Bluetooth ® communication. It takes role as a diagnostic assistant to perform operative telemedicine applications. It amplifies adventitious sounds up to 24x as against to acoustical stethoscopes. The frequency range filters are Bell (20-200 Hz), Diaphragm (100-500 Hz), and Extended (20-1000 Hz). The 16 channels of auscultation sounds are embedded into extensible mark-up language file with the zsa file extension. The file is comprised of all auscultation parameters, subject name and 16 auscultation sounds. The auscultation sounds in the zsa files had been converted to waveform audio file format (wav) with a sampling frequency of 4000 Hz using the Littmann API.



Figure 3.17. Littmann 3200 Digital Stethoscope

The database has been variegated with both lung and heart sounds from subjects with different severities of the COPD, asthma, chronic bronchitis and healthy subjects.

Volunteer admittance was signed on a voluntary basis form with minimal information. The patients aged 38 to 68 were selected from different occupational groups, socio-economic status, sexuality for skilful capability of the diseases. The database population consists of 13 female and 64 male subjects. Distribution of diseases in regard to sexuality and severities of diseases is shown in Table 3.3.

Table 3.3. Distribution of diseases according to sexuality

Diseases	#Records	Genders	
		Male	Female
Asthma	6	4	2
COPD0	5	4	1
COPD1	5	4	1
COPD2	7	7	-
COPD3	7	6	1
COPD4	17	13	4
Healthy	30	26	4
TOTAL	77	64	13

The COPD is not an idiopathic for specialists. The biggest factor for the COPD is extreme smoking for years. In the light of this artefact case, the healthy auscultation sounds had been chosen among subjects who have never smoked for achieving homogeneous and reliable database. It has been paying attention that healthy subjects had never been diagnosed a chronical lung dis-functionality. Considering genetic factor of the COPD and asthma, the subjects whose close relative has asthma or the COPD were not appended into the database group. The patient specific detailing and listening module of the designed CMI is depicted in Figure 3.19.

File
Functions

RESPIRATORY DATABASE

Records

H001_L

☒ Bell
☐ Diaphragm
☐ Extended

ID	Field Name	Sound Type
L1	Posterior- Upper Left Lung	Vesicular-Normal
L2	Posterior- Middle Left Lung	Crackles-Rales
L3	Posterior- Lower Left Lung	Wheeze
L4	Posterior- Left Costophrenic Angle	Rhonchi
L5	Anterior- Upper Left Lung	Bronchial
L6	Anterior- Lower Left Lung	Bronchovesicular
L7	Pulmonary Heart	Vesicular-Normal
L8	Mitral Heart	Crackles-Rales

Diagnose Phase
☐ COPD 0 ☐ COPD I ☐ COPD II ☒ COPD III ☐ COPD IV ☐ Healthy

Other Diseases
Diabetes, CHF

PatientID	Recording Time
H001_L	8.3.2017 11:09:36
H001_R	8.3.2017 11:09:52
H002_L	8.3.2017 11:10:07
H002_R	8.3.2017 11:10:21

Figure 3.18. Patient specific listening and detailing module of the CMI

A total number of 16-channels auscultation sounds including lung and heart sounds are recorded from 8 basic foci for right and left sides severally on subjects. All recordings were converted to 3 various frequency ranges using Bell, Diaphragm, and Extended filters. Each subject has 48 (8x2x3) auscultation sounds. If the entire database is taken into consideration, the total number of 3696 (77x48) auscultation sounds labelled as five different COPD severities, asthma and healthy subjects in the CMI auscultation sound module.

3.4.4.Sound Synchronizer

The left and right sides of body are auscultated, simultaneously. The synchronization is one of the most crucial processes that may cause the durational deviations of

milliseconds. The simultaneously recorded 2-channel auscultation sounds were synchronized using an indicator point to state the synchronizing data point for recordings. Setting one trig point as the beginning data point of the sounds by cropping the previous data points can manage the synchronization. The trig point can be marked with a soundless duration or a high noisy action such as superior pick that is consequence of coughing. The coughing in the first 5s is selected for the synchronizing the auscultation both lung and heart sounds in the acquisition stage of the RespiratoryDatabase@TR.

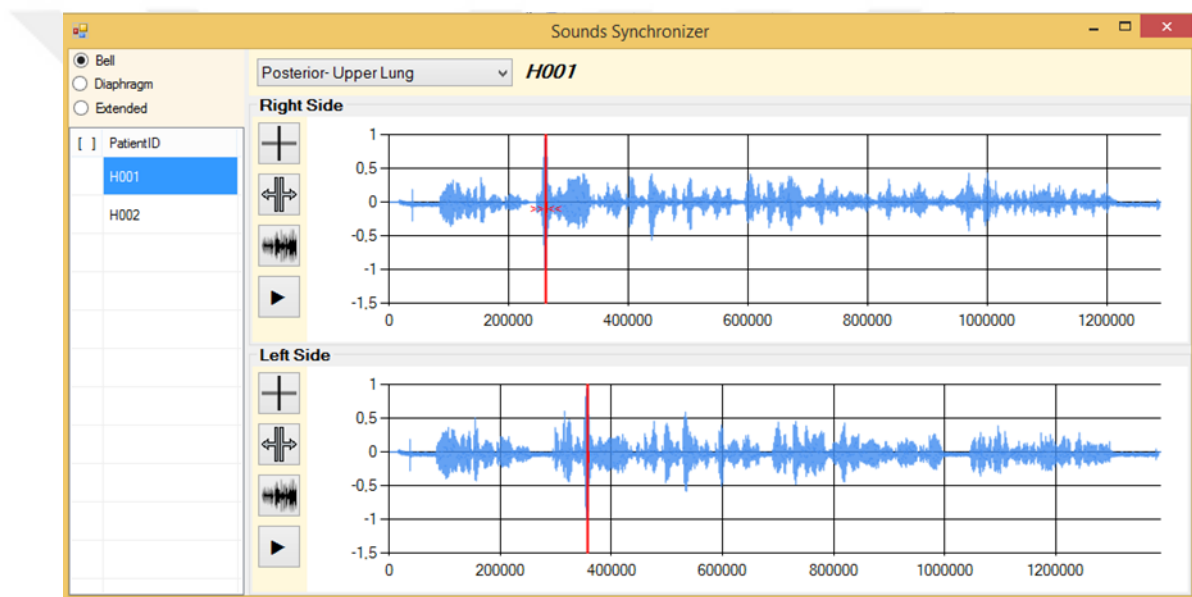


Figure 3.19. Sounds synchronization Module of the CMI

In the recording scenario of the RespiratoryDatabase@TR, the pulmonologist requested the subjects to cough in the first 5s and deep mouth breathing in the continuation of coughing. The coughing in the recording reasons an unexpected extreme peak in the auscultation sound. The selected auscultation sounds area in the comprised peak points can be discerned in definitive ranges of the sounds by the aid of the proposed CMI and can be stated using the annotation bar. In waveforms of both left and right auscultation sounds, the extreme peaks can be pointed out. Afterwards the annotation bars are placed at the higher peaks, synchronizer process is applied. The CMI module crops the previous data points and

sets the pointed annotation bar positions as the starting of the auscultated inner body sounds in interface module. The view of the module is indicated in Figure 3.20.

3.4.5.Sound Annotation

The auscultation sounds may have unlike characteristics in inhalation and exhalation, certainly. Abnormal sounds such as crackle and wheezing sounds may occur for short cycles during both inspiration and expiration. In some instances, they can be heard only in inspiration duration, or only one type of the pathological sounds is heard. For as much as unexpected occurrence in abnormal auscultation sounds, independent characteristics demand on the areal labelling for the identical selection of murmur on hearth sounds, crackle and wheezing sounds on the lung sounds.

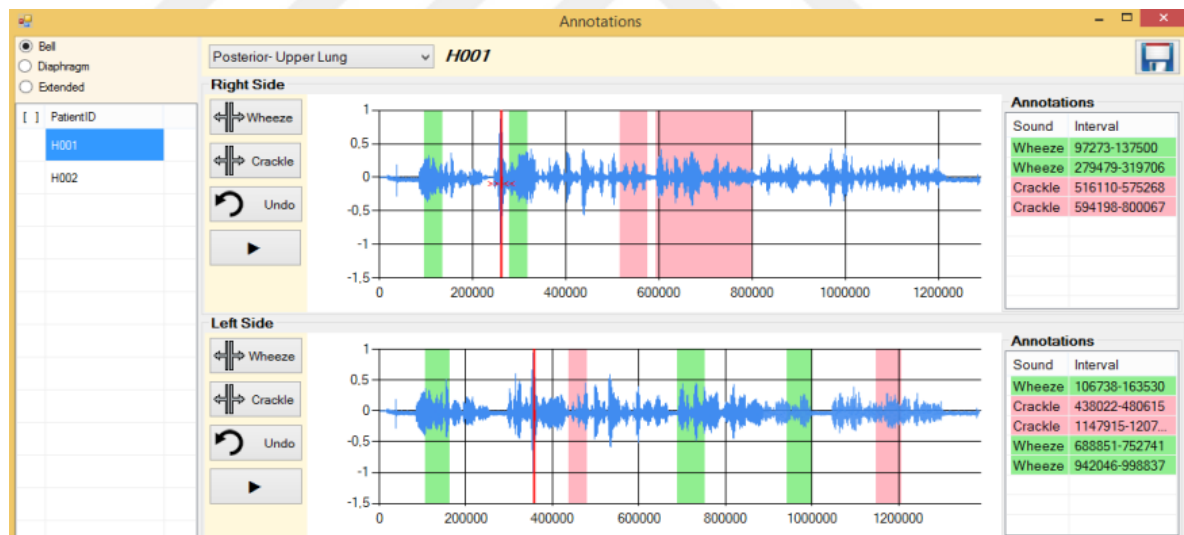


Figure 3.20. Auscultation Sounds Annotation Module of the CMI

The patient-based labelled auscultation annotations can be re-listened and can be analysed at different frequency ranges on the annotation module. On patient-based auscultation areas, the sounds can be annotated for adventitious wheezing and crackle types can be marked regionally. The time variables at the annotated regions are utilized to mark the waveforms and are stored in the system database for each auscultation areas. The

annotated regions can be re-listened merely, by getting rid of normal areas on respiratory sounds. The view of annotation module is indicated in Fig. 3.21.

3.4.6. Significance of RespiratoryDatabase@TR

Most of respiratory disorders are chronic seasonal affective disorders that need to be tracked and kept under control. The RespiratoryDatabase@TR is designed to manage the requirements of respiratory and cardio-pulmonary diseases within the attacks. It consists of a unique auscultation and pulmonary multimedia data which enables analysing capacity to diagnose the lungs and the heart diseases. It is composed of digitized auscultation sounds from 16 of different channels synchronized for left and right sides, a distributable CMI that is user friendly for labelling on analysis, the PFT measurements and chest X-rays.

The COPD has no healing process and no cure at the severe levels. On the account of it is an uncomfortable social position for both physicians and subjects with tough managing routines, early diagnosis and treatment of the COPD and the severity of the COPD have a vital significance to prevent disease progression at early severities by holding on leash. The COPD and asthma need routine check. The previous treatments, medicine history, and the attacks on the seasonal conditions affect the procedure on treatment, critically. On the ground that RespiratoryDatabase@TR is focused on chronic respiratory diseases, it prepares for major analysis capacity in advance by allowing the subjects to check against the symptoms of the severities with current states, concluding the scope of the treatment in a prosperous manner, and leading a constructive support for various disciplines in the course of diagnosis the severity on respiratory diseases.

The RespiratoryDatabase@TR is a rare database which includes chest X-rays, the PFT measurements, SGRQ-C questionnaire analysis, 16 channels of auscultation sounds, and also a CMI to prepare text, graphics, and sound signals for computer-aided analysis and labelling the sound types and disorders.

The PFT and chest X-rays are the fundamental diagnostics which are applied considering particular criterion throughout the world. Lung auscultation has not a protocol related to specific criterion, notably. However, auscultation areas that were utilized for

hearing purer and decisive respiratory sounds in the physical examinations, the CORSA standardizations (Sovijärvi et al., 2000) were handled as superior for peripheral and physical examination routines such as breathing skills in the data acquisition. Performing auscultation or physical examination with definite standardizations makes capable the RespiratoryDatabase@TR to be shared all over the world. The subject population can be intensified by expert physicians. Including chest X-ray, auscultation sounds, the PFT measurements, and a CMI with user friendly modules provides outstanding potential and profits in signal analysis applications and educational clinical skills.

Many lung sound analysing researches were based on classification of lung sounds from the healthy and pulmonary subjects or detecting pathologic lung sounds. One of the most hard to accept steps for the medical health estimation against engineering approaches is approving each patient as unique. The symptoms and treatment of the diseases are inconstant. It is essential that examining as many indications as possible during the diagnosis and managing processes of diseases. The RespiratoryDatabase@TR enables analysing chest X-ray, the PFT measurements, SGRQ-C questionnaire answers, digitized lung and heart sounds simultaneously for computer-aided approaches on respiratory, cardiovascular and cardiopulmonary diseases. Chronic respiratory diseases purpose to cardiovascular diseases in the advanced severities for aged patients. The RespiratoryDatabase@TR enables the estimations of heart and lung sounds together, and specifying of considerable amount for cardiopulmonary diseases. Likelihood of assessing the heart and lung sounds together gives occasion obtaining the connection between chronic respiratory diseases and cardiovascular diseases. In a different view, it paves the way for whether diagnosing and assessments on the chronic pulmonary diseases using only heart sounds or alternative multimedia respiratory data. Simultaneous analysis of heart sounds and lung sounds from 16-channels, and other RespiratoryDatabase@TR multimedia has made studying capable occasions to arrive more special functionality in the early diagnosis of cardio-pulmonary, cardiovascular and respiratory diseases.

The chest X-rays, PFT measurements, SGRQ-C questionnaire, and 16-channels of digitized auscultation sounds enable a particular estimation of the subjects and examining visceral sounds on 16 incompatible auscultation points. Analysing 16-channels biomedical

signals has a high capability for diagnosis models, because the digitized multimedia data can achieve higher accurate than analogue auscultation, and can be filtered in various frequency ranges. The auscultation module of the RespiratoryDatabase@TR has invariable recording standardizations for analogy of long-term estimations and can distribute interdisciplinary information among specialists for cardiologists, radiologists and pulmonologists specialists. The coded CMI allows an easy access patient-based respiratory multimedia data; it is reusable reproduced for many times with no decrement.

Digitized auscultation sounds provide quantization, visualization and analysis for diagnosis models and pointing out of similarities between current severity and preventable severities of respiratory diseases. Computerized biomedical signals enables the designing novel mathematical algorithms in the analysing of assorted pulmonary, cardiovascular and cardio-pulmonary diseases, severities of diseases. It also provides substructure for developing models on chest X-rays, researches on machine learning algorithms, clinical decision support systems, producing embedded systems to diagnostic tools. Considering that analysis of medical imaging is one of the most preferred disciplines, the RespiratoryDatabase@TR has a potential to be continually referred for obstructions and abnormalities detection in chest X-rays, beside the digitized auscultation sounds and the PFT measurements.

3.5. Feature Extraction

Digital Signal Processing has been a prominent approach for many disciplines of engineering sciences in order to evaluate the signal characteristics. For quite a long time now, the scientists have developed innumerable analysis methods, tools and mathematical models, such as Short-time Fourier Transform, Wavelet transform, and involution of them for extracting significant features and explaining the meaning of the characteristics in data processing discipline. The signal processing methods have been using almost in every step of everyday life such as researching areas, scientific problems, in mobile applications and are proved the usefulness in medicine, biomedical signal processing disciplines, communication systems, and more. The aims of the data analysis are defining time scale or

frequency, defining energy density, and defining joint frequency-energy distribution as a function of time.

3.5.1. Hilbert-Huang Transform

Non-stationary and nonlinear signal processing had long been a hindrance for scientific researches. The HHT is an adaptable and efficient transformation method to overcome the non-linearity and non-linearity signal problems. The HHT is a frequently-used method in the feature extraction, filtering the signals, basing the novel algorithms, and similar processes. The raising course on processing of non-stationary and non-linear signals has guided to occasions of the analysis capability to develop technical requirements (Huang and Shen, 2005). The HHT has a versatile and widespread mathematical model that can be taken into account in last decades. The HHT has been put into practice for lots of fields such as biomedical signal processing, communication systems, medical decision support systems and geophysics (Wu and Huang, 2009).

The mathematical formulation of the HHT algorithm could not be stated definitely and obviously, in the consequence of the flexibility of the stoppage criteria in HHT procedure (Attoh-Okine et al., 2008). The HHT consists of two-step analysis: Firstly Empirical Mode Decomposition (EMD), and subsequently the Hilbert Transform (HT) for analysing the appropriate signal in frequency domain. The EMD is overhead operation for the original signal to assay the time-domain features by sifting Intrinsic Mode Functions (IMF) and residual signal. Each IMF is a set of components which represents the frequency modulation of the input signal. The number of the IMFs are related to the oscillations in the signal. The HT implements extracting instantaneous frequency and amplitude amount of IMF at the time-frequency domain (Duman et al., 2012; Attoh-Okine et al., 2008). The HHT has ability to perform more definitive, discriminative and evident capability compared to the other methods in terms of time-frequency-energy characteristics for non-stationary and nonlinear signals (Altan et al., 2016).

3.5.1.1. Empirical Mode Decomposition

The EMD is a responsive transformation technique that is used for obtain significant information from non-linear and non-stationary signals. The most distinguishing quality of the EMD against to other transformations is the capability of generating self-distinct oscillations by adopting self-oscillations at unusual frequency ranges. Each self-oscillation is associated in a symmetrical manner to local mean of local minimum and local maximum extrema. Each different frequency oscillation is represented by an IMF. The IMF is sifted from the signal under the following circumstances are met (Huang et al., 1998; Attoh-Okine et al., 2008):

- I. The number of the local extrema and zero-crossing must be either equal or differ at most by one
- II. The symmetrical envelopes on upper and lower envelopes must be obtained at any t time

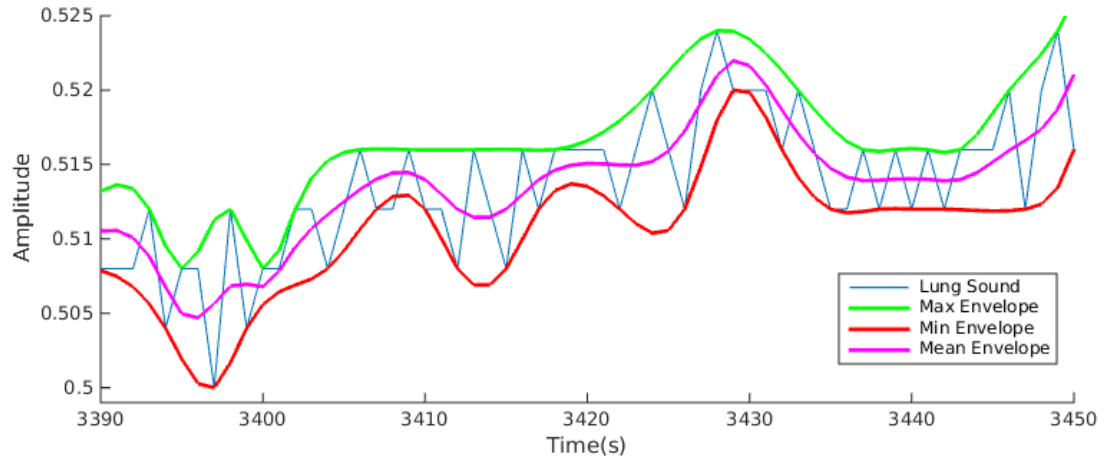


Figure 3.21. EMD process on a random part of lung sound

Aforementioned IMF extraction circumstances are used for avoiding negative frequency bands, and placing the instantaneous frequency value of small band width at the frequency band while calculating the instantaneous frequency information (Huang and Shen, 2005).

The EMD process starts with distinguishing all minimum extreme and maximum extreme and plotting spline of the envelopes with an interpolation function. The local mean curve is estimated averaging of the variable on the plot of minimum envelope and the maximum envelope (seen in Figure 3.22). The obtained local mean curve for the whole signal is sifted from the current form of signal. The new formed signal is checked if it meets with the IMF circumstances. If the new formed signal does not meet with the IMF circumstances, the local mean curve is iterated by utilizing the local maximum and local minimum envelopes of new formed signal. The sifting process continues until IMFs are extracted (Huang et al., 1998; Shukla et al., 2009).

The input signal is $x(t)$ and the mean curve is represented by $Mean_1$. The new form of the signal is difference between the current signal and $Mean_1$ is the first component C_1 .

$$C_1 = x(t) - Mean_1 \quad (3.1)$$

After the first cycle of the sifting process, the new formed signal may become a local maximum. In the following consecutive sifting process, C_1 can only be proceeding as a pre-IMF. In the next step, C_1 is tackled as the input signal, then

$$C_{11} = C_1 - Mean_{11} \quad (3.2)$$

After iterated sifting process up to k times, C_1 becomes an IMF, that is

$$C_{1k} = C_{1(k-1)} - Mean_{1k} \quad (3.3)$$

then it is extracted as the first IMF

$$IMF_1 = C_{1k} \quad (3.4)$$

The sifting process is ended with two ways. The first way is the stoppage criterion which is resolved by a Cauchy type of convergence test (Huang et al., 1998). When amount

of the SD_k of the signal is equal or smaller than pre-defined criteria, the sifting EMD is halted

$$SD_k = \frac{\sum_{t=0}^T |h_{k-1}(t) - h_k(t)|^2}{\sum_{t=0}^T h_k^2(t)} \quad (3.5)$$

The second way is defining a number which will be checked if the new formed signal has that the same number of zero-crossings and extrema, and differs at most by one.

When the IMF circumstances are met C_1 is identified as IMF_1 and can be separated from the rest of data by

$$r_1 = x(t) - IMF_1 \quad (3.6)$$

The residual signal (r) is established by subtraction of whole IMFs from the original signal.

$$r_n = r_{n-1} - IMF_n \quad (3.7)$$

When the new formed signal is a monotonic function which does not restrain riding waves or in other words it has only a local extreme, sifting IMF gets impossible and the EMD process is stopped (Duman et al., 2012). The extracted IMFs are depicted in Figure 3.23.

r_n represents for the last residual signal, $x(t)$ is the original signal, and n is the number of extracting the IMF processes.

$$x(t) = r_n(t) + \sum_{j=1}^n IMF_j(t) \quad (3.8)$$

Sincere performing of sifting process propagates mode mixing problems because of the IMF reparation. The sifting process end when the sub-signals meet monotonicity.

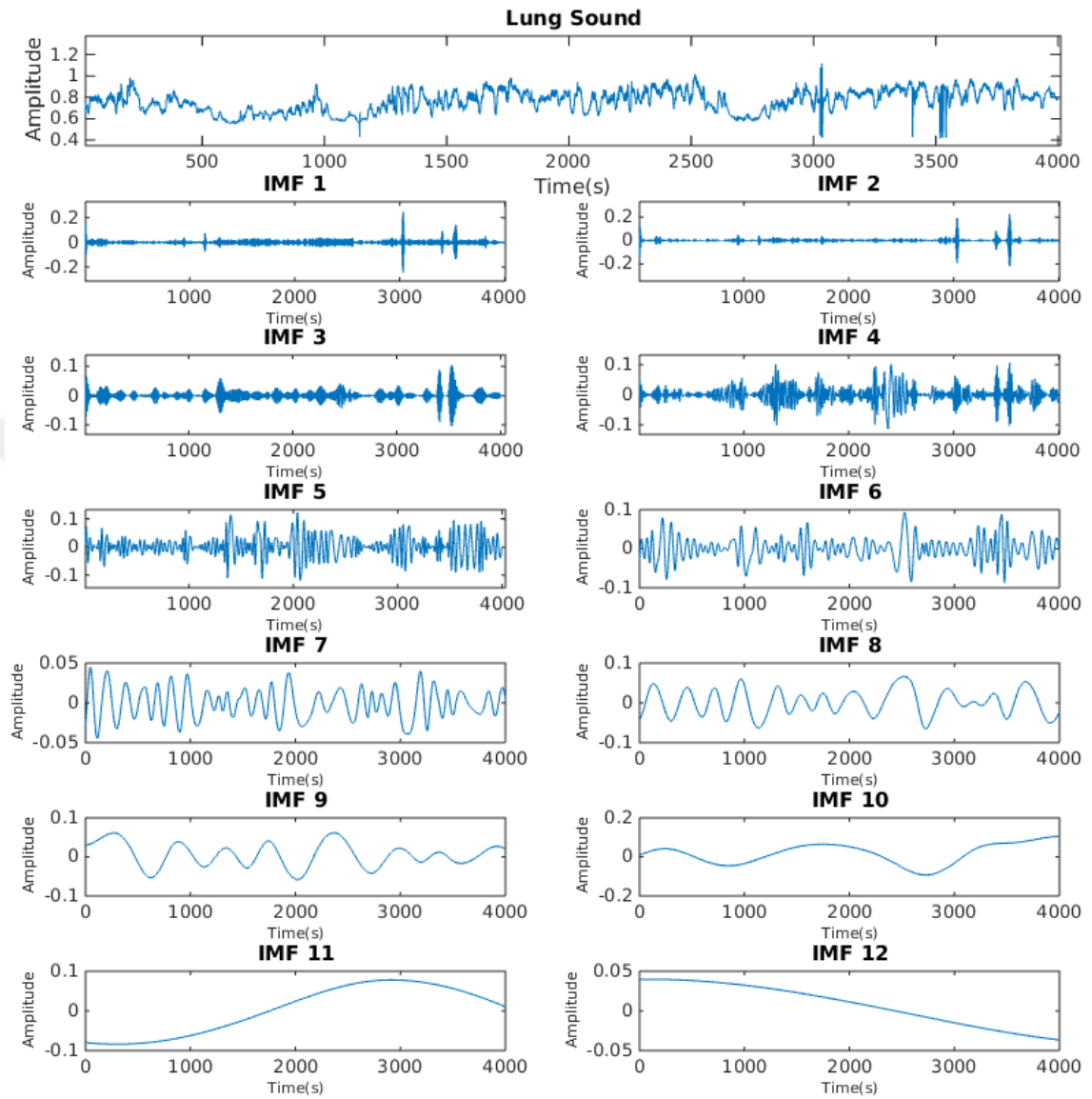


Figure 3.22. Extracted IMFs and the original lung signal

Various numbers of IMFs may be obtained for same original signal due to the intermittency at the high frequency, signal sacrifice, and noises in the EMD. The Ensemble EMD model is utilized to reduce the possible noises causing mode-mixing problem. The Ensemble EMD handles the mean of the successive IMFs that are extracted using traditional EMD by adding white noise series errors at each sifting of adaptively and particularly decomposition. An unequalled residual signal is estimated for extracting each

modulation. The Ensemble EMD model keep adding white noise series in as much as the IMF circumstances are met (Wu and Huang, 2009).

3.5.1.2. Hilbert Spectral Analysis

The non-linear signals have internal wave frequency modulations. The mentioned modulations are the fundamental and leading characteristics of the various signal types. These frequency modulations have the instantaneous frequency description in a single period. The HT is a decomposition technique that concludes the amplitude-frequency-time description of the given signal (Huang et al., 1998). The HT assays to represent non-stationary signal, locally. The formulation indicates the HT, $\hat{y}(t)$, PV denotes Cauchy's principle value integral.

$$H[x(t)] \equiv \hat{y}(t) = \frac{1}{\pi} V \int_{-\infty}^{\infty} \frac{X(\tau)}{t - \tau} d\tau \quad (3.9)$$

The analytic function with the HT is denoted as

$$z(t) = x(t) + i\hat{y}(t) = A(t)e^{i\theta(t)} \quad (3.10)$$

where

$$A(t) = \sqrt{x^2 + \hat{y}^2}, \theta(t) = \tan^{-1} \left(\frac{\hat{y}}{x} \right) \text{ and } i = \sqrt{-1} \quad (3.11)$$

$A(t)$ and $\theta(t)$ are the instantaneous amplitudes and phase functions, respectively. The instantaneous frequency can be indicated as the time derivative of the phase:

$$\omega = \frac{d\theta(t)}{dt} \quad (3.12)$$

The amplitude and the frequency modulations are also obviously sifted using IMF distribution. Therefore, the limitation of the stable amplitude and frequency representation of the Fourier distribution has been overcome using inconstant amplitude and frequency scales. The HT is basically utilized to extract the analytic representation of signal (Huang and Shen, 2005). Hilbert spectral analysis of the lung sound is plotted in Figure 3.24.

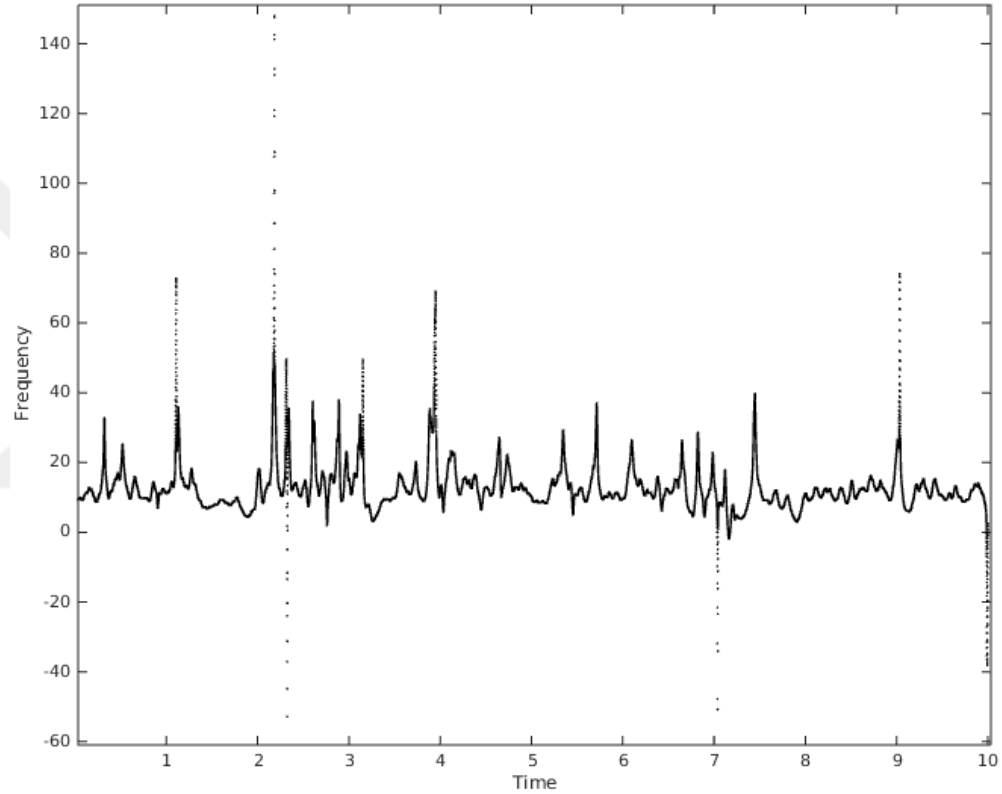


Figure 3.23. Hilbert Spectral Analysis of lung sound

The Hilbert spectrum exhibits the comparative amplitude or energy representations for a particular frequency value and denoted as $H(\omega, t)$. Afterwards, a marginal spectrum can be calculated considering the spectrum is summed over the time domain of 0 and T. The marginal spectrum stands for the sum of all amplitudes (energies) over the complete signal (Huang et al., 1998, Huang and Shen, 2005).

ω represents for the instantaneous frequency function. The frequency-time distribution of the amplitude is called as Hilbert Spectrum, $H(\omega, t)$ and is the relative amplitude or energy contributions for a certain frequency at a t time. \mathbb{R} states for the real

part of terms. Using equations $z(t)$ and $A(t)$, The analytic function of the HHT can be formed as :

$$E(\omega) = \int_0^T H(\omega, t) dt \quad (3.13)$$

$$x(t) - r_n(t) = \Re \left[\sum_{j=1}^n A_j(t) e^{i \int \omega_j(t) dt} \right] \quad (3.14)$$

$$x(t) = \Re \left[\sum_{j=1}^n A_j e^{i \omega_j t} \right] \quad (3.15)$$

The equations prove the IMFs are amplitude and frequency modulated signals. The EMD is contented with the influence by analysis usability on the non-stationary signals in the different amplitude and frequency scales (Flandrin et al., 2003).

3.5.2. Discrete Wavelet Transform

Spectral analysis methods make it possible to utilize frequency components in resulting pathological indications. Fourier analysis transforms a signal from the time domain to the frequency domain, but the time domain disappears when the frequency domain is obtained. It can be important that the specific spectral components occur in which the time and Fourier analysis is insufficient overcoming this situation (Yazgan and Korürek, 1996). Wavelet Transform is the most effective method for time-frequency analysis of impermanent signals (Adeli et al., 2002). The main advantage of wavelet transform is having different window sizes that are narrow for high frequencies, narrow for the low frequencies. In this way, optimum time-frequency resolution can be achieved over all frequency ranges (Daubechies, 1990). There are two main types of wavelet transform. The Continuous Wavelet Transform (CWT) is defined as the multiplication of the modified

and scaled versions of the wavelet function with the total time of the signal. The calculation of wavelet coefficients for each scale is difficult and time consuming as the scaling and transforms parameters change continuously. Therefore DWT is selected more (Chen, 1998).

Calculation of the wavelet coefficients for every possible frequency ranges handles meaningless information in the signal leads to the prolongation of the transformation process and hence the analysis processes (Rioul and Vetterli, 1991). As the DWT analyses both frequency and timing domain features of the signal, it is frequently used to explain more progressive signal difficulties such as signal denoising, data compression, and more. One of the most principle difficulties in multi-scale analysis is the reliance on the total energy of the wavelet coefficients at various scales with the fractional changes. If the selected scale and positions for the analysis are varied in the form of superscripts by doubles, the analysis gets more efficient and faster. It enables the extraction of unwanted meaningless data from the analysis process and is called as DWT. The DWT is performed using various filters and first performed by Mallat in 1988. This very practical filtering algorithm allows Wavelet transform to be performed faster than the CWT (Graps, 1995). At the most basic filter algorithm separates the low and high frequencies in the signal. The low-pass Filter is for removing higher frequency data and the high-pass filter is designed for removing lower frequency data. The filtering process generates two separate signals called as Approximation and Detail. The approach signals represent the original signal and give the definition of the signal. Details include the characterization or detail of the signal (Misiti et al., 2004). If the higher frequencies are removed from signal, the content reaches significance. However, if low frequencies are filtered, unrecognizable, and meaningless data will be handled. The Approximation represents the original of the signal and is obtained with a high scale, the Detail is low-level information and high-frequency components of the signal for wavelet transform. DWT coefficients are pictured in the Figure 3.25.

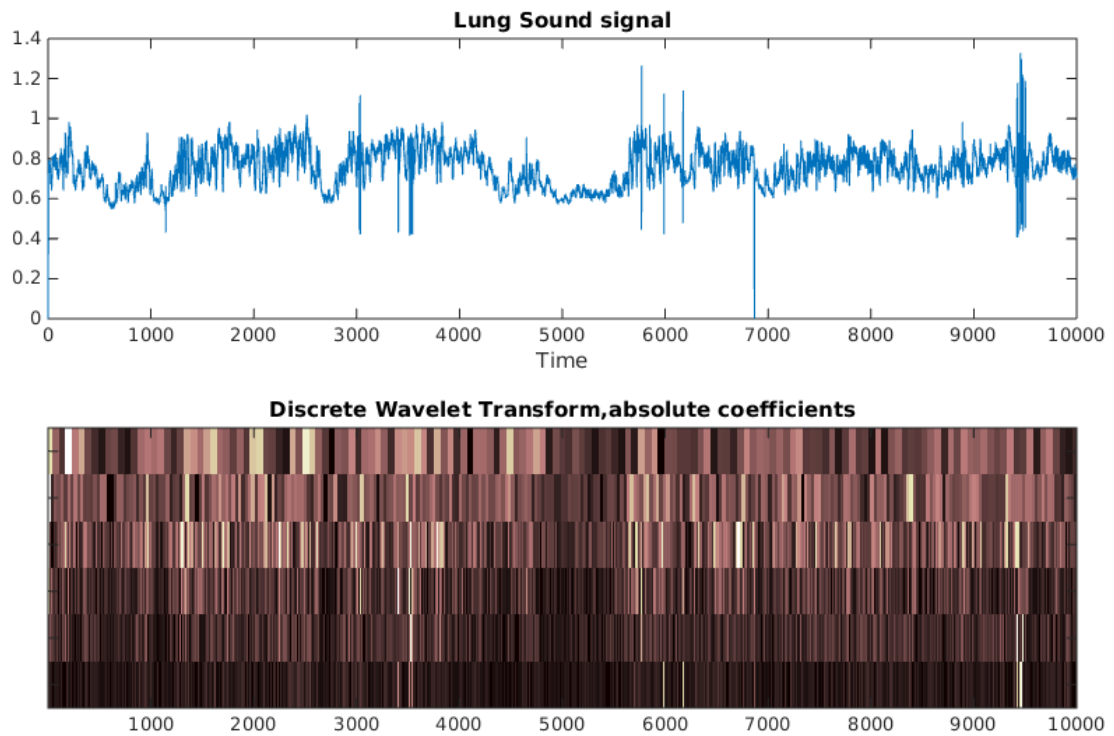


Figure 3.24. Discrete Wavelet Transform Coefficients with sym2 wavelet in 6 levels

The DWT can be obtained by applying low-pass and high-pass filters to the signals and dividing the resulting data into two frequency ranges. The DWT is an implementation of the wavelet transform for discrete set of the wavelet types. That is to say, DWT separates the signal into simpler compounds by convolving jointly orthogonal set of wavelets. In contrast with several types of DWT implementation, the most used one is the Mallat (pyramidal) algorithm in which two filters - smoothing and non-smoothing forms are decomposed using the wavelet coefficients. As an outcome of the DWT, the ordered subbands with same length as the input signal and are commonly sorted from the largest frequency scales to the smallest scales. The filters are repeatedly applied to obtain subbands for analysing all the scales. If the process is applied to the obtained two frequency ranges separately, the multi-resolution analysis of the signal is realized. The Detail and Approximation that arise at each level of decomposition are seen in Figure 3.26. A downsampling process is performed in downward.

The wavelet can be established using scaling functions. The disadvantage of the scaling functions is that, it must be orthogonal to its discrete and integer translations. Dilation equation overcomes this necessity. If we assume S is a scaling factor

$$\Phi(x) = \sum_{k=-\infty}^{\infty} a_k \Phi(Sx - k) \quad (3.16)$$

In addition to scaling function, the area between the function must be normalized

$$\int_{-\infty}^{\infty} \Phi(x) \Phi(x + l) dx = \delta_{0,1} \quad (3.17)$$

The finite set of coefficients a_k which define the scaling function, composes the wavelet.

$$\psi(x) = \sum_{k=-\infty}^{\infty} (-1)^k a_{N-1-k} \psi(2x - k) \quad (3.18)$$

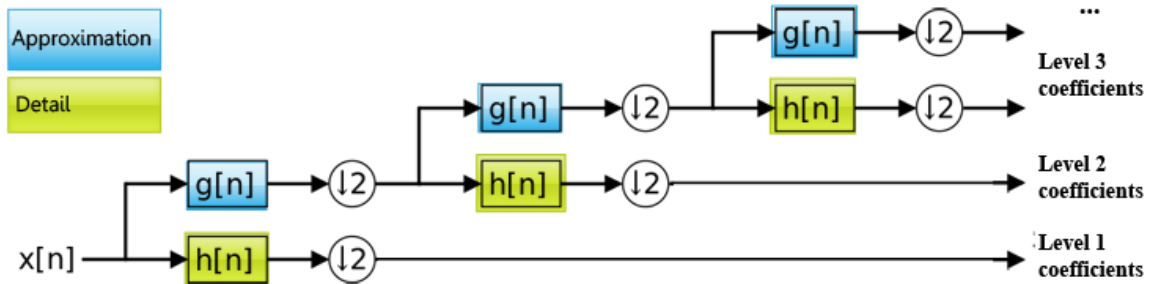


Figure 3.25. Discrete Wavelet Decomposition at Level 3

The inverse DWT can reconstruct the original signal from the wavelet subbands using the same wavelet type. The information in the $x[n]$ signal is the Approximation signals. The Detail subbands of the DWT are the high frequency parts of the different frequency values, and the signal $x[n]$ equals the sum of all the Details subbands and the Approximation subbands. After the decomposition, the Detail or Approximation information at the any

level with frequency range can be selected to analyse. The advantages and disadvantages of most used transform methods are compared in Table 3.4.

Table 3.4. The comparison of the transformations

Basis	Fourier Transform	Wavelet Transform	Hilbert Transform
	<i>a priori</i>	<i>a priori</i>	adaptive
Frequency	convolution: global, uncertainty	convolution: regional, uncertainty	differentiation: local, certainty
Presentation	energy-frequency	energy-time-frequency	energy-time-frequency
Nonlinear	non applicable	non applicable	applicable
Non-stationary	non applicable	applicable	applicable
Feature extraction	non applicable	discrete: non-applicable, continuous: applicable	applicable
Theoretical base	theory complete	theory complete	empirical

3.5.3. The Proposed 3D Second Order Difference Plot

The SODP is an optional signal visualization technique which is based on the Chaos Theory. It is proved the efficiency on computerized biomedical signals such as EEG (Pachori and Patidar, 2014) and ECG (Thuraisingham, 2009; Altan and Kutlu, 2015). It clarifies the quantity of non-symmetrical functions for non-linear data. The quantization of sign dispersion, binomial dispersion and the geometric sectional approximations on the SODP can derive characteristic features and can improve the statue of the abnormality classification model for medical diagnosis difficulties. The SODP charts the distinctions of the two consecutive data points. The SODP denotes the permanency rate of signal distribution. If $x(n)$ is considered as the time-series to be analysed,

$$X(n) = [x(n + 1) - x(n)] \quad (3.19)$$

$$Y(n) = [x(n + 2) - x(n + 1)] \quad (3.20)$$

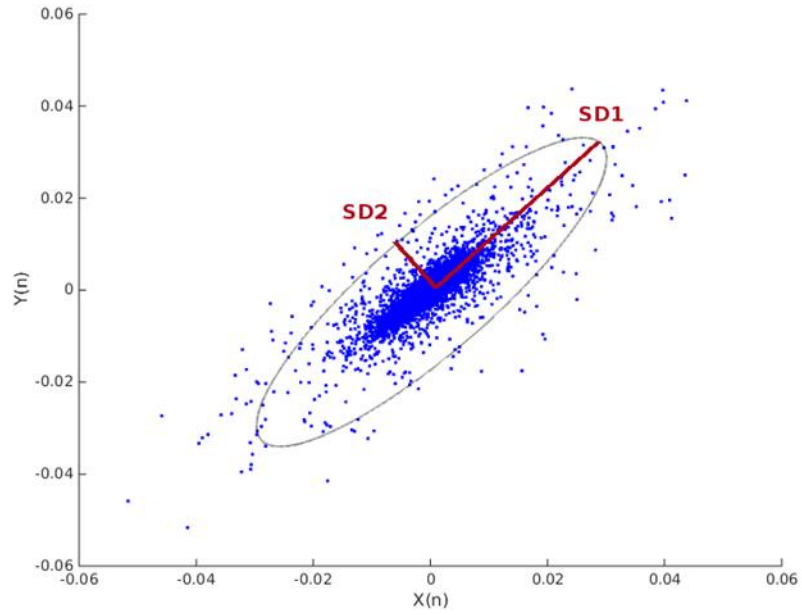


Figure 3.26. Elliptical Distribution of lung sound using SODP

$$S_X = \sqrt{\frac{1}{N} \sum_{n=0}^{N-1} X(n)^2} \quad (3.21)$$

$$S_Y = \sqrt{\frac{1}{N} \sum_{n=0}^{N-1} Y(n)^2} \quad (3.22)$$

$$S_{XY} = \frac{1}{N} \sum X(n)Y(n) \quad (3.23)$$

$$Dist(i) = \sqrt{(S_X^2 + S_Y^2) - 4(S_X^2 S_Y^2 - S_{XY}^2)} \quad (3.24)$$

$$SD1 = 1.7321 \sqrt{(S_X^2 + S_Y^2 + D)} \quad (3.25)$$

$$SD2 = 1.7321 \sqrt{(S_X^2 + S_Y^2 - D)} \quad (3.26)$$

The data points are plotted in an elliptical distribution as seen in Figure 3.27. The horizontal radius (SD1) and vertical radius (SD2) are the principle amounts for the SODP (Pachori and Patidar, 2014; Thuraisingham, 2009; Isler and Kuntalp, 2007).

The proposed quantization allows three-dimensional analysis using the distance of the plotted three points in space, on the contrary the sectional quantization methods. The model deals with the consecutive three data points in space. The distribution of the SODP is seen in Fig. 3.27. Z coordinate is obtained as follows;

$$Z(n) = [x(n + 3) - x(n + 2)] \quad (3.27)$$

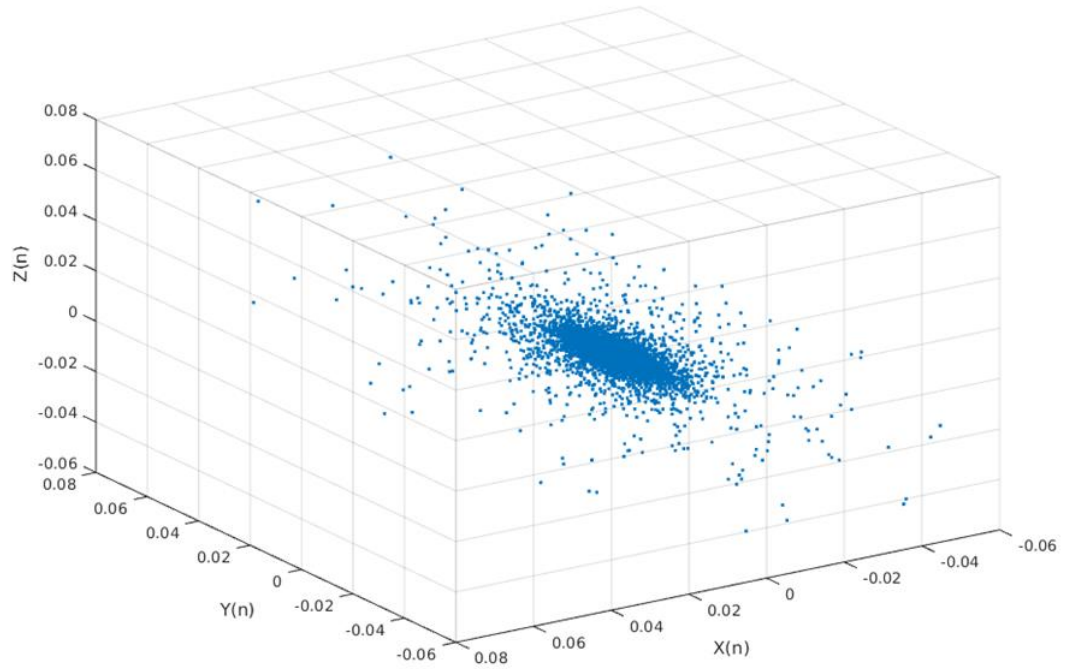


Figure 3.27. The dispersion of the proposed 3D-SODP

The depth analyse has already the maintained elliptical form in the 3D-SODP as depicted in Figure 3.28. The visualized third dimension depth is regarded to derive intact attributes at various proportion ranges. The schemed 3D-SODP space is fragmented into plane sections and sign-based spaces are observed. The proposed 3D-SODP quantifies self-similarity by detecting the presence variations in non-linear dynamics using chaos from the randomness. In the light of the Euclidean theorem, whereas the dispersion of data points with one dimensional line at a range provides assessing limited number of features and the plot of data points with two-dimensional plane (SODP) increases the assessing ability with many features, the 3D-SODP allows for detailed analysis of the data points with too many features at different depths.

$$\delta(oct_k(i)) = \begin{cases} \delta(oct_1(i)) = 1, \text{ if } X(n) \geq 0, Y(n) \geq 0, Z(n) \geq 0 \\ \delta(oct_2(i)) = 1, \text{ if } X(n) \geq 0, Y(n) \geq 0, Z(n) < 0 \\ \delta(oct_3(i)) = 1, \text{ if } X(n) \geq 0, Y(n) < 0, Z(n) \geq 0 \\ \delta(oct_4(i)) = 1, \text{ if } X(n) \geq 0, Y(n) < 0, Z(n) < 0 \\ \delta(oct_5(i)) = 1, \text{ if } X(n) < 0, Y(n) \geq 0, Z(n) \geq 0 \\ \delta(oct_6(i)) = 1, \text{ if } X(n) < 0, Y(n) \geq 0, Z(n) < 0 \\ \delta(oct_7(i)) = 1, \text{ if } X(n) < 0, Y(n) < 0, Z(n) \geq 0 \\ \delta(oct_8(i)) = 1, \text{ if } X(n) < 0, Y(n) < 0, Z(n) < 0 \\ \delta(oct_k(i)) = 0, k = 1, 2, 3, \dots, 8 \text{ Otherwise} \end{cases} \quad (3.28)$$

The 3D-SODP has segmented into eight octants using XY-plane, YZ-plane, and XZ-plane in the light of the probable combinations of abscissa, ordinate and applicate coordinates. Figure 3.29 shows the octants and the coloured planes on the 3D-SODP. The octant 1 space is settled by positive axes; the octant 2 space has positive ordinate and applicate coordinates, and negative abscissa axis values; the octant 3 space has only positive applicate, the abscissa and the negative ordinate values; the octant 4 space has positive the x-axis and z-axis, and negative y-axis; the octant 5 space has positive abscissa and ordinate values, and negative z-axis value, the octant 6 is settled with positive y-axis values and negative x-axis and the z-axis values, the octant 7 space has negative

coordinates, the octant 8 space is settled by positive abscissa, the negative ordinate and applicate values.

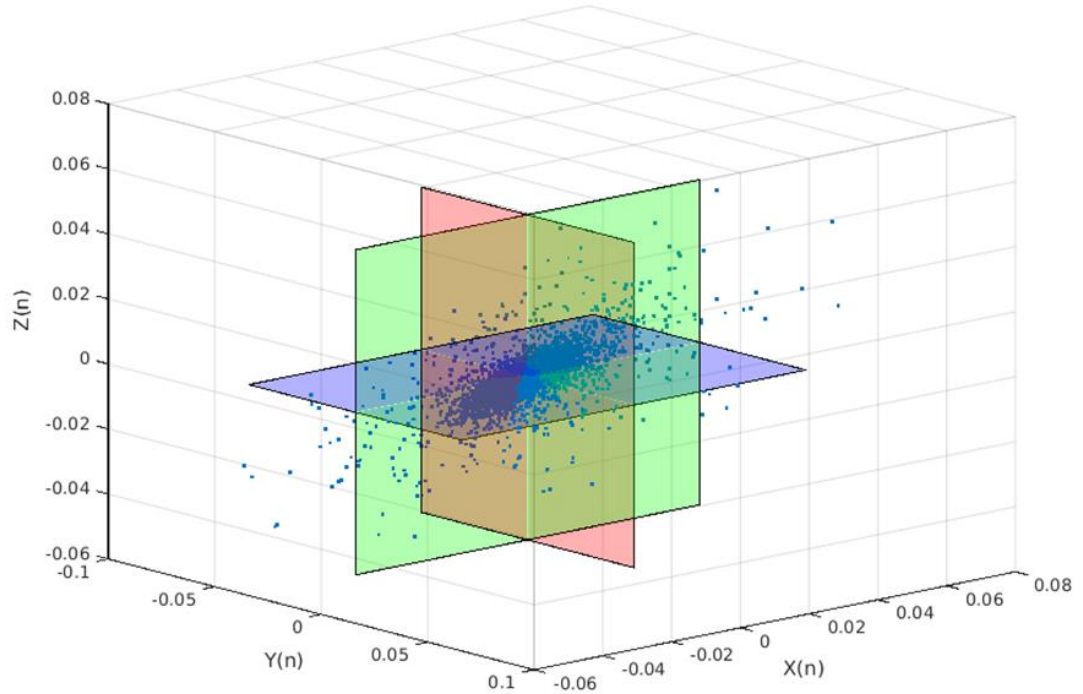


Figure 3.28. The octant regions of the proposed 3D-SODP

3.5.4. Statistical Feature Extraction

The statistical and high order statistical features are calculated from the obtained subbands of third level DWT and the IMFs. While the first and second order statistics include mean and variance, higher order statistics include higher order moments and cumulants.

Minimum is the value in extracted subbands and IMFs. It is the data point which is less than all other data points in the subbands and IMFs. If the subbands were ordered in ascendingly, the minimum of the subband or IMFs would be the first data point.

Maximum is the value in extracted subbands and IMFs. It is the data point which is greater than all other data points the subbands and IMFs. If the subbands were ordered in descending case, the maximum of the subband or IMFs would be the first data point.

Mode is the most frequently appearing amount in extracted subbands and IMFs. To define the mode value the signal is put in order and the number of repetitions of the data points is counted. The highly repeated data point is determined as the mode value.

Median is data point which splits the higher partial from lower partial on the extracted subbands and IMF. It is measurement of central tendency in basic. The subbands were ordered in ascendingly or descending. The data point in the middle of extracted subbands and IMFs is determined as statistical median. x stands for the input signal, and n is the number of data points. The median is calculated for the odd number n using (3.29), for even number n using (3.30).

$$Median = x_{\frac{(n-1)}{2}} \quad (3.29)$$

$$Median = \frac{1}{2} \left(x_{\left(\frac{n}{2}\right)} + x_{\left(\frac{n}{2}+1\right)} \right) \quad (3.30)$$

Mean is average of the entire data point in extracted subbands and IMFs, often symbolized by \bar{X} . It is calculated with the summation of entire data points dividing by the number of data points in extracted subbands and IMFs.

$$Mean = \bar{X} = \frac{1}{n} \sum_{i=1}^n x_i \quad (3.31)$$

Standard Deviation is the amount of dispersement which represents how much each of the extracted subbands and IMFs is dispersed. Particularly, it is distributed around the statistical mean for the extracted subbands and IMFs.

$$Standart Deviation = \sqrt{\frac{\sum |x - \bar{x}|^2}{n - 1}} \quad (3.32)$$

Moments of the extracted subbands and IMFs are explained as the coefficients in the Taylor expansions. The moment is the measure which quantizes the extracted subbands and IMFs data points' distribution shape. The moment has a close relationship within the probability and statistics. It represents an appropriate approach for resuming particular statistics. Nevertheless the high capability of the moments, Higher-order levels (over the fourth order) are difficult to predict and to define in Layman's terms.

$$\text{Moment} = \mu_n = \mathbb{E}[x^n] \quad (3.33)$$

First moment stands for the mean, second moment stands for the variance, the third moment stands for the skewness, and fourth order moment equals to kurtosis statistics.

Kurtosis describes the position and variability of the extracted subbands and IMFs. Kurtosis is the representation of the thickness or heaviness of the tails on extracted subbands and IMFs dispersion. It was produces with Karl Pearson approach with scaled form of the fourth moment (μ_4/σ^4) of extracted subbands and IMFs. The kurtosis and tails of the dispersion are proportional to each other. $\mathbb{E}[\cdot]$ symbolizes the average over the probability distribution $p(x)$:

$$\text{Kurtosis} = \mathbb{E} \left[\left(\frac{X - \mu}{\sigma} \right)^4 \right] = \frac{\mu_4}{\sigma^4} = \frac{\mathbb{E}[(X - \mu)^4]}{(\mathbb{E}[(X - \mu)^2])^2} \quad (3.34)$$

Skewness is the quantization of the asymmetry of the extracted subbands and IMFs distribution. Skewness is produced by a related scaled form of to the third moment about the mean. The distribution of extracted subbands and IMFs is symmetric if it attendances same to the left and right of the centre on the distribution.

$$\begin{aligned} \text{Skewness} &= \mathbb{E} \left[\left(\frac{X - \mu}{\sigma} \right)^3 \right] = \frac{\mu_3}{\sigma^3} = \frac{\mathbb{E}[X^3] - 3\mu \mathbb{E}[X^2] + \mu^2 \mathbb{E}[X] - \mu^3}{\sigma^3} \\ &= \frac{\mathbb{E}[X^3] - 3\mu \sigma^2 + \mu^2 \mathbb{E}[X] - \mu^3}{\sigma^3} \end{aligned} \quad (3.35)$$

Cumulants are the coefficients in the Taylor expansion about the origin. The specific nonlinear combinations of moments stand for cumulants, appear artlessly if analysis on summation of independent the extracted subbands and IMFs. It is solved with the derivative of the logarithm of moment estimation. Nevertheless the high capability of the cumulants, Higher-order levels (over the fourth order) are difficult to predict and to define in Layman's terms. The cumulant are presented in the following equations.

$$k_n = \ln \mathbb{E}[x^n] = \ln \mu_n \quad (3.36)$$

$$k_1 = \frac{\mu_1}{\mu_0} \quad (3.37)$$

$$k_2 = \frac{\mu_2}{\mu_0} - \left(\frac{\mu_1}{\mu_0}\right)^2 \quad (3.38)$$

$$k_3 = \frac{\mu_3}{\mu_0} - 3 \frac{\mu_1 \mu_2}{\mu_0^2} + 2 \left(\frac{\mu_1}{\mu_0}\right)^3 \quad (3.39)$$

$$k_4 = \frac{\mu_4}{\mu_0} - 3 \left(\frac{\mu_2}{\mu_0}\right)^2 - 4 \frac{\mu_1 \mu_3}{\mu_0^2} + 12 \frac{\mu_1^2 \mu_0}{\mu_0^3} - 6 \left(\frac{\mu_1}{\mu_0}\right)^4 \quad (3.40)$$

3.6. Classification

Classification is one of the most famously used practice in machine learning, with a completely layout of processes such as biomedical signal analysis, risk estimations, medical diagnosis and image classification. The main aim of classification is predicting the referring class using the measured or counted feature inputs. In addition to the existing and fundamental models and algorithms used in classification, as well as core machine learning concepts, the classification performances have been achieved with very high accuracy rates, sensitivity and precision values using new algorithms and mathematical model. Novel approaches are distinguished by the integration of existing models, by the inclusion of

different decompositions, differences in evaluation criteria, and different kernels for the classifier models. Classification approaches iterates various learning models and presentations to apply reduction of error on training data (Duda et al., 2012).

Learning of the machines in pattern recognition systems is in either supervised or unsupervised ways. The classification with supervised learning approach concludes a function which is based on relationship between features set (input) and labels (output) using training process. In unsupervised learning (clustering), there is no training; learning is achieved by similarity-based statistical approaches and regressions with unlabelled data (Mitchell, 1997).

Rather than covering all aspects and conventional classification models, this thesis focused on novel core techniques, which are widely used in the real-world to get state-of-the-art performance, other image processing techniques, speech recognition, emotive tasks, biomedical signal analysing task. In this subsection conventional ELM kernel, novel ELM kernels (Hess-ELM, Lu-ELM), Deep Learning approaches, Deep Belief Networks classifier and proposed multi-kernel Deep ELM classifier are explained in detail using the mathematical model of ELM kernels, Deep Belief Networks model. By following Deep ELM approach, implementation of analysing the features using linear algebra on multiple real-world tasks, and deeply grasp the core techniques needed to be successful in practice.

3.6.1. Deep Learning

Deep learning is a machine learning algorithm that trains a computer to carry out human-like tasks, such as recognizing speech, identifying images, interpreting the images, other visuals, additionally making predictions and inferences. Instead of unionizing the data to obtain a function through predefined equations, deep learning arranges the fundamental optimization parameters about the input and constrains to learn on the model's own by recognizing the data in detail using many hidden layers. Deep learning models have enhanced the performance on classification, recognition, detection and also diagnosis approaches. Contemporarily, the most used field of the Deep Learning is on image processing such as analysing objects, segmentation, interpreting entire image, object and

human framing and labelling of the images. In last decade, Deep learning has been used in the modelling of biomedical signal processing and diagnosis systems with an increasing acceleration.

The characteristic developments improve the deeply analysing the data for Deep Learning. The novel algorithmic capabilities have boosted the performance of deep learning methods. New machine learning approximations have increased the accuracy of deep learning models. The augmentation of the available data to build large neural networks with many hidden layers, including textual data from social media, physician's notes, diagnostic multimedia tools and searching and treatment transcripts.

Deep Learning is not a new approach. It was first theorized for machine learning by Rina Detcher (1986), and was based through Boolean threshold neurons for ANN by Igor Aizenberg et al. (2000) through neural networks for reinforcement learning. In 2006, Geoff Hinton and Osindero (2006) offered a pre-training algorithm to prove the efficiency of training one layer at a time for multi layered feedforward neural network by layer wise treating each layer in unsupervised restricted Boltzmann machine algorithm. Then the calculated parameters including weights, biases are optimized using supervised backpropagation fine-tuning (Hinton et al., 2006). The model referred to learning for deep belief nets. The Deep Learning needs too sophisticated hardware and data requirements. That is why Deep Learning has only recently become useful and become popular contemporarily. The Computational advances of distributed cloud computing and graphics processing units have brought the algorithm incredible computing power. The power at the parallel computing and cloud computing has satisfied the demands to train deep algorithms. Deep Learning requires large amounts of labelled data for an accurate training stage.

The most significant dissimilarity of Deep Learning from the actual classification algorithms is that, it does not need any feature extraction stage for the analyses. It consists of both the feature extraction including pooling, filtering, convolution, autoencoder, unsupervised stages and the neural network model including many hidden layers, fully connected layers, back propagation algorithms, activation functions, and iterations. The main model of the Deep Learning on analysis of the images is indicated in Figure 3.30.

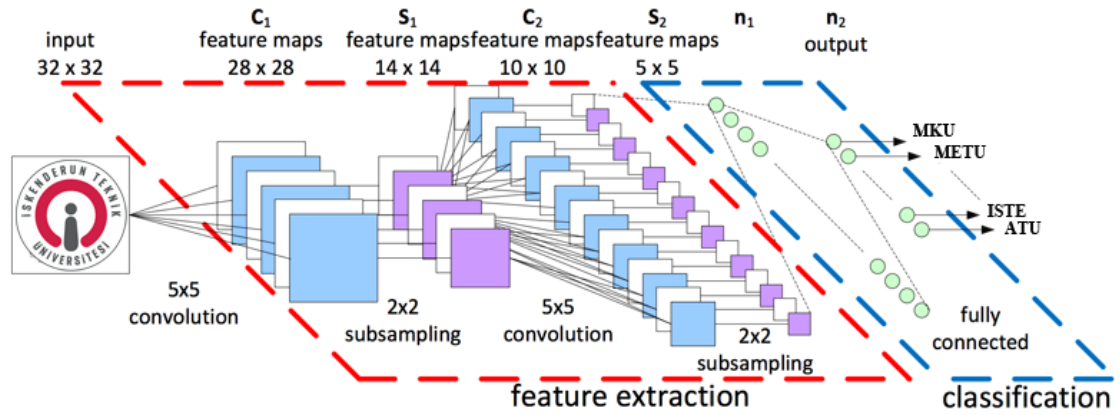


Figure 3.29. The Deep Learning model which is based on Convolutional Neural Network on image analysis

The Deep Learning is inclusive of many different classification models such as Convolution Neural Networks, Deep Belief Networks, Recurrent Neural Networks, Deep Neural Networks, Sparse Autoencoders, and Deep Convolution Networks. In this thesis, the DBN algorithm was utilized in the analysis of the lung sounds. Deep ELM model with novel kernels are proposed to enhance deep analyse capacity of the ELM learning algorithms. New unsupervised ELM autoencoder kernels are proposed.

3.6.1.1. Deep Belief Networks

The DBN, semi-supervised learning algorithm, are probabilistic and stochastic generative models which are comprised of at least two layers hidden variables. The top two layers have undirected linking within them. The other layers provide top-down directed linking from the layer above. The DBN structure with three hidden layers is indicated in Figure 3.31.

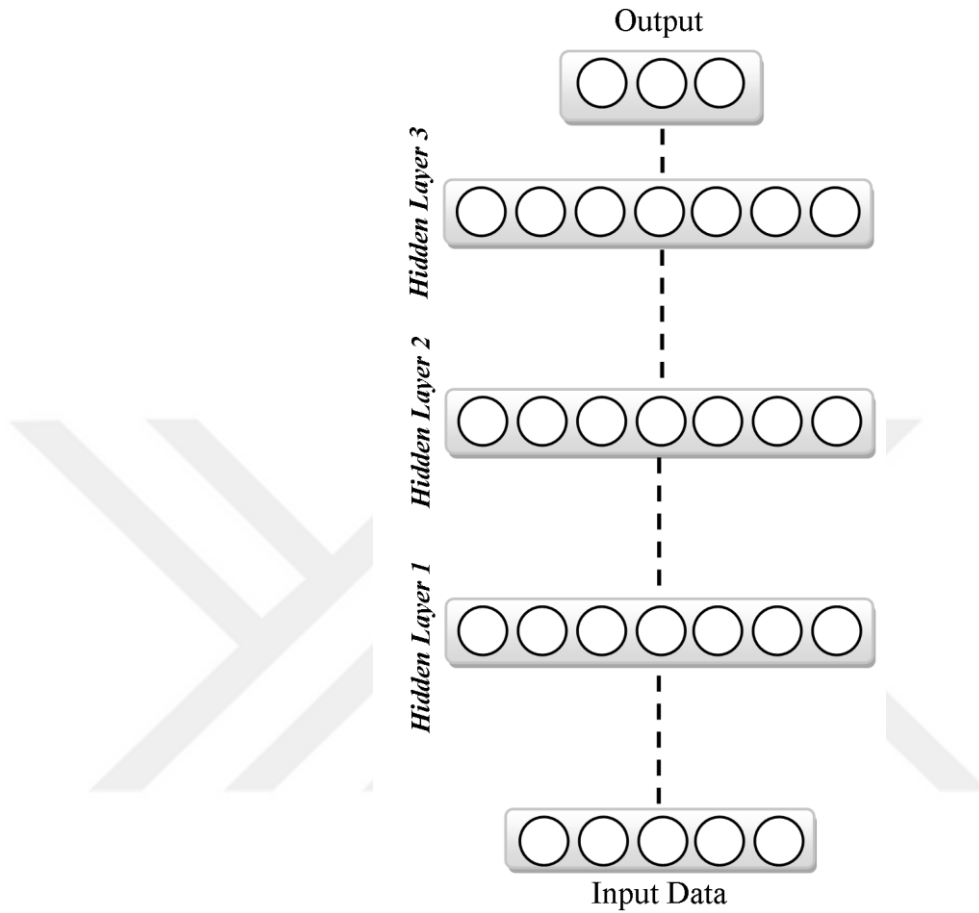


Figure 3.30. The Deep Belief Network structure

The DBN is an originaive Deep Learning approach that comprises of both unsupervised training and supervised training stages. The idea on pre-training of the input data for the classification parameters including the weights, biases, and the other parameters is most prominent advantage of the DBN. The most popular unsupervised training algorithms for the DBN are Sparse Autoencoder and Restricted Boltzmann Machines (RBM) (Bengio and Lamblin, 2007; Hinton et al., 1986). In this thesis, the RBM is selected as pre-training kernel of the DBN.

The RBM is stacked between two adjacent visible-hidden layers or adjacent hidden-hidden layers. Each double adjacent layer is grouped as an RBM. The RBM has no contact between visible-visible layers, hidden-hidden layers, and the units within the same layer. The RBM is energy-based functions. The direction of the unsupervised training between

the nodes is estimated using its energy function. The classification parameters including weights of the nodes, biases of the layers on the DBN model are evaluated by means of the probabilistic amount of greedy layer-wise method using a set of inputs. On the other hand, the stacking of the RBM can constitute the DBN with contrastive divergence algorithms, too (Bengio et al., 2007). In the RBM, visible units (inputs) are linked to hidden units that represent the linked previous layer features considering undirected weighted connections (Hinton et al., 2006; Bengio et al., 2008). Enduring the top-down directed training, iteratively the RBMs at upper layers are trained using outputs of lower layers, thus the upper features in a lower hidden layer become the visible layer with input parameters for an upper hidden layer in the unsupervised stage. The RBM training is demonstrated in Figure 3.32.

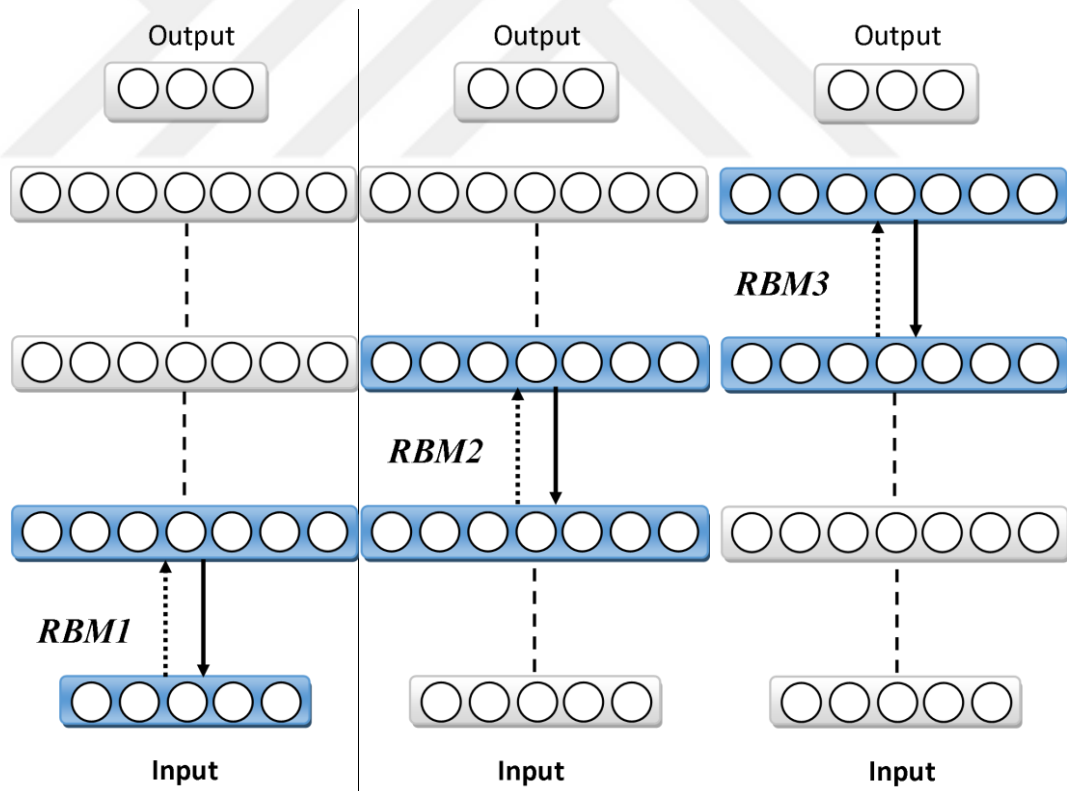


Figure 3.31. The presentation of RBM training in the DBN

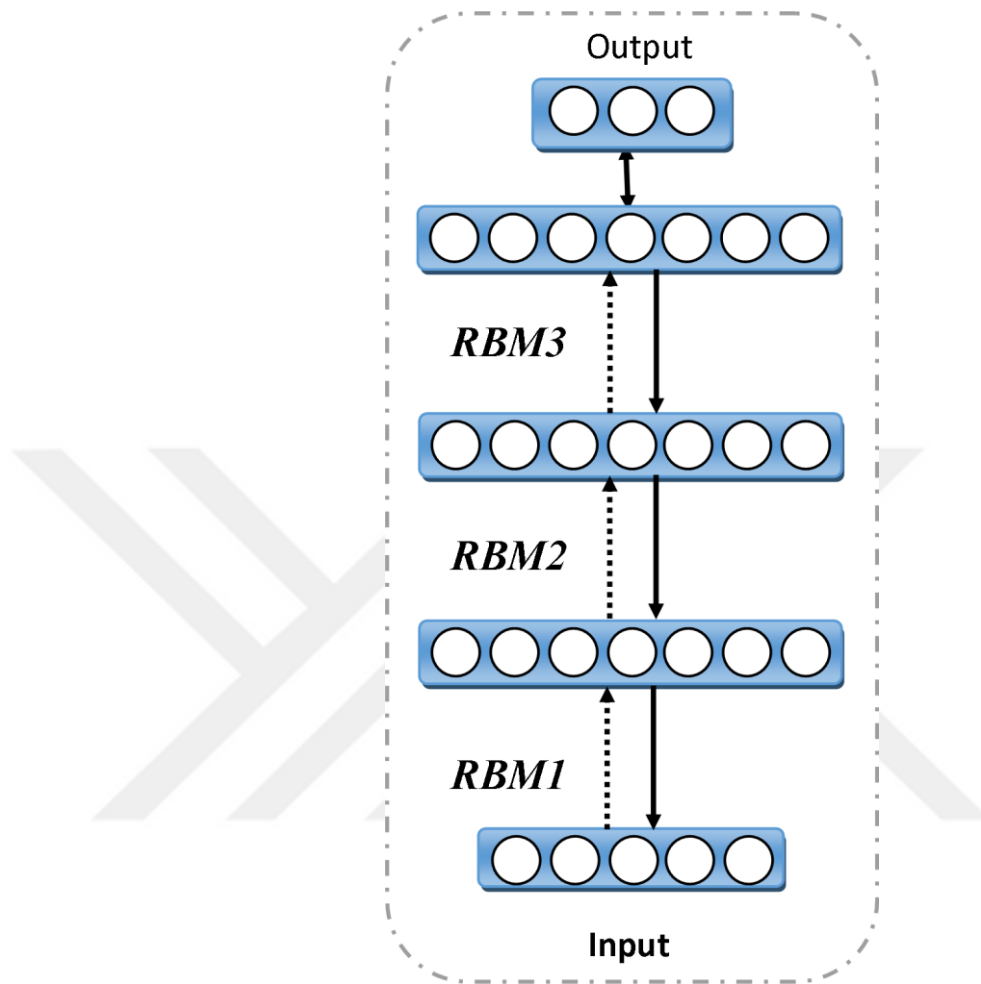


Figure 3.32. The Deep Belief Network training

The adjacent previous hidden layer attends as the visible layer for the next adjacent hidden layer applying contrastive divergence and the probabilistically recalculation of the shared weights is realized (Bengio and Delalleau, 2009). In the supervised training phase of the DBN, the classification parameters obtained unsupervised ways including weights of neurons, biases and the structure of classifier model are unfolded to a neural network structure for optimization of the parameters using fine-tuning approach (Bengio and Lamblin, 2007). The DBN must be structured at least two hidden layers. The number of the hidden layers is iteratively selected and is relevant with the how deep analysis of the input features is performing (Bengio and Lamblin, 2007; Hinton et al., 2006). The DBN training with three RBM is demonstrated in Figure 3.33.

The probability distribution of RBM using the visible nodes v and hidden nodes h can be impersonated by energy function $E(v, h)$, where b_i is bias of visible nodes i , and b_j is bias of hidden nodes j :

$$E(v, h) = - \sum_{i,j} v_i h_j \omega_{ij} - \sum_i b_i v_i - \sum_j b_j h_j \quad (3.41)$$

The probability of the energy function, $P(v, h)$:

$$P(v, h) = \frac{e^{-E(v, h)}}{\sum_{v, g} e^{-E(v, g)}} \quad (3.42)$$

The derivative of the log probability of a training vector with respect to a weight:

$$\frac{\partial \log P(v, h)}{\partial w_{ij}} = \langle v_i h_j \rangle_{data} - \langle v_i h_j \rangle_{model} \quad (3.43)$$

The binary nodes of the hidden layer are Bernoulli random variables. The probability formulation when node h_j is activated, considering given visible layer v

$$P(h_j = 1 | v) = \sigma \left(b_j + \sum_i w_{ij} v_i \right) \quad (3.44)$$

where σ is a sigmoid function

$$\sigma(x) = \frac{1}{1 + e^{-x}} \quad (3.45)$$

The probability formulation when node v_i is activated, considering the visible layer h

$$P(v_i = 1 | h) = \sigma \left(b_i + \sum_j w_{ij} h_j \right) \quad (3.46)$$

The scope of the RBM is reaching the maximum probability amount, correspondingly the log likelihood amount for training examples X

$$\operatorname{argmax}_w \prod_{x \in X} P(x) \quad (3.47)$$

$$\operatorname{argmax}_w \sum_{x \in X} \log P(x) \quad (3.48)$$

Contrastive divergence algorithm with k iterations of Gibbs sampling is a fast recommended solution for calculating change of weights (Hinton, 2002) where η represents the learning rate as follows:

$$\Delta w_{ij} = \eta \left(\langle v_i h_j \rangle^0 - \langle v_i h_j \rangle^k \right) \quad (3.49)$$

A DBN with the joint distribution between estimated sample x and l hidden layers h_k is solved as follows:

$$P(x, h^1, \dots, h^l) = \left(\prod_{k=1}^{l-2} P(h^k | h^{k+1}) \right) P(h^{l-1}, h^l) \quad (3.50)$$

3.6.2. Extreme Learning Machines

The word “extreme” stands for advancing traditional artificial learning approaches and drawing close biological brain similar to learning procedure. The ELM purposes to improve the efficiency of the traditional artificial learning models as same as biological learning procedure.

The ELM is related with the some fundamental biological learning procedures. The machine-based learning capacity was approved by Huang et al. (Huang et al., 2004). The universal estimation ability was precisely established for generalized single layer neural network model in 2006–2008 (Huang and Chen, 2008; Huang et al., 2006; Huang and Chen, 2007). The randomly generated hidden nodes with given numbers of neuron size ensure no-tuning is needed for the ordinary implementations in ELM. Nevertheless, ELM also increases in variety with many other kernels and decomposition techniques (Huang,

2014; Huang et al., 2012). The machine learning algorithms are based on the fundamental requirements for compression, feature learning, clustering, regression and classification. The ELM approaches are intended to accomplish these roles by the integration of the kernel algorithms.

The ELM has a revealing learning algorithm for the generalized single hidden layer feedforward neural networks. It is fast and influential procedure with randomly defined hidden node parameters and simply calculated output weights by simple analytical mathematics (Tang et al., 2016).

The deepest analysis of the big data needs high requirements for computing time. The poor learning speed on usual ANN algorithms including gradient descent based methods has been a big deficiency considering the required training time in machine learning implementations and has readily converged to local minimums for past decades. Iterative learning epochs are demanded by learning algorithms for achieving accurate learning rates (Huang et al., 2004). The provisional reasons were widely using the slow gradient-based learning algorithms in training stages of ANN and necessity on optimization of weights, biases and node parameters in a repetitious manner by tuning with lazy learning algorithms. Unlike the traditional lazy approximations, the ELM appear with the capability of coming up with fast and generalized results for complex classification circumstances. The ELM may manage the learning process thousands times faster than classic ANN learning algorithms with more attractive generalization performance.

The ELM learning is based on Moore-Penrose generalized matrix inverse circumstances. Input weights are stacks that bunch up input nodes to hidden nodes, and output weights are stacks that bunch up hidden nodes to output layer nodes. The input weights are the random values, but output weights are estimated using learning process. The hidden layer biases are threshold amounts which are calculated to avoid the zero convergence. The structure of a traditional ELM is pictured in Figure 3.34.

The ELM is especially utilized to overcome the classification and regression problems including ECG-based arrhythmia classification (Kim et al., 2009), image processing based face recognition (Mohammed et al., 2011; Zong and Huang, 2011), image

processing based digit recognition (Chacko et al., 2012), EEG-based epileptic seizure detection (Song and Liò, 2010) and other time series (Sun et al., 2008).

Even though the ELM has demonstrated the ability to not only shorten learning time, but also improve learning capability and generalization performance. In whatever way, the computational stability of ELM hasn't been verified, yet.

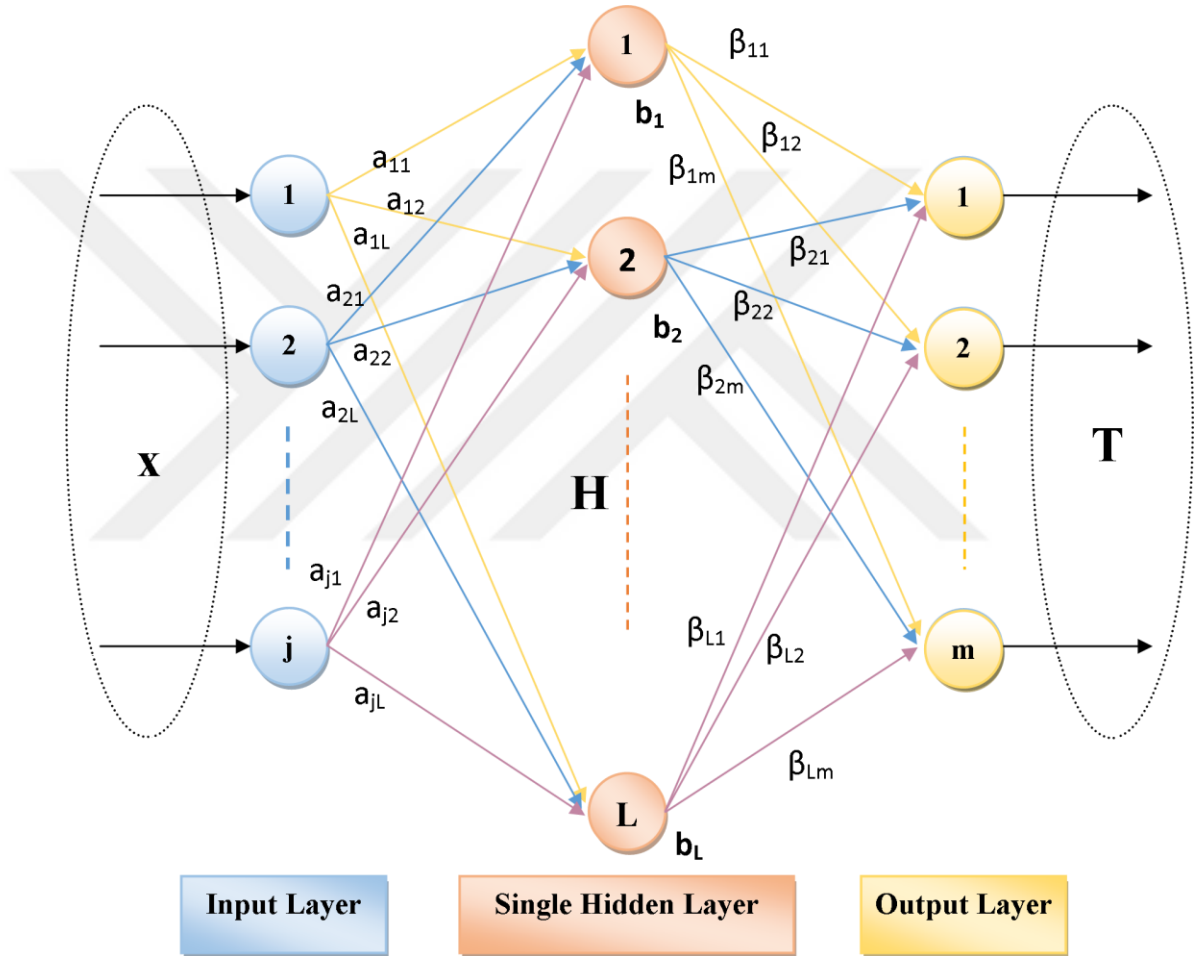


Figure 3.33. The structure of Single Layer Feedforward network based Extreme Learning Machines

Determining the parameters for spacious datasets is a troublesome situation for machine learning approaches in which it is fixed using singular value decomposition in traditional ELM. Even so, it has disabilities on convergence of the models into real circumstance with slow extrapolating.

The prominent advantages of the ELM are non-iterative tuning of hidden nodes, layer wise training, randomly stated hidden neurons or inheritable hidden neurons, and learning the output weights for each hidden layer separately with application based optimization constraints.

The ELM theory is formulated as the equations given below:

The SLFN with L hidden nodes is demonstrated as

$$f_L(x) = \sum_{i=1}^L G_i(x, a_i, b_i) \cdot \beta_i, \quad a_i \in R^d, b_i, \beta_i \in R \quad (3.51)$$

where $G_i(\cdot)$ represents the activation function of i^{th} hidden node, a_i is the input weight vector of i^{th} hidden layer, b_i is the bias of i^{th} hidden layer, β_i is output weights. The summation node activation function is denoted as g and G_i is represented by the following equation:

$$G_i(x, a_i, b_i) = g(a_i \cdot x + b_i) \quad (3.52)$$

The radial basis function (RBF) nodes with activation function g , G_i is presented as by following equation:

$$G_i(x, a_i, b_i) = g(b_i ||x - a_i||) \quad (3.53)$$

The SLFN has ability to converge any continuous target function over any condensed subset $X \in R^d$ (d : dimensional Euclidean space) with above random stated nodes or RBF nodes. $|f|^2$ is integrable $\int_X |f(x)|^2 dx < \infty$. Inner product $\langle u, v \rangle$ is defined as

$$\langle u, v \rangle = \int_X u(x)v(x)dx \quad (3.54)$$

$\|\cdot\|$ function estimates the adjacency amount of initial function f_n and the target function f_t

$$\|f_L - f\| = \left(\int_X |f_n(x) - f(x)|^2 dx \right)^2 \quad (3.55)$$

$\lim_{n \rightarrow \infty} \|f - f_n\| = 0$ goes along with probability one if the β_i is estimated by regular least square to minimize $\|f(x) - \sum_{i=1}^L \beta_i g_i(x)\|$.

The given theorem (Huang et al., 2006; Huang and Chen, 2007; Huang and Chen, 2008) proves that randomly stated input weights have ensures fast learning and the universal estimation ability using least mean square algorithm for defining outputs.

The machine learning algorithms purpose achieving the smallest training error and also the smallest norm of β_i

$$\text{Minimize } \|\beta\|_v^{\sigma_1} + \lambda \|H\beta - T\|_u^{\sigma_2} \quad (3.56)$$

$\sigma_1 > 0, \sigma_2 > 0, u, v = 0, (1/2), 1, 2, \dots, +\infty$, H is randomly stated hidden layer output matrix

$$H = \begin{bmatrix} h(x_1) \\ \vdots \\ h(x_N) \end{bmatrix} = \begin{bmatrix} h_1(x_1) & \cdots & h_L(x_1) \\ \vdots & \vdots & \vdots \\ h_1(x_N) & \vdots & h_L(x_N) \end{bmatrix} \quad (3.57)$$

T is the training data target matrix

$$P(x, h^1, \dots, h^l) = \left(\prod_{k=1}^{l-2} P(h^k | h^{k+1}) \right) P(h^{l-1}, h^l) \quad (3.58)$$

$$T = \begin{bmatrix} t_1^T \\ \vdots \\ t_N^T \end{bmatrix} = \begin{bmatrix} t_{11} & \cdots & t_{1m} \\ \vdots & \vdots & \vdots \\ t_{N1} & \cdots & t_{Nm} \end{bmatrix}$$

Training of the ELM is handled as follows:

$$\beta = H^\dagger T \quad (3.59)$$

H^\dagger is the Moore-Penrose inverse of matrix of H . Pseudoinverse comply according to Moore-Penrose inversing operations

$$H H^\dagger H = H \quad (3.60)$$

$$H^\dagger H H^\dagger = H^\dagger$$

$$(H^\dagger H)^* = H^\dagger H$$

$$(H H^\dagger)^* = H H^\dagger$$

The orthogonal projection method can be efficiently used for the calculation of Moore-Penrose inverse: $H^\dagger = (H^T H)^{-1} H^T$, if $H^T H$ is non-singular; or $H^\dagger = H^T (H H^T)^{-1}$, if $H H^T$ is non-singular. According to the ridge regression theory, it was suggested that a positive value $(1/\lambda)$ is added to the diagonal of $H^T H$ or $H H^T$ in the calculation of the output weights β .

$$\beta = H^T \left(\frac{1}{\lambda} + H H^T \right)^{-1} T \quad (3.61)$$

the output function of ELM is formulated as

$$f(x) = h(x)\beta = h(x)H^T \left(\frac{1}{\lambda} + H H^T \right)^{-1} T \quad (3.62)$$

if β is selected

$$\beta = \left(\frac{1}{\lambda} + H H^T \right)^{-1} H^T T \quad (3.63)$$

the output function of ELM is formulated as

$$f(x) = h(x)\beta = h(x) \left(\frac{1}{\lambda} + H H^T \right)^{-1} H^T T \quad (3.64)$$

3.6.3. The Proposed ELM Autoencoder Kernels

An autoencoder is an ANN algorithm which stands for performing unsupervised learning in effective ways (Liou et al., 2008; Liou et al., 2014). The autoencoder generates a representation of input data with decreased or increased size of dimensionality models. In the last decades, the autoencoder algorithms have been frequently used along the popularization of Deep Learning approaches (Pascal et al., 2010).

The structure of the autoencoder is a feedforward model which is very similar to ANN with having input layer, output layer and hidden layer(s) as seen in Figure 3.35. The autoencoder constructs the outputs with the same number of nodes as the input layer from unlabelled data. Hence, the autoencoder approach is an unsupervised learning model which is commonly performed for pre-training of the models for preventing randomization. The ELM and ELM Autoencoder are universal approximations (Kasun et al., 2013). The autoencoder aims to learn a function to identify construction and deconstruction of the input as output nodes.

The autoencoder is comprised of two stages, the encoding stage and the decoding stage. Encoding transition, defined as Φ , employs the hidden layer weights to determine a function for outputs, decoding transition, defined as ψ employs the calculated hidden weights to reconstruct input such that:

$$\Phi: \mathcal{X} \rightarrow \mathcal{F} \quad (3.65)$$

$$\psi: \mathcal{F} \rightarrow \mathcal{X}$$

$$\psi, \Phi = \underset{\Phi, \psi}{\operatorname{argmin}} \|X - (\psi \circ \Phi)X\|^2$$

In the simplest form of autoencoder, one hidden layer exist and x is the input of the autoencoder

$$z = \sigma(Wx + b) \quad (3.66)$$

z is referred to the latent presentation of the given x , b is the bias vector of the hidden layer, W is the weight matrix. σ is the activation function for the encoding process. And the following equation is the decoding function:

$$x' = \sigma'(W'z + b') \quad (3.67)$$

Autoencoder aimed to train minimizing reconstruction errors.

$$\mathcal{L}(x, x') = \|x - x'\|^2 = \|x - \sigma'(W'\sigma(Wx + b) + b')\|^2 \quad (3.68)$$

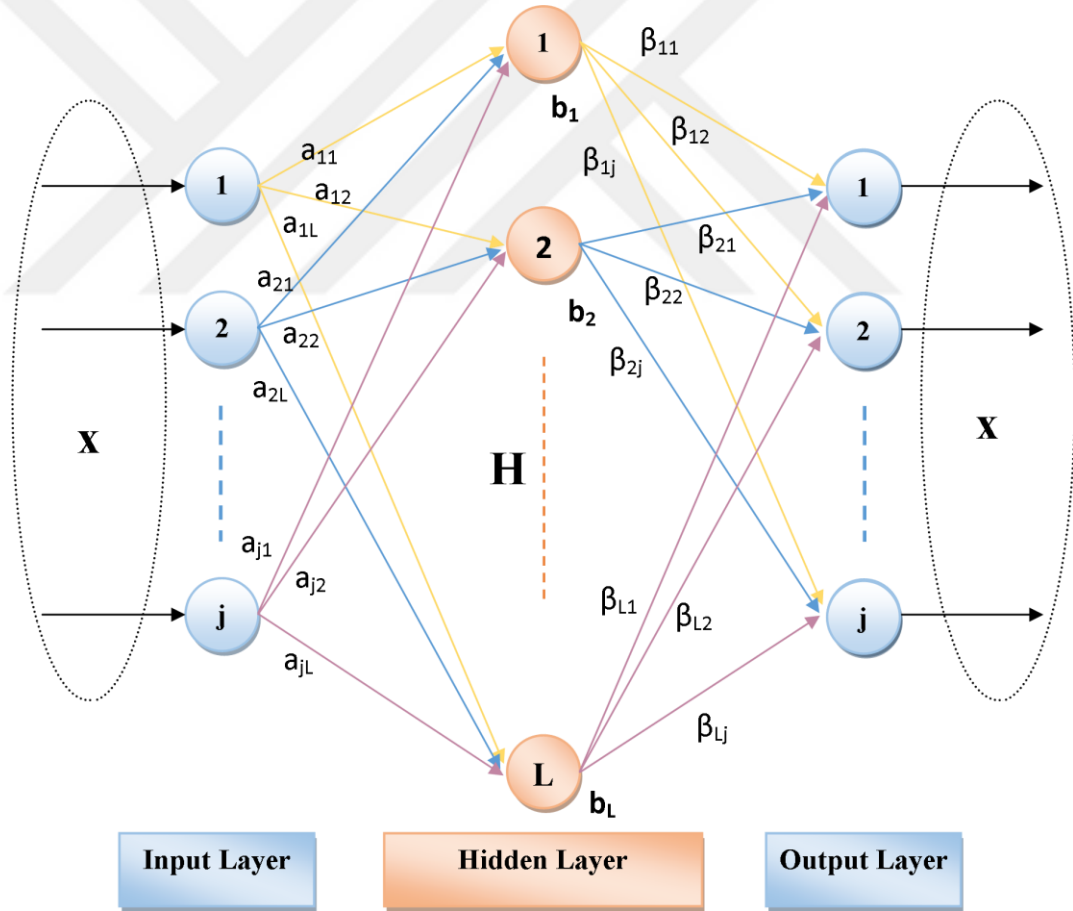


Figure 3.34. The ELM Autoencoder model

The ELM Autoencoder handles representing the input data in three representation ways considering the input size and output size. Compressed representation is performed

when the input dimension is higher than output dimension and reduces dimensional feature spaces. Sparse representation is performed when the input dimension is lower than output dimension and enlarges dimensional feature spaces using sparsity parameter. Equal dimension representation is performed when feature space dimensions of input and output dimension is well-matched (Kasun et al., 2013). The representations are calculated by Johnson-Lindenstrauss Lemma which declares that the Euclidean distances of various dimensional spaces can stand for the corresponding distances in both lower and higher dimensional spaces equally (Johnson and Lindenstrauss, 1984).

$$h = g(ax + b) \quad (3.69)$$

$$a^T a = I, \quad b^T b = 1 \quad (3.70)$$

a stands for orthogonal random weight vector and b is the orthogonal random bias between the input layer and hidden layer of ELM autoencoder. The output weights vector is β , H vector is the hidden layer outputs, X is the output and input data of the ELM autoencoder

When the number of training samples is more than the number of hidden layer node which means sparse ELM autoencoder.

$$\beta = \left(\frac{I}{C} + H^T H \right)^{-1} H^T X \quad (3.71)$$

When the number of training samples is less than the number of hidden layer node which means compressed ELM autoencoder.

$$\beta = H^T \left(\frac{I}{C} + H H^T \right)^{-1} X \quad (3.72)$$

When the number of training samples is equal to the number of hidden layer node which means equal dimension representation ELM autoencoder

$$\beta = H^{-1} X \quad (3.73)$$

$$\beta^T \beta = I \quad (3.74)$$

The input weights, bias of hidden layers of ELM Autoencoder are orthogonal. Different presentations of the given X can be analysed for various models with the help of the output matrix β .

3.6.4. The Proposed Multi-kernel Deep ELM

ELM Autoencoder enables composing output weights with an expected number of dimensionality. It has ability to compress the input data with dimensional reduction, to sparse the input data with a defined parameter amount. In ELM Autoencoder model the input and output have equal dimensions to obtain the weights of the connected nodes.

Sequential integration of more than one ELM Autoencoder constructs Multilayer ELM model. Multilayer ELM provides using ELM Autoencoder to train the parameters layer-by-layer. Multilayer ELM hidden layers' activation functions may be chosen in a manner of linear and nonlinear analysis. If the last hidden layer in multilayer ELM is handled with a kernel ELM model, Multilayer ELM model is expanded to the Deep ELM model (seen in Figure 3.36).

$$H_{k+1}H_{k+1}^T = \Theta_{Deep} \quad (3.75)$$

The output weight matrix β_{Deep} in Deep ELM can be formulated as in (3.94) and the classification of formula of Kernel ELM can be formulated as in (3.95):

$$\beta_{Deep} = \left(\frac{I}{C} + \Theta_{Deep} \right)^{-1} T \quad (3.76)$$

$$f(x) = h_{k+1}(h_k(x))H_{k+1}^T \beta_{Deep} = \begin{bmatrix} K(h_k(x), H_k(:, 1)) \\ \vdots \\ K(h_k(x), H_k(:, N)) \end{bmatrix}^T \left(\frac{I}{C} + \Theta_{Deep} \right)^{-1} T \quad (3.77)$$

The proposed Multi-kernel Deep ELM model is consists of the traditional ELM autoencoder, Lower Upper decomposition based ELM autoencoder, and Hessenberg decomposition based ELM autoencoder models.

3.6.4.1. The Proposed Lower Upper Decomposition based ELM Autoencoder

Many theoretical approaches are focused on how to find inverses of matrices in effective ways. Lower Upper (LU) triangularization method is a proper method which is moderately easy to implement. LU decomposition was uttered by Alan Turing in 1948 (Bunch and Hopcroft, 1974). The LU decomposition has ability to solve a set of simultaneous linear equations. It might also provide a learning capability on more advanced matrix factorization for machine learning algorithms. The biggest advantage of LU decomposition is the time-consuming elimination. This process can be formulated requiring only matrix H (Bunch and Hopcroft, 1974; Golub and Van Loan, 2012). Additionally, It decomposes stability inverse once for calculating several matrices of b for $Hx = b$.

Matrix H can be decomposed as $H = LU$, where L is a lower triangular matrix and U is an upper triangular matrix (Golub and Van Loan, 2012; Press et al., 1992).

$$\begin{bmatrix} h_{11} & h_{12} & h_{13} \\ h_{21} & h_{22} & h_{23} \\ h_{31} & h_{32} & h_{33} \end{bmatrix} = \begin{bmatrix} l_{11} & 0 & 0 \\ l_{21} & l_{22} & 0 \\ l_{31} & l_{32} & l_{33} \end{bmatrix} \begin{bmatrix} u_{11} & u_{12} & u_{13} \\ 0 & u_{22} & u_{23} \\ 0 & 0 & u_{33} \end{bmatrix} \quad (3.78)$$

The decomposition enables the original equation, substituted into $(LU)W = b$:

$$\left(\begin{bmatrix} l_{11} & 0 & 0 \\ l_{21} & l_{22} & 0 \\ l_{31} & l_{32} & l_{33} \end{bmatrix} \begin{bmatrix} u_{11} & u_{12} & u_{13} \\ 0 & u_{22} & u_{23} \\ 0 & 0 & u_{33} \end{bmatrix} \right) \begin{bmatrix} W_1 \\ W_2 \\ W_3 \end{bmatrix} = \begin{bmatrix} b_1 \\ b_2 \\ b_3 \end{bmatrix} \quad (3.79)$$

If we assume that $(LU)W = b$, and $UW = d$, where d is a different column vector considering b , we obtain two different $HW = b$ formulation

$$\begin{bmatrix} l_{11} & 0 & 0 \\ l_{21} & l_{22} & 0 \\ l_{31} & l_{32} & l_{33} \end{bmatrix} \left(\begin{bmatrix} u_{11} & u_{12} & u_{13} \\ 0 & u_{22} & u_{23} \\ 0 & 0 & u_{33} \end{bmatrix} \begin{bmatrix} W_1 \\ W_2 \\ W_3 \end{bmatrix} \right) = \begin{bmatrix} b_1 \\ b_2 \\ b_3 \end{bmatrix} \quad (3.80)$$

We can resolve all the elements of W and d matrix. We first calculate $Ld = b$ for matrix d , then we substitute into $UW = d$ to calculate matrix W .

$$\begin{bmatrix} l_{11} & 0 & 0 \\ l_{21} & l_{22} & 0 \\ l_{31} & l_{32} & l_{33} \end{bmatrix} \begin{bmatrix} d_1 \\ d_2 \\ d_3 \end{bmatrix} = \begin{bmatrix} b_1 \\ b_2 \\ b_3 \end{bmatrix} \quad (3.81)$$

$$\begin{bmatrix} u_{11} & u_{12} & u_{13} \\ 0 & u_{22} & u_{23} \\ 0 & 0 & u_{33} \end{bmatrix} \begin{bmatrix} W_1 \\ W_2 \\ W_3 \end{bmatrix} = \begin{bmatrix} d_1 \\ d_2 \\ d_3 \end{bmatrix}$$

In the matrix L all elements above the diagonal are zero, in the matrix U , all the elements below the diagonal are zero.

The following circumstances must be met for LU decomposition (Bunch and Hopcroft, 1974):

- The matrix H must be square matrix,
- The matrix H must be non-singular (invertible) matrix to avoid producing singular L and U .
- Some of the amounts in the L and U matrices must be known before the decomposition to avoid too many unknowns and equations. Diagonal matrix may set to 1.

For solving L and U matrixes, following equations are used

for $i=1, 2, \dots, n$ and $j=2, 3, \dots, n$

$$l_{i1} = h_{i1} \quad (3.82)$$

$$u_{1j} = \frac{h_{1j}}{l_{11}} \quad (3.83)$$

for $j=2, 3, \dots, n-1$ and $i=j, j+1, \dots, n$

$$l_{ij} = h_{ij} - \sum_{k=1}^{j-1} l_{ik} u_{kj} \quad (3.84)$$

for $k=j+1, j+2, \dots, n$

$$u_{jk} = \frac{h_{jk} - \sum_{j=1}^{j-1} l_{ji} u_{ik}}{l_{jj}} \quad (3.85)$$

$$l_{nn} = h_{nn} - \sum_{k=1}^{n-1} l_{nk} u_{kn} \quad (3.86)$$

In the LU based ELM process, decompose of matrix H for solving $UW = y$, and $Ly = b$ using forward substitutions

$$HW = (L U)W = L(U W) = b \quad (3.87)$$

$$y_1 = \frac{b_1}{l_{11}} \quad (3.88)$$

$$y_2 = \frac{b_2 - (l_{21} * y_1)}{l_{22}} \quad (3.89)$$

$$\vdots$$

$$y_i = \frac{1}{l_{ii}} \left(b_i - \sum_{j=1}^{i-1} l_{ij} y_j \right)$$

where $i = 2, \dots, N$. For solving triangular system $UW = y$ for W using backward substitution

$$W_{end} = \frac{y_{end}}{u_{end,end}} \quad (3.90)$$

$$W_{end-1} = \frac{y_{end-1} - (u_{end-1,end} * W_{end})}{u_{end-1,en-1}} \quad (3.91)$$

$$\vdots$$

$$W_i = \frac{1}{u_{ii}} \left(y_i - \sum_{j=i+1}^N u_{ij} W_j \right)$$

3.6.4.2. The Proposed Hessenberg Decomposition based ELM Autoencoder

Hessenberg decomposition is a matrix decomposition of a real symmetric matrix A into a unitary matrix P and a tri-diagonal symmetric Hessenberg matrix H such that (Golub and Van Loan, 1996).

$$P H P^H = A \quad (3.92)$$

where P^H symbolizes the conjugate transpose.

The eigenvectors of matrix H are in general different from the eigenvectors of matrix A . Hessenberg decomposition has ability to handle only square matrix. It needs least square solution to decompose rectangular matrix. It is utilized as intermediate staging of a wide variety of mathematical models that can profit positively from its structure close to the structure of an upper-triangular matrix (Golub and Van Loan, 1996).

If we assume H as the pseudoinverse of hidden layer output

$$H^+ = H^T (H^T H)^{-1} \quad (3.93)$$

to retrieve H^+ , square matrix $H^T H$ needs to be decomposed using Hessenberg decomposition

$$H^T H = Q U Q^* \quad (3.94)$$

where Q is a unitary matrix, and U stands for the upper Hessenberg matrix,

$$H^+ = H^T (Q U Q^*)^{-1} \quad (3.95)$$

$$H^+ = H^T Q U^{-1} Q^*$$

As a result, the decomposed matrix U is non-singular (invertible) and $|U| \neq 0$. The Hessenberg decomposition based ELM is performed by substituting H^{-1} and with H^+ and the output weights were calculated.

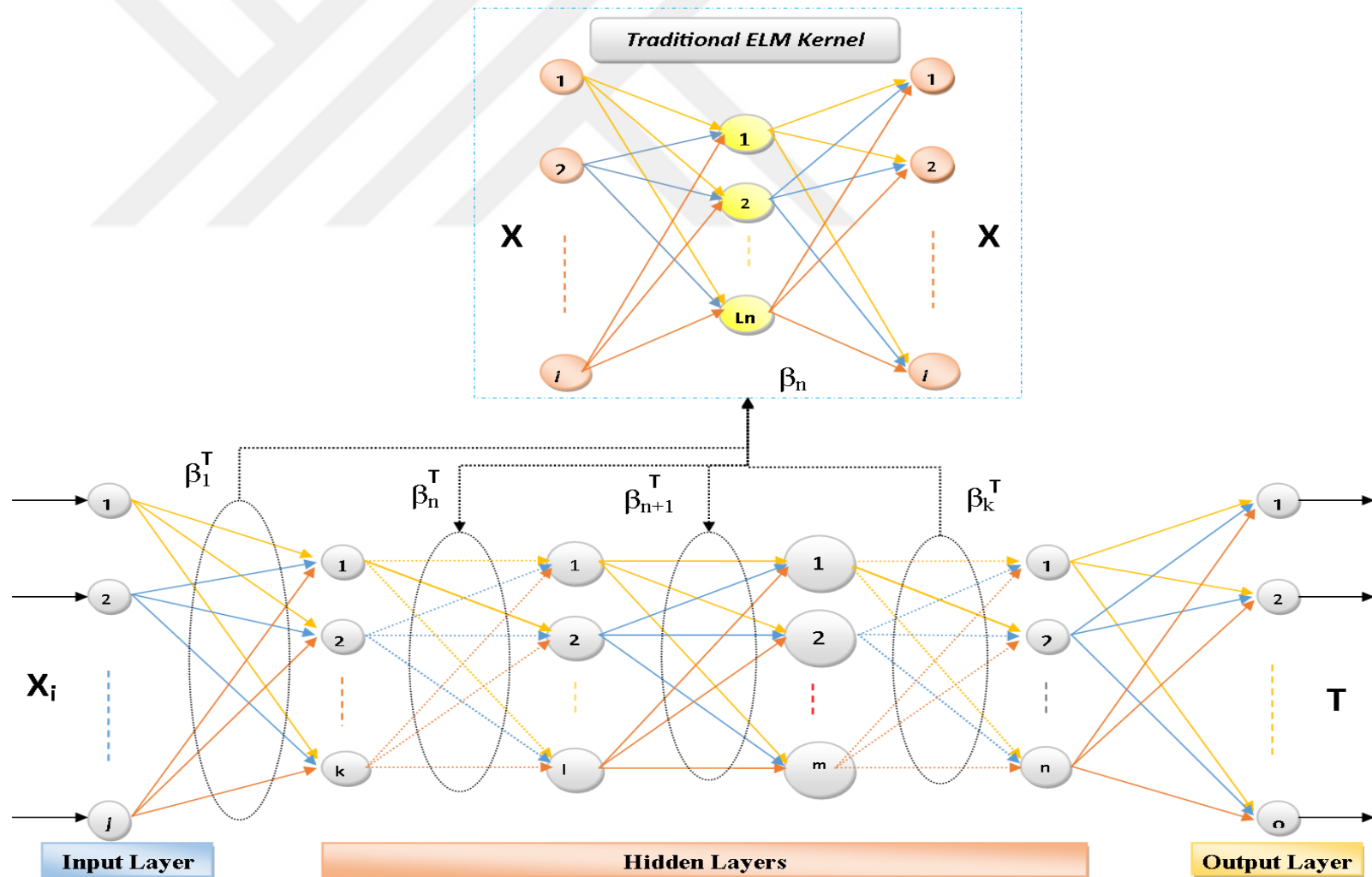


Figure 3.35. Deep ELM Mode

The proposed Multi-kernel Deep ELM model differentiates from the Deep ELM model from with the kernel selection optionality. The proposed model encapsulates both traditional ELM kernels, Lower Upper (LU) decomposition based ELM autoencoder kernel, and Hessenberg decomposition based ELM autoencoder kernel in its kernel module (seen in Figure 3.37). This structure enables Deep ELM models to realize with different mathematical solutions with the same hidden layer sizes and to analysis the different depths more quickly and effectively in the both autoencoder stages and supervised learning stages.

3.7. Feature Selection

One of the most significant steps in pattern recognition approaches is feature selection. The feature selection process aims to reduce the dimensionality of the feature set and to define the features which are high responsible for the models. Especially, a high feature dimension in the training stages is a big problem that needs to be overcome. According to “No free lunch” and “Ugly Duckling” theorems which are the fundamental approaches for pattern recognition, features are not labelled for a specific class, the dataset needs to include as much as possible features to detect the responsible characteristic information. Feature selection approaches are used to denote the meaningless, useless features for recognition. In pattern recognition and statistics terminology it is also called as attribute selection and feature dimensionality reduction.

The features from 16-channels are fed into the classifier for the respiratory sounds analysis models. The feature selection algorithm is used to archive the highest classification performances by removing meaningless features.

Determining the responsibility of feature for the proposed models is an essential approximation to reach the high classification performances including specificity, accuracy and more. The high dimensional features also results with long training times. The training time is a restriction on data mining and machine learning models with the supervising approximations. A variety of feature selection techniques have been proposed to determine high responsible features in the literature for classification or clustering.

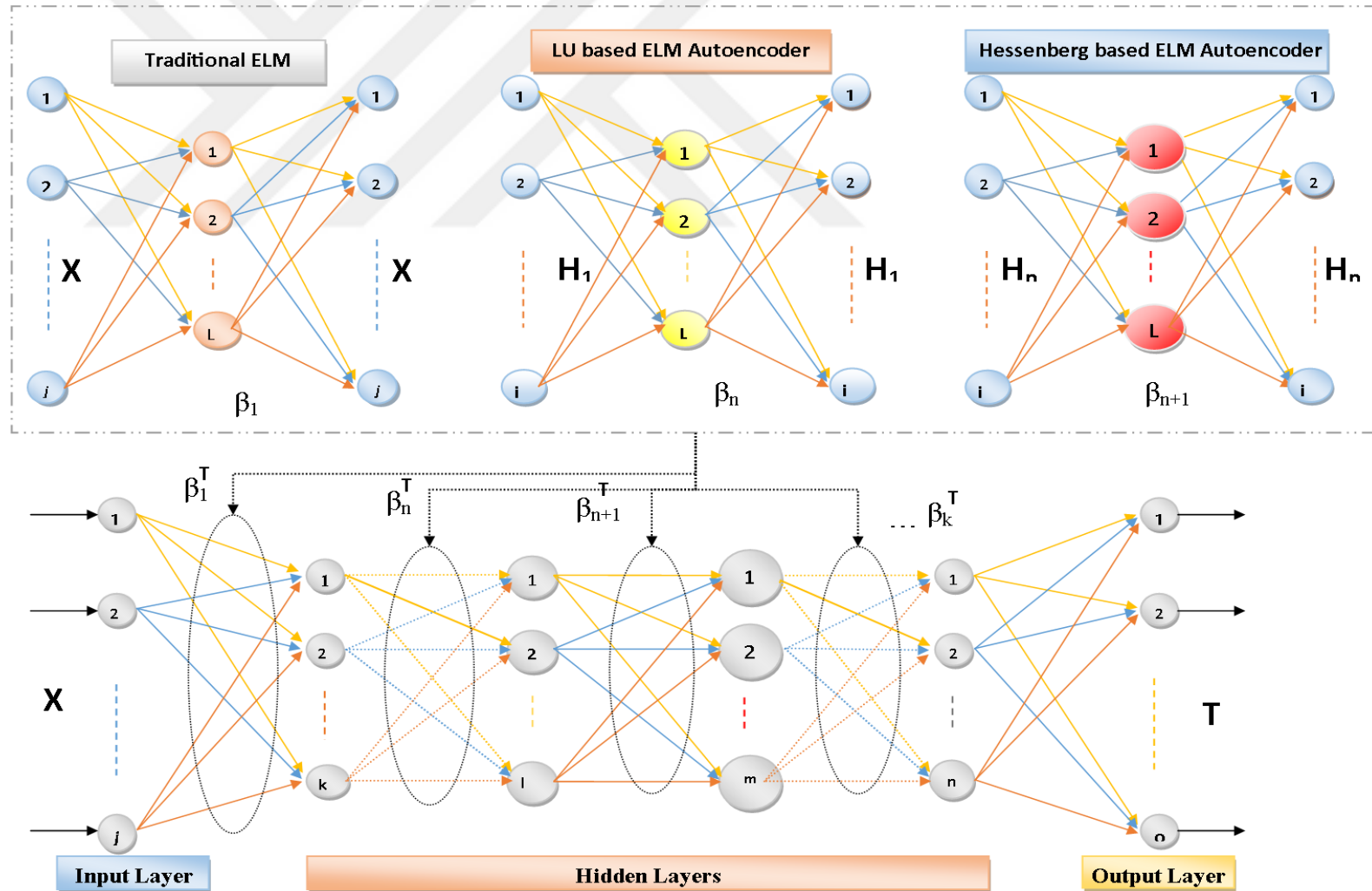


Figure 3.36. The proposed Multi-kernel Deep ELM Model

3.7.1. Least-Square Method

Let $AX = Y$ be a system of linear equation with n equations and m variables. If there are more equations than variables, $n > m$, system of linear equation is said to be overdetermined. And in contrast, if variables outnumber equations, $m > n$, such system of linear equation is said to be underdetermined. Least-square method shed light for solving systems of linear equations that are overdetermined or underdetermined. Since A is not a square matrix, in general A^{-1} does not exist. However pseudoinverse matrix, $\text{pinv}(A)$, that converges to inverse matrix can be used for solving such systems of linear equations. This is not exact true solution we expected but it is a close solution that can be reached.

If $AX = Y$ is an overdetermined system of equation,

$$\text{pinv}(A) = A^+ = (A^T A)^{-1} A^T \quad (3.96)$$

$$X = A^+ Y$$

If $AX = Y$ is an underdetermined system of equation,

$$A^+ = \text{pinv}(A) = A^T (A^T A)^{-1} \quad (3.97)$$

$$X = A^+ Y$$

As it can be observed, $A^T A$, which is used in both cases, is a square matrix. Therefore $(A^T A)^{-1}$ exists. Least square solution is used in proposed Hess-ELM and kernel ELM models.

3.7.2. Sequential Forward Feature Selection

The redundancy of feature dimension ceaselessly ascends because of analysing the high number of the channels from the biomedical signals and signal processing methods. The SFFS approach embeds the ELM model for the classification process with the

objective to decrease consumption and associated costs of training and testing time during classification by reducing feature dimension (Rückstieß et al., 2011).

The SFFS algorithm learns which features are most responsible for the confidence of the machine learning problem by attaching the next best feature to the already composed feature set. The main idea for the SFFS is deciding which feature achieves better classification performance to select next feature considering the previously-selected together (Reunanen, 2006; Rückstieß et al., 2011).

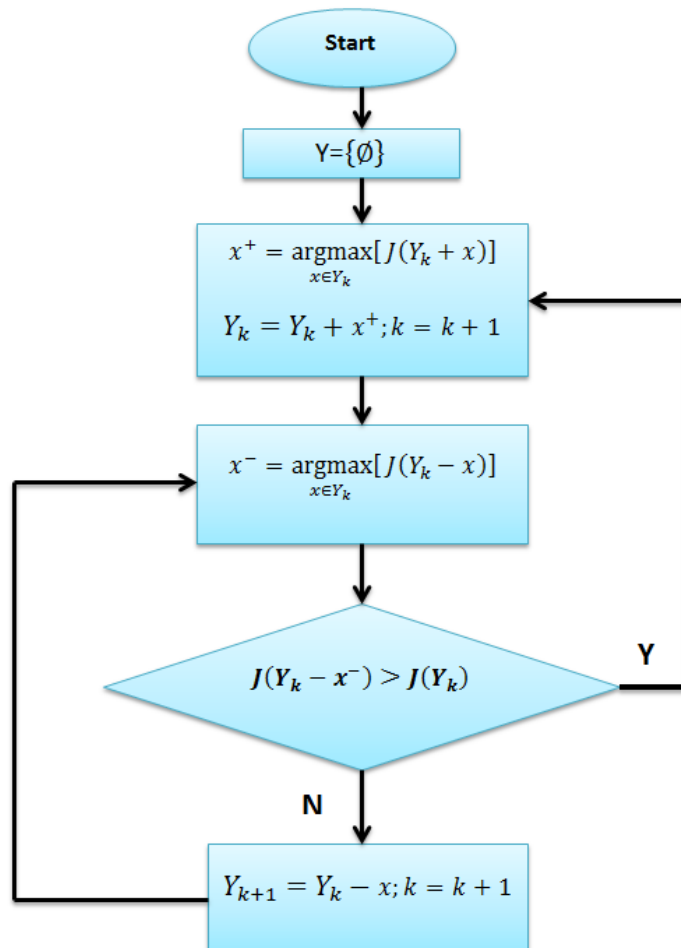


Figure 3.37. The SFFS algorithm

The fundamental SFFS algorithm starts with an empty feature set and attaches the most responsible feature at each step to the previously composed feature set until a

predefined number of feature dimension is achieved, or the classification performance does not achieve further metrics anymore. In rout thesis, the SFFS algorithm is preceded to the end. At each step of the SFFS, every candidate feature is separately attached into the current feature set and the performance measurements are evaluated subsequently. If the most responsible new feature set enlarges more than reached threshold, the SFFS continues with the feature in process, otherwise the SFFS is terminated. The SFFS algorithm is given in Figure 3.38.

3.7.3. Cross Validation

Cross-validation is an algorithm which iterates various feature sets to generalize to new feature sets. The algorithm is named as *k*-Fold Cross Validation. The *k* represents the dividing parameter for the dataset. The entire dataset is homogenously and randomly divided into *k* equal size subsets (McLachlan, 2004). The *k* parameter is selected as four. 4-Fold cross validation means 75% of the samples are fed into the training, and remaining 25% of the dataset is utilized to test the trained model. To prevent the overfitting in learning phases, homogenous distribution is selected in many studies. In this thesis, an equal number of samples from various COPD severities are folded into *k* sub-feature sets. The *k-1* fold are gathered and used in the training of the model, and the remaining last fold is utilized in the test stage of the model. This process is repeated for *k* times leaving one unique fold for estimation and the average of the performance measurements are evaluated as the system performance. However, in our dataset randomly dividing data into train and test data may result in problems considering the various sample sizes (seen in Figure 3.39). So the smallest sample size, the COPD1, is handled as the base for feature sizes. The remaining samples from the other classes are homogenously deployed to testing sets. It was noticed that each feature set encloses all samples for training and testing the proposed model.

3.8. Performance Measurements and Statistical Analysis

In this thesis, the classification of five types of the COPD severity is evaluated due to the fact that output is a five-class condition. One of most coherent models for estimating the performance of classifiers is based the confusion matrix analysis. The confusion matrix for n class output is seen in Table 3.5. The number of correctly classified samples is not enough to judge the accurate of the proposed methods. Especially, the heterogeneous distributed sample size results inaccurate assessments, although achieving high classification accuracy. This circumstance needs various metric requirements for the machine learning approaches.

True Positive Rate (TPR, Recall, and Sensitivity) defined as the number of true positives in total number of samples that actually belong to positive class.

True Negative Rate (TNR, Specificity) is the number of true negatives (TN) in divided by total number of elements that actually belong to negative class.

Table 3.5. Confusion Matrix for n classes.

		Predicted			
		Class 1	Class 2	...	Class n
Actual	Class 1	x_{11}	x_{12}	...	x_{1n}
	Class 2	x_{21}	x_{22}	...	x_{2n}
	...				
	Class n	x_{n1}	x_{n2}	...	x_{nn}

$$FN_i = \sum_{\substack{j=1 \\ j \neq i}}^n x_{ij} \quad (3.98)$$

$$FP_i = \sum_{\substack{j=1 \\ j \neq i}}^n x_{ji} \quad (3.99)$$

$$TN_i = \sum_{\substack{j=1 \\ j \neq i}}^n \sum_{\substack{k=1 \\ k \neq i}}^n x_{jk} \quad (3.100)$$

$$TP_{all} = \sum_{j=1}^n x_{jj} \quad (3.101)$$

$$\text{Overall Accuracy} = \frac{TP_{all}}{\text{Total Number of Samples}} \quad (3.102)$$

$$\text{Sensitivity}_i = \frac{TP_{all}}{TP_{all} + FN_i} \quad (3.103)$$

$$\text{Specificity}_i = \frac{TN_i}{TN_i + FP_i} \quad (3.104)$$

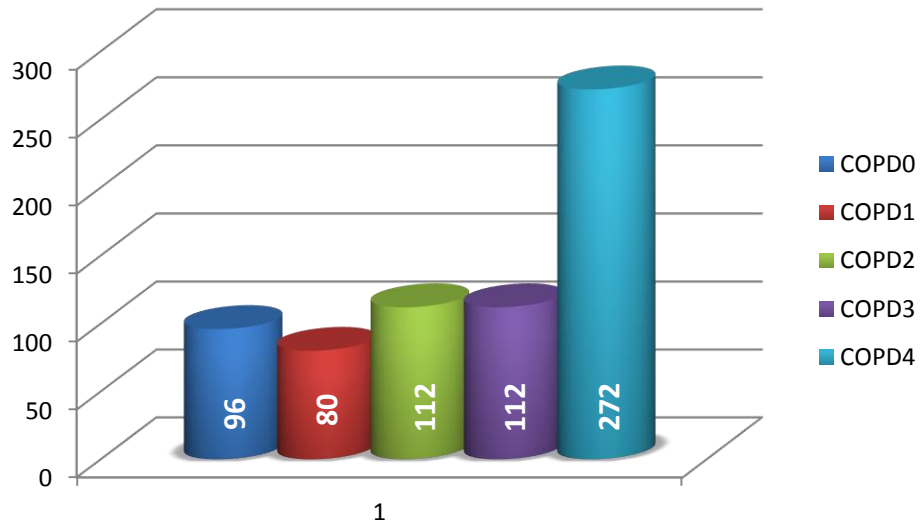


Figure 3.38. Class distribution of COPD severity

4. RESEARCH FINDINGS AND RESULTS

The developments achieved through extensive studies on the Computer-aided respiratory analysis have increased the usefulness of the monitoring, detection, diagnosis and analysis competencies as well as the findings about the patients and the functionality that ensures the preservation of the laboratory tests. Enabling easy and online access to the clinical data provides a great way to modernize the acquired data to a large patient cloud that aims meeting quality assurance needs. Sensitivity and reliability in computer-aided respiratory analysis are judge independent test characteristics used for the analysis and testing of processes in which the patient population is not very large and homogeneous (Duda et al., 2012).

In this thesis, a unique multimedia respiratory database, named RespiratoryDatabase@TR, is presented. The database consists of chest X-rays, auscultation sounds including 4-channel heart sounds and 12-channel lung sounds the PFT measurements, the SGRQ-C questionnaire answers. The RespiratoryDatabase@TR enables assessments on respiratory diseases using computerized signal analysis techniques. All analyses are based on the auscultation sounds.

The SGRQ-C questionnaire is the highest validity patient situation based grouping questionnaire with detailed information about the stages of the COPD. The SGRQ-C questionnaire answers collected from the subjects from RespiratoryDatabase@TR are evaluated with the statistical tests to check against the thesis analysis results.

A multi-kernel Deep ELM model is proposed. The conventional ELM kernel, Lu-based ELM kernel and Hessenberg decomposition-based ELM kernel integration constructed the multi-kernel model. In each layer ELM autoencoder, the kernel is selected sequentially. Performances of proposed models are compared to the DBN classifier. Different signal transform methods are applied to the lung sounds or entire auscultation sounds to diagnose the COPD and the COPD severity classification. The classification performances, namely all over accuracy (ACC), weighted sensitivity (WA-SEN), and weighted specificity (WA-SPE) are compared with each other.

In the classification processes, dataset is divided into four fold using 4-fold cross validation algorithm. Three folds are used to train the classifier models when subsequent fold is used to test the proposed model. In this way, all circumstances are counted in the training and testing separately to evaluate performance measurements.

Proposed classifier and transform techniques integration is tested on 77 subjects for various respiratory diseases on RespiratoryDatabase@TR. In the COPD analysis the highest responsible features from DWT, HHT and proposed 3D-SODP quantization are specified for the SFFS algorithm and results are evaluated.

4.1. The Statistical Analysis of SGRQ-C

Analysis of variance (ANOVA) is a great approximation for comparing the differences between group means. The ANOVA has ability to extract the assessment metrics which are related with how different alloys are close to the mean strength of the results. The ANOVA provides assessing response variables simultaneously. ANOVA is applied to evaluate the accuracy of the SGRQ-C and physician patient labelling to validate efficiency of patient selection analysis. Dependent variable and independent variable are given below. The results are presented in Table 4.1, and Table 4.2.

Dependent variable: SGRQ-C answers. It is comprised of information of related the patient conditions.

Hypothesis to compare mean values are given below (p significance value: 0.05):

H_0 : There is no statistical meaningful difference between SGRQ-C answers and patient decisions with 95 % confidence.

H_1 : There is statistical meaningful difference between SGRQ-C answers and patient decisions with 95 % confidence.

The SGRQ-C questionnaire answers collected from the subjects in RespiratoryDatabase@TR are statistically analysed with ANOVA to check against the thesis analysis results. The results indicate the most distinctive questions with high significance close to zero.

Table 4.1. ANOVA Statistical Analysis of the SGRQ-C Questions

Question No	Sum of Squares	df	Mean Square	F	Sig.
General	1,897	3	,632	1,671	,189
1.1	9,951	3	3,317	2,666	,061
1.2	9,385	3	3,128	1,241	,308
1.3	21,491	3	7,164	7,556	,000
1.4	15,120	3	5,040	2,859	,049
1.5	11,431	3	3,810	10,895	,000
1.6	5,130	3	1,710	4,296	,010
1.7	,796	3	,265	1,154	,340
2.8	6,197	3	2,066	7,164	,001
2.9.a	2,839	3	,946	7,635	,000
2.9.b	1,635	3	,545	2,723	,057
2.9.c	1,930	3	,643	4,369	,010
2.9.d	,310	3	,103	6,047	,002
2.9.e	,310	3	,103	6,047	,002
2.10.a	,064	3	,021	,109	,954
2.10.b	1,326	3	,442	3,323	,029
2.10.c	1,630	3	,543	3,231	,033
2.10.d	1,122	3	,374	4,425	,009
2.10.e	,878	3	,293	2,027	,126
2.10.f	,789	3	,263	2,346	,088
2.11.a	,869	3	,290	1,544	,218
2.11.b	,382	3	,127	,907	,447
2.11.c	,835	3	,278	1,100	,361

Table 4.2. (Continued) ANOVA Statistical Analysis of the SGRQ-C Questions

Question No	Sum of Squares	df	Mean Square	F	Sig.
2.11.d	2,614	3	,871	8,720	,000
2.11.e	1,444	3	,481	6,312	,001
2.11.f	1,198	3	,399	1,889	,147
2.11.g	2,839	3	,946	7,635	,000
2.12.a	2,281	3	,760	6,134	,002
2.12.b	2,281	3	,760	6,134	,002
2.12.c	1,727	3	,576	6,534	,001
2.12.d	2,117	3	,706	7,351	,001
2.12.e	1,444	3	,481	6,312	,001
2.12.f	,432	3	,144	2,379	,084
2.12.g	,983	3	,328	3,718	,019
2.12.i	,654	3	,218	2,856	,049
2.13.a	2,539	3	,846	5,844	,002
2.13.b	4,495	3	1,498	9,352	,000
2.13.c	3,492	3	1,164	6,300	,001
2.13.d	5,658	3	1,886	17,902	,000
2.13.e	2,464	3	,821	4,589	,008
Additional 1	2,497	3	,832	4,170	,012
Additional 2	2,038	3	,679	3,144	,036
Additional 3	2,492	3	,831	4,926	,005
Additional 4	,666	3	,222	1,235	,310
Additional 5	3,884	3	1,295	9,736	,000
Additional 6	,561	3	,187	,901	,449
Additional 7	1,786	3	,595	3,188	,034
Additional 8	,578	3	,193	1,422	,251
Additional 9	,067	3	,022	,201	,895

Table 4.3. Levene's Test and T-test Statistical Analysis of the SGRQ-C Questions

Questions	Levene's Test for Equality of Variances		t-test for Equality of Means						
	F	Sig.	t	df	Sig. (2- tailed)	Mean Difference	Std. Error Difference	95% Confidence Interval of the Difference	
								Lower	Upper
General	,774	,396	,350	12	,732	,121	,346	-,634	,876
1.1	75,429	,000	4,342	12	,001	2,000	,461	,997	3,003
1.2	,510	,489	-,413	12	,687	-,303	,733	-1,901	1,295
1.3	75,429	,000	4,342	12	,001	2,667	,614	1,329	4,005
1.4	33,541	,000	3,768	12	,003	2,485	,660	1,048	3,922
1.5	,454	,513	2,776	12	,017	1,212	,437	,261	2,164
1.6	9,172	,010	2,562	12	,025	1,061	,414	,159	1,963
1.7	,829	,381	1,699	12	,115	,485	,285	-,137	1,107
2.8	18,857	,001	3,761	12	,003	1,000	,266	,421	1,579
2.9.a	75,429	,000	-4,342	12	,001	-,667	,154	-1,001	-,332
2.9.b	3,229	,098	-2,439	12	,031	-,576	,236	-1,090	-,061
2.9.c	3,229	,098	-2,439	12	,031	-,576	,236	-1,090	-,061
2.9.d	75,429	,000	-2,171	12	,051	-,333	,154	-,668	,001
2.9.e	75,429	,000	-2,171	12	,051	-,333	,154	-,668	,001
2.10.a	,829	,381	-,531	12	,605	-,152	,285	-,773	,470
2.10.b	75,429	,000	-4,342	12	,001	-,667	,154	-1,001	-,332
2.10.c	3,229	,098	-2,439	12	,031	-,576	,236	-1,090	-,061
2.10.d	75,429	,000	-4,342	12	,001	-,667	,154	-1,001	-,332

Table 4.4. (Continued) Levene's Test and T-test Statistical Analysis of the SGRQ-C Questions

Questions	Levene's Test for Equality of Variances		t-test for Equality of Means						
	F	Sig.	t	df	Sig. (2- tailed)	Mean Difference	Std. Error Difference	95% Confidence Interval of the Difference	
								Lower	Upper
2.10.e	3,229	,098	-2,439	12	,031	-,576	,236	-1,090	-,061
2.10.f	75,429	,000	-2,171	12	,051	-,333	,154	-,668	,001
2.11.a	,774	,396	-,350	12	,732	-,121	,346	-,876	,634
2.11.b	,123	,732	,191	12	,852	,061	,317	-,631	,752
2.11.c	,123	,732	-1,241	12	,238	-,394	,317	-1,085	,297
2.11.d	75,429	,000	-4,342	12	,001	-,667	,154	-1,001	-,332
2.11.e	75,429	,000	-4,342	12	,001	-,667	,154	-1,001	-,332
2.11.f	3,229	,098	-2,439	12	,031	-,576	,236	-1,090	-,061
2.11.g	75,429	,000	-4,342	12	,001	-,667	,154	-1,001	-,332
2.12.a	75,429	,000	-4,342	12	,001	-,667	,154	-1,001	-,332
2.12.b	75,429	,000	-4,342	12	,001	-,667	,154	-1,001	-,332
2.12.c	75,429	,000	-4,342	12	,001	-,667	,154	-1,001	-,332
2.12.d	75,429	,000	-4,342	12	,001	-,667	,154	-1,001	-,332
2.12.e	75,429	,000	-4,342	12	,001	-,667	,154	-1,001	-,332
2.12.f	75,429	,000	-2,171	12	,051	-,333	,154	-,668	,001
2.12.g	75,429	,000	-2,171	12	,051	-,333	,154	-,668	,001
2.12.i	75,429	,000	-2,171	12	,051	-,333	,154	-,668	,001
2.13.a	75,429	,000	-4,342	12	,001	-,667	,154	-1,001	-,332
2.13.b	3,229	,098	-2,439	12	,031	-,576	,236	-1,090	-,061

Table 4.5. (Continued) Levene's Test and T-test Statistical Analysis of the SGRQ-C Questions

Question	Levene's Test for Equality of Variances		t-test for Equality of Means					95% Confidence Interval of the Difference	
	F	Sig.	t	df	Sig. (2- tailed)	Mean Difference	Std. Error Difference	Lower	Upper
2.13.c	3,229	,098	-2,439	12	,031	-,576	,236	-1,090	-,061
2.13.d	75,429	,000	-4,342	12	,001	-,667	,154	-1,001	-,332
2.13.e	,123	,732	-1,241	12	,238	-,394	,317	-1,085	,297
Additional 1	3,229	,098	-2,439	12	,031	-,576	,236	-1,090	-,061
Additional 2	9,874	,008	-2,619	12	,022	-,727	,278	-1,332	-,122
Additional 3	1,270	,282	5,071	12	,000	,909	,179	,518	1,300
Additional 4	9,874	,008	,982	12	,345	,273	,278	-,332	,878
Additional 5	75,429	,000	-4,342	12	,001	-,667	,154	-1,001	-,332
Additional 6	3,229	,098	-1,027	12	,325	-,242	,236	-,757	,272
Additional 7	,829	,381	1,699	12	,115	,485	,285	-,137	1,107
Additional 8	3,229	,098	-1,027	12	,325	-,242	,236	-,757	,272
Additional 9	1,270	,282	,507	12	,621	,091	,179	-,300	,482

Judging by the significance (sig) results of the questions with the ANOVA statistical test given in Table 4.1 and Table 4.2, eight questions (including 1.2, 1.7, 2.10.a-e, 2.11.a-b-c-f) have no statistical meaningful for the classification of the COPD severity. The apart from the eight questions have achieved a severely statistical difference between SGRQ-C answers and patient decisions with 95 % confidence. In addition to the ANOVA test, the significance of the SGRQ answers and the COPD severities also have statistical meaning with the Levene's Test and T-test Statistical Analysis results which are presented for evaluating a complete comparison for statistical meaningful between COPD severity classification and SGRQ-C questionnaire in Table 4.3, Table 4.4, and Table 4.5.

4.2. Signal Length Impact

In the signal processing models different characteristics can be determined depending on the signal length. Depending on the analysis problem, some biomedical analysis address short-term signals, while others on long-term signals. Among the main causes of this situation is that, the deterministic features searched depending on the type of the processed signal appear in certain periods in time for disorders, and some abnormalities can be encountered suddenly and independently in the time. The pathological sounds on the lung sounds can be evaluated as short-term signal because of the obstacles in the lungs and the persistence and continuity of the narrowing of the airways.

Whereas the long-term signals provide detailed analysis possibility for various scenarios on applications such as designing management systems, computer-assisted models, diagnosis models, and optimizing classification structures, detailed and in-depth analyses of shorter signature portions are more practical and should be selected to investigate. The most important and common feature for medical diagnostic models and machine learning applications is to achieve high discrimination performance as fast as possible. The deep breathing scenario takes about 5 seconds for the entire patient and healthy population for 1 cycle duration. Therefore, the lung sound recordings from RespiratoryDatabase@TR are analysed for at least 5s, 10s, and 15sn segments and attempting has been performed to determine an optimum signal length for the COPD severity classification by benchmarking the performances. The high accurate COPD severity classification kernel LU decomposition based Deep ELM kernel is utilized as the classifier model for length impact. The classification performances of the proposed LU based Deep ELM COPD severity classification model for SFFS is presented in Table 4.6 for 5s, 10s, and 15s lung sounds.

Table 4.6. The classification overall accuracy (%) of the proposed LU based Deep ELM model for various signal lengths on COPD severity classification

	5s	10s	15s
Accuracy	64.23	93.29	81.71

The same iteration ranges of classification parameters for the proposed LU based Deep ELM structures are fixed for three signal lengths. 15s short-term lung sounds are the most ineffective signal length for the COPD severity classification using the proposed multi-kernel Deep ELM and 3D-SODP for SFFS. The best discrimination rates of COPD severities are achieved analysing 10s lung sounds. The achieved results show that, too short lung sounds have low discrimination capability and lose the significant characteristic information for COPD severity classification considering the auscultation areas, and the proposed LU based Deep ELM model with 3D-SODP. 10s duration of lung sounds has a better separation performance for the proposed structures. Extracting 10s short-term lung sounds provides the correspondent sub-signature portions for further deterministic.

4.3. The COPD Analysis

The diagnosis of the COPD has a significant importance, because of aforementioned characteristics of the COPD. The wheeze analysis in literature was based on frequency analysis mostly. The proposed COPD analysis is focused on DWT application. The COPD diagnosis model is comprised of segmentation 10s lung sounds from RespiratoryDatabase@TR, applying DWT to lung sounds with various wavelets, statistical feature extraction and evaluating the features with the DBN and Deep ELM.

12-channel lung sounds from RespiratoryDatabase@TR are analysed to prepare the decisive and non-restrictive cases in 15 subjects with healthy subjects and the 15 patients with COPD including 3 subjects from each COPD severities. The lung sounds has a frequency rate of 4000 samples. Hence, the 5th level DWT is applied to lung sounds including 40000 data points. The five level DWT extracts Detail, Approximation-Detail, Approximation-Approximation-Detail, Approximation-Approximation-Approximation-

Detail, Approximation-Approximation-Approximation-Approximation-Detail, and Approximation-Approximation-Approximation-Approximation-Approximation subbands from the each lung sounds using Haar, Daubechies (db), and Symlets (sym) wavelets with various scaling functions (Altan et al., 2017). The aforementioned statistical and higher order statistical features were calculated from the subbands. The All feature set is comprised of the Haar, Daubechies (db4-db12), Symlets (sym4-sym12) wavelets.

The HHT is also applied to the 12-channel lung sounds from RespiratoryDatabase@TR. The EMD was applied to the lung sounds and IMFs were extracted with different characteristics of the signals. Since the number of the IMFs extracted from auscultation sounds can vary according to the frequency range and state of the signal, the number of IMFs varied between 5 and 7. The HHT analysis has been finalized by applying the Hilbert transformation to each IMF signal forms. The dataset is comprised of 12 statistical features including standard deviation, mean, median, maximum, minimum, variance, mode, correlation coefficient, kurtosis, moment, cumulant, and energy of the signal from all extracted IMFs except the residual signal were calculated.

Each statistical feature set is analysed independently using DBN, Multi-kernel Deep ELM model. The signal processing-based results are presented in the sub sections.

4.3.1. Deep Belief Networks Results

The features are fed into The DBN and the proposed multi-kernel Deep ELM classifiers. The DBN is iterated for 50 epochs. The proposed classification models were iterated within a limited range neuron size and hidden layer size. The neuron size is tested with a variety between 100-600 units and two hidden layers were placed in the both the proposed multi-kernel Deep ELM and DBN classifier models. The iterations are necessary for detecting the optimum parameters for classification problem. The DBN has a learning rate for backpropagation at the supervised phase. The learning rate is selected as 2 and the sigmoid activation function is utilized as the output function for the DBN model. The proposed DBN structure has 2 hidden layers with 340 neurons in first hidden layer and 580

neurons in second hidden layer. The classification performances of the DBN for each wavelet coefficient are given in the Table 4.7 and for HHT features are given in Table 4.8.

Table 4.7. The classification performances (%) of the DBN model for COPD diagnosis on each wavelet

Wavelets	ACC	WA-SEN	WA-SPE	Time(s)
Haar	39.17	35.56	42.78	0.49
db4	49.72	40.56	58.89	0.59
db5	43.89	40.56	47.22	0.56
db6	33.89	35.00	32.78	0.56
db7	44.44	41.11	47.78	0.63
db8	50.28	54.44	46.11	0.62
db9	45.28	44.44	46.11	0.67
db10	47.78	47.22	48.33	0.53
db11	40.83	41.11	40.56	0.63
db12	66.39	75.56	57.22	0.61
sym4	58.89	60.56	57.22	0.53
sym5	49.17	47.78	50.56	0.59
sym6	26.11	23.89	28.33	0.58
sym7	25.56	27.78	23.33	0.67
sym8	43.06	40.56	45.56	0.64
sym9	45.28	46.11	44.44	0.64
sym10	63.06	61.11	65.00	0.50
sym11	32.50	29.44	35.56	0.57
sym12	47.22	46.67	47.78	0.53
All	57.22	55.56	58.89	12.28

The highest DBN performance achievements for DWT wavelets are performed with classification rates of 66.39%, 75.56%, and 57.22% for accuracy, weighted average of sensitivity (WA-SEN), and the weighted average of specificity (WA-SPE), separately by using db12, sym10 wavelets.

Table 4.8. The classification performances (%) of the DBN model for COPD diagnosis on each HHT-based feature set

	ACC	WA-SEN	WA-SPE	Time(s)
IMF1	33,61	28,89	38,33	0.69
IMF2	62,78	66,67	58,89	0.53
IMF3	50,83	53,33	48,33	0.72
IMF4	47,50	54,44	40,56	0.63
IMF5	38,06	36,67	39,44	0.67
All	70,28	67,22	73,33	3.32

The highest DBN classification performance achievements for HHT-based IMF features are achieved with rates of 62.78%, 66.67%, and 58.89% for ACC, WA-SEN, and WA-SPE, separately by using IMF2 features. Using whole IMF feature sets as input of the DBN model has increased the classification performance to 70.28%, 67.22%, and 73.33% for ACC, WA-SEN, and WA-SPE, respectively.

4.3.2. The Proposed Multi-kernel Deep ELM Results

The performance metrics for the each kernel of Deep ELM model are evaluated in this section. The Deep ELM model with traditional ELM autoencoder kernel, LU decomposition based ELM autoencoder kernel, and Hessenberg decomposition based ELM autoencoder kernel is performed on both DWT and HHT features, respectively.

The proposed multi-kernel Deep ELM model with traditional ELM autoencoder kernel has achieved the highest performance using the experimented range of 2 hidden

layers with 210 neuron size in the first hidden layer, and unlike 470 neurons in second hidden layer.

Table 4.9. The classification performances (%) of the Deep ELM model with traditional ELM Autoencoder kernel for COPD diagnosis on each wavelet

Wavelets	ACC	WA-SEN	WA-SPE	Time(s)
Haar	41.67	47.78	35.56	0.07
db4	43.06	45.56	40.56	0.10
db5	36.39	46.11	26.67	0.11
db6	45.28	54.44	36.11	0.19
db7	31.67	27.22	36.11	0.16
db8	32.50	47.22	17.78	0.13
db9	54.72	56.11	53.33	0.15
db10	59.17	62.22	56.11	0.19
db11	63.61	59.44	67.78	0.15
db12	58.33	60.56	56.11	0.15
sym4	53.61	51.67	55.56	0.14
sym5	36.11	26.67	45.56	0.11
sym6	40.28	37.22	43.33	0.10
sym7	36.67	37.22	36.11	0.19
sym8	61.11	60.56	61.67	0.14
sym9	65.83	63.33	68.33	0.11
sym10	50.28	49.44	51.11	0.23
sym11	58.33	58.89	57.78	0.18
sym12	51.94	50.56	53.33	0.10
All	72.22	68.89	75.56	3.17

The highest performance achievements using Deep ELM model with traditional ELM Autoencoder kernel for DWT wavelets are presented in Table 4.9. It is performed with classification rates of 65.83%, 63.33%, and 68.33% for ACC, WA-SEN, and WA-SPE, separately by using sym9 wavelet.

Table 4.10. The classification performances (%) of the Deep ELM model with traditional ELM Autoencoder kernel for COPD diagnosis on each HHT-based feature set

	ACC	WA-SEN	WA-SPE	Time(s)
IMF1	31.67	26.67	36.67	0.14
IMF2	49.44	53.33	45.56	0.14
IMF3	61.67	61.11	62.22	0.13
IMF4	41.67	38.89	44.44	0.18
IMF5	32.50	29.44	35.56	0.15
All	64.17	66.67	61.67	1.32

The highest classification performance achievements using the Deep ELM model with traditional ELM Autoencoder kernel for HHT-based IMF features are achieved with rates of 61.67%, 61.11%, and 62.22% for ACC, WA-SEN, and WA-SPE, separately by using IMF3 features. The classification performances and time consuming are presented in Table 4.10. Using whole IMF feature sets as input of the Deep ELM model with traditional ELM Autoencoder kernel has increased the classification performance to 64.17%, 66.67%, and 61.67% for ACC, WA-SEN, and WA-SPE, respectively.

The proposed multi-kernel Deep ELM model with LU decomposition based ELM autoencoder kernel has achieved the highest performance using the experimented range of 2 hidden layers with 340 neuron size in the first hidden layer, and unlike 410 neurons in second hidden layer.

Table 4.11. The classification performances (%) of the Deep ELM model with LU decomposition based ELM Autoencoder kernel for COPD diagnosis on each wavelet

Wavelets	ACC	WA-SEN	WA-SPE	Time(s)
Haar	37.50	40.56	34.44	0.09
db4	35.83	31.11	40.56	0.26
db5	27.22	36.67	17.78	0.17
db6	51.11	53.33	48.89	0.17
db7	54.72	53.33	56.11	0.19
db8	57.50	56.11	58.89	0.12
db9	52.22	53.33	51.11	0.12
db10	55.28	56.11	54.44	0.11
db11	76.67	75.56	77.78	0.10
db12	71.39	71.11	71.67	0.16
sym4	66.67	62.78	70.56	0.12
sym5	47.22	46.11	48.33	0.13
sym6	25.83	25.56	26.11	0.16
sym7	33.89	32.22	35.56	0.15
sym8	56.67	53.89	59.44	0.19
sym9	68.33	71.11	65.56	0.14
sym10	74.17	77.78	70.56	0.12
sym11	54.72	56.11	53.33	0.21
sym12	60.28	56.11	64.44	0.17
All	83.06	80.56	85.56	3.72

The highest performance achievements using Deep ELM model with LU decomposition based ELM Autoencoder kernel for DWT wavelets are presented in Table 4.11. It is performed with classification rates of 66.39%, 75.56%, and 57.22% for ACC, WA-SEN, and WA-SPE, separately by using db11 wavelet.

Table 4.12. The classification performances (%) of the Deep ELM model with LU decomposition based ELM Autoencoder kernel for COPD diagnosis on each HHT-based feature set

	ACC	WA-SEN	WA-SPE	Time(s)
IMF1	45.28	47.78	42.78	0.11
IMF2	60.56	62.22	58.89	0.16
IMF3	61.94	64.44	59.44	0.19
IMF4	50.83	53.89	47.78	0.15
IMF5	37.78	39.44	36.11	0.12
All	73.06	68.89	77.22	1.32

The highest classification performance achievements using the Deep ELM model with LU decomposition based ELM Autoencoder kernel for HHT-based IMF features are achieved with rates of 61.94%, 64.44%, and 59.44% for ACC, WA-SEN, and WA-SPE, separately by using IMF3 features. The classification performances and time consuming are presented in Table 4.12. Using whole IMF feature sets as input of the Deep ELM model with LU decomposition based ELM Autoencoder kernel has increased the classification performance to 73.06%, 68.89%, and 77.22% for ACC, WA-SEN, and WA-SPE, respectively.

The proposed multi-kernel Deep ELM model with Hessenberg decomposition based ELM autoencoder kernel has achieved the highest performance using the experimented range of 3 hidden layers with 360 neuron size in the first hidden layer, unlike 270 neurons in second hidden layer, and 180 hidden neurons in third layer. In consequence of the hidden layer size of the proposed Deep ELM model, the training time is longer than the LU decomposition based ELM autoencoder kernel and traditional ELM autoencoder kernel. Both proposed ELM autoencoder kernels are more effective with high classification performances than the traditional ELM autoencoder kernel on the lung sounds for diagnosis of the COPD.

Table 4.13. The classification performances (%) of the Deep ELM model with Hessenberg decomposition based ELM Autoencoder kernel for COPD diagnosis on each wavelet

Wavelets	ACC	WA-SEN	WA-SPE	Time(s)
Haar	63.89	60.56	67.22	0.18
db4	45.28	47.78	42.78	0.24
db5	38.89	37.22	40.56	0.26
db6	29.17	25.56	32.78	0.24
db7	60.28	64.44	56.11	0.16
db8	33.89	32.78	35.00	0.31
db9	40.83	42.78	38.89	0.23
db10	64.72	60.56	68.89	0.19
db11	43.06	46.67	39.44	0.19
db12	65.83	62.78	68.89	0.26
sym4	49.72	53.33	46.11	0.25
sym5	38.06	36.67	39.44	0.23
sym6	56.94	58.33	55.56	0.19
sym7	71.11	73.33	68.89	0.31
sym8	39.72	40.56	38.89	0.24
sym9	66.67	62.78	70.56	0.29
sym10	59.44	63.33	55.56	0.19
sym11	45.28	43.33	47.22	0.20
sym12	51.11	54.44	47.78	0.21
All	80.28	79.44	81.11	6.70

The highest performance achievements using Deep ELM model with Hessenberg decomposition based ELM Autoencoder kernel for DWT wavelets are presented in Table 4.13. It is performed with classification rates of 71.11%, 73.33%, and 68.89% for ACC, WA-SEN, and WA-SPE, separately by using sym8 wavelet.

Table 4.14. The classification performances (%) of the Deep ELM model with Hessenberg decomposition based ELM Autoencoder kernel for COPD diagnosis on each HHT-based feature set

	ACC	WA-SEN	WA-SPE	Time(s)
IMF1	34,17	35,56	32,78	0.26
IMF2	61,11	59,44	62,78	0.17
IMF3	57,78	59,44	56,11	0.19
IMF4	45,83	43,89	47,78	0.21
IMF5	49,72	53,33	46,11	0.21
All	68,61	71,67	65,56	1,80

The highest classification performance achievements using the Deep ELM model with Hessenberg decomposition based ELM Autoencoder kernel for HHT-based IMF features are achieved with rates of 61.11%, 59.44%, and 62.78% for ACC, WA-SEN, and WA-SPE, separately by using IMF2 features. The classification performances and time consuming are presented in Table 4.14. Using whole IMF feature sets as input of the Deep ELM model with Hessenberg decomposition based ELM Autoencoder kernel has increased the classification performance to 68.61%, 71.67%, and 65.56% for ACC, WA-SEN, and WA-SPE, respectively.

The highest Deep ELM performance achievements for DWT wavelets are performed by Deep ELM model with LU decomposition based ELM autoencoder kernel. When all wavelet features are evaluated together, the highest classification performances are also achieved with an accuracy rate of 83.06% by the Deep ELM model with LU decomposition based ELM autoencoder kernel. The combination of the all wavelet features increased the separating capability for the Deep ELM, contrarily no affect it increased the DBN classifier if compared with the db12 wavelet performance achievements. In the light of the achievements presented in Table 4.15 and Table 4.15, the Deep ELM model has better classification performance than the DBN model. It is noted that Deep ELM model has a poor performance for low dimensional feature sets.

Table 4.15. The best classification performances (%) of the proposed multi-kernel Deep ELM and DBN models for COPD classification using proposed and traditional ELM autoencoder kernels on HHT features

	ACC	WA-SEN	WA-SPE	Time(s)
LU based ELM Autoencoder	94.17	95.56	92.78	1.6
Hessenberg ELM Autoencoder	92.22	89.44	95.00	2.7
Traditional ELM Autoencoder	80.83	88.89	72.78	1.3
DBN	90.83	94.44	87.22	6.2

Table 4.16. The best classification performances (%) of the proposed multi-kernel Deep ELM and DBN models for COPD classification using proposed and traditional ELM autoencoder kernels on DWT features

	ACC	WA-SEN	WA-SPE	Time(s)
LU based ELM Autoencoder	91.39	93.89	88.89	1.9
Hessenberg ELM Autoencoder	86.11	85.56	86.67	2.3
Traditional ELM Autoencoder	89.17	87.78	90.56	1.7
DBN	87.78	86.67	88.89	5.1

The SFFS is applied independently for combination of all wavelet features and IMF-based HHT features for obtaining the optimal DBN model and training set. The DBN classification model with the SFFS reached the maximum performance using 5 wavelet features among all feature set. The DBN model classified the COPD lung sounds and healthy lung sounds with high classification performance rates of 87.78%, 86.67% and 88.89% for ACC, WA-SEN and WA-SPE, separately using DWT features. If performance is evaluated considering the wavelets, the db12 is highly responsible method for the SFFS to separate the healthy subject and COPD patients. Table 4.15 presents the classification performances of the proposed kernels, traditional ELM autoencoder and DBN. In spite of the fastest training speed, the proposed multi-kernel Deep ELM model with Hessenberg decomposition kernel achieved the lowest classification performances among the DBN and the proposed kernels. The proposed multi-kernel Deep ELM model with LU based ELM

autoencoder achieved better classification performances than both traditional Deep ELM autoencoder and the DBN. The best separation performances for the COPD and non-COPD subjects are achieved using the proposed Lu based ELM autoencoder with rates of 91.39%, 93.89% and 88.89% for ACC, WA-SEN and WA-SPE on DWT features. Haar, Daubechies (db8, db12), Symlets (sym4, sym10) wavelets are the most significant wavelet subbands for COPD diagnosis model with the SFFS algorithm.

The DBN model classified the COPD lung sounds and healthy lung sounds with high classification performance rates of 90.83%, 94.44% and 87.22% for ACC, WA-SEN and WA-SPE, separately using IMF-based features. If performance is evaluated considering the IMF-based features, the IMF2 is highly responsible method for the SFFS to separate the healthy subject and COPD patients. Table 4.16 presents the classification performances of the proposed kernels, traditional ELM autoencoder and DBN. In spite of the fastest training speed, the proposed multi-kernel Deep ELM model with traditional ELM autoencoder kernel achieved the lowest classification performances among the DBN and the proposed autoencoder kernels. The proposed multi-kernel Deep ELM model with LU based ELM autoencoder kernel and Hessenberg decomposition based ELM autoencoder kernel achieved better classification performances than both traditional Deep ELM autoencoder and the DBN. The best separation performances for the COPD and non-COPD subjects are achieved using the proposed Lu based ELM autoencoder with rates of 94.17%, 95.56% and 92.78% for ACC, WA-SEN and WA-SPE on IMF-based HHT features. The contingency tables for the best performance using the proposed multi-kernel Deep ELM with LU decomposition and Hessenberg decomposition based ELM autoencoder kernels on HHT features for diagnosis of the COPD are presented in Table 4.17 and Table 4.18. The tested COPD patient population is homogenously grouped within 3 subjects from each COPD severity including COPD0, COPD1, COPD2, COPD3, and COPD4. The Detail presentations of FP and FN are for assessing the misclassified lung sounds and detecting the misclassified lung sound severity.

Table 4.17. The contingency table and detailed misclassified COPD severities for the best performance using the Deep ELM with traditional ELM autoencoder kernel with HHT features for COPD classification

		Predicted	
		Non-COPD	COPD
Actual	Non-COPD	160	49
	COPD	20	131

Details of FP

16	COPD0
8	COPD1
10	COPD2
9	COPD3
6	COPD4

Details of FN

8	COPD0
5	COPD1
2	COPD2
3	COPD3
2	COPD4

COPD0 is so similar to healthy subjects. It only gives a rise to short wheezing pathological forms in the lung sounds. The Detail presentation of FN indicates that the misclassified lung sounds are from COPD0 mostly. The lung sounds from the mild levels to very severe levels have been deformed with pathological waveforms. Therefore, the deformation of the lung sounds in the severe levels of The COPD has enables separation of the COPD and non-COPD patients with efficient performances. Similarly, the Detail presentation of the FP consists of mostly misclassified lung sounds from the COPD0. The Table 4.17 presents the contingency table and the detailed presentation of misclassified COPD severities of the Deep ELM model with traditional ELM autoencoder kernel.

Table 4.18. The contingency table and detailed misclassified COPD severities for the best performance using the proposed Deep ELM with LU decomposition based ELM autoencoder kernel with HHT features for COPD classification

		Predicted	
		Non-COPD	COPD
Actual	Non-COPD	172	13
	COPD	8	167

Details of FP →

6	COPD0
3	COPD1
2	COPD2
1	COPD3
1	COPD4

↓ Details of FN

3	COPD0
2	COPD1
1	COPD2
1	COPD3
1	COPD4

The Table 4.18 presents the contingency table and the detailed presentation of misclassified COPD severities of the Deep ELM model with proposed LU decomposition based ELM autoencoder kernel. The contingency table and the detailed presentation of the FP and FN for the Deep ELM model with Hessenberg decomposition based ELM autoencoder kernel is presented in Table 4.19. As it is clearly seen in the contingency tables demanding on the ELM autoencoder kernels, the proposed Deep ELM model with both LU decomposition based ELM autoencoder kernel and Hessenberg decomposition based ELM autoencoder kernel have better generalization capability for the diagnosis of COPD patients using HHT analysis on 12-channel lung sounds. The Deep ELM model with traditional ELM autoencoder kernel misclassifies most of lung sounds with COPD0 and also big number of lung sounds from COPD4.

Table 4.19. The contingency table and detailed misclassified COPD severities for the best performance using the proposed multi-kernel Deep ELM with Hessenberg decomposition with HHT features for COPD classification

		Predicted		
		Non-COPD	COPD	
Actual	Non-COPD	161	9	Details of FP →
	COPD	19	171	

4	COPD0
2	COPD1
2	COPD2
1	COPD3
0	COPD4

↓ Details of FN

11	COPD0
4	COPD1
2	COPD2
1	COPD3
1	COPD4

The proposed multi-kernel Deep ELM and the DBN models are both reached the highest performance using the same wavelet features. The proposed multi-kernel Deep ELM model classified the lung sounds from COPD and non-COPD subjects almost 2x faster than the DBN. The proposed multi-kernel Deep ELM model with novel autoencoder kernels has achieved better classification performances using IMF-based HHT features against the DWT features.

4.4. The COPD Severity Analysis

The COPD diagnosis model is comprised of segmentation 10s lung sounds from RespiratoryDatabase@TR, plotting 3D-SODP, quantization of the 3D-SODP using various lengths of cuboid polyhedrons, counting the cuboid-based data points and evaluating the

counted features with the DBN and Deep ELM. The quantization of 3D-SODP space which is obtained plotting consecutive data points on the lung sounds stands for deterministic significance for reversals on the signal. The 3D plots enable visualization of lung sounds and wave characteristics. At the beginning of the belief, the lung sounds from different severities of the COPD are plotted, the differences and similarities are visually analysed. While the difference of consecutive three data points on lung sounds are aligned so close to the centre of the 3D-SODP with the early stages of the COPD, contrarily, the difference of consecutive three data points on lung sounds point out a distant distribution from the centroid of 3D-SODP with the very severe levels of COPD. For a clear distribution view, the 3D-SODP from the COPD0 and COPD4 are pictured in Figure 4.1.

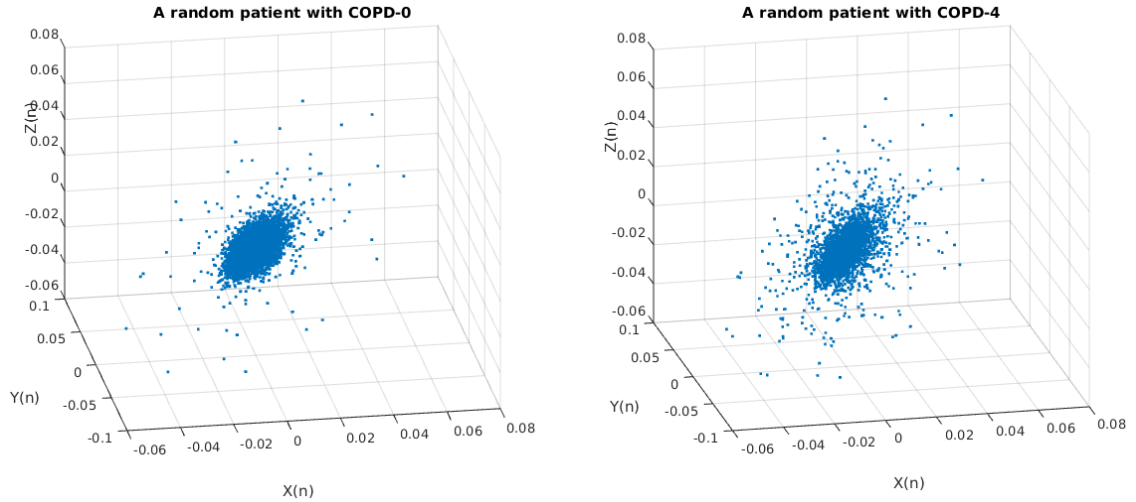


Figure 4.1. 3D-SODP of lung sounds from random subjects with COPD0 and COPD4

Using the different aptitudes of the 3D-SODP, assessing the intension of the data points by segmentation of the space with various sizes of cuboid polyhedrons is bethought to extract the deterministic measures from lung sounds. The segment numbers were experimentally decided at a range between 3 and 6 scopes. The 3D-SODP space is segmented into octants; origin centred 3-6 spaces entwined cuboid polyhedrons. The quantity of data points within the segmented cuboids and the octant regions are counted on the 3D-SODP using the distances-base metrics to the centroid. The feature set includes 22 of cuboid polyhedrons-based quantization, and 8 of octant-based quantization. The max

limit of the cuboid polyhedron size is set to the mean SD1, the data points at outer space of the limited solids are also counted as outer features for each quantization method.

12-channel lung sounds from RespiratoryDatabase@TR are analysed to perform COPD severity classification for 5 patients with COPD0, 5 patients with COPD1, 7 patients with COPD2, 7 patients with COPD3, and 17 patients with COPD4. The lung sounds has a frequency rate of 4000 samples. 5 patients at each COPD severity were utilized in the training process of the proposed models to ensure a homogeneous patient distribution. The remaining patients were included in testing folds for once to incorporate all patients.

4.4.1. Deep Belief Networks Results

The DBN is iterated for 50 epochs within a limited range neuron size and hidden layer size. The neuron size is tested with a variety between 100-600 units and two hidden layers were placed in the both Deep ELM and DBN classifier models. The learning rate is selected as 2 and the sigmoid activation function is utilized as the output function for the DBN model. The proposed DBN structure has 2 hidden layers with 150 and 290 neurons, respectively. The classification performances including overall accuracy, weighted mean sensitivity, and weighted mean specificity of the DBN classifier for 3D-SODP quantization are presented in Table 4.20.

Table 4.20. The classification performances (%) of the DBN model for COPD severity classification on each quantization models

	Cuboid₃	Cuboid₄	Cuboid₅	Cuboid₆	Cuboid_{all}	Octant	All
ACC	32.32	35.77	48.58	30.49	52.03	45.73	64.43
WA-SEN	27.73	29.36	39.52	26.80	40.19	37.98	55.55
WA-SPE	27.54	29.20	39.64	26.66	40.61	38.27	57.22
Time(s)	0.73	0.96	1.32	1.53	5.99	2.12	7.21

The highest DBN performance achievements for cuboid quantization model are performed with classification rates of 48.58%, 39.52%, and 39.64% for ACC, WA-SEN, and WA-SPE, separately by using Cuboid₅ on 3D-SODP.

4.4.2. The Proposed Multi-kernel Deep ELM Results

The Deep ELM model with the highest performance at the experimented range has also 2 hidden layers with 310 and 520 neurons, respectively. Both two hidden layer is decomposed by Lu-based ELM autoencoder. The classification performances including overall accuracy, weighted mean sensitivity, and weighted mean specificity of the proposed multi-kernel Deep ELM classifiers for each Cuboid and octant quantization methods are presented in Table 4.21.

Table 4.21. The classification performances (%) of the Deep ELM model for COPD severity classification on each quantization models

	Cuboid₃	Cuboid₄	Cuboid₅	Cuboid₆	Cuboid_{all}	Octant	All
ACC	26.22	28.86	38.82	31.91	76.83	49.39	90.04
WA-SEN	22.50	24.75	33.93	28.70	71.71	46.23	87.79
WA-SPE	21.41	24.57	35.29	29.18	72.92	48.01	89.11
Time(s)	0.21	0.32	0.35	0.49	3.24	0.73	4.63

The highest Deep ELM performance achievements are performed with classification rates of 49.39%, 46.23%, and 48.01% for accuracy, sensitivity, and specificity, separately by using octant-based quantization features on 3D-SODP.

When all cuboid features evaluated together as Cuboid_{all}, the highest classification performances with accuracy rate of 76.83% by the Deep ELM model. The combination of the all Cuboid features increased the separating capability for the both Deep ELM and the DBN classifiers. Taken in terms of segmentation methods, the octant based 3D-SODP quantization has achieved better performance even though it has simple mathematical analysis than Cuboid model for Deep ELM classifier.

In the light of the achievements presented in Table 4.20 and Table 4.21, the Deep ELM model has better classification performance than the DBN model. It is noted that Deep ELM model has a poor performance for low dimensional feature sets.

The SFFS is applied for combination of all features for obtaining the optimal DBN model and feature set. The DBN classification model reached the maximum performance using 21 features among feature set. The DBN model classified the COPD lung sounds from different severities with classification performance rates of 74.59%, 69.27% and 69.60% for ACC, WA-SEN and WA-SPE, separately. The Deep ELM model separated the five types of COPD severities with performance rates of 93.29%, 98.75% and 98.40% for ACC, WA-SEN and WA-SPE, respectively. If performances are evaluated considering the methods, the octant and Cuboid₅ quantization methods with the SFFS are highly responsible for the COPD severity classification. When the performances are evaluated considering the whole feature set, the octant quantization, and the outer space quantization extract the most remarkable characteristics from lung sounds for the proposed model with the SFFS.

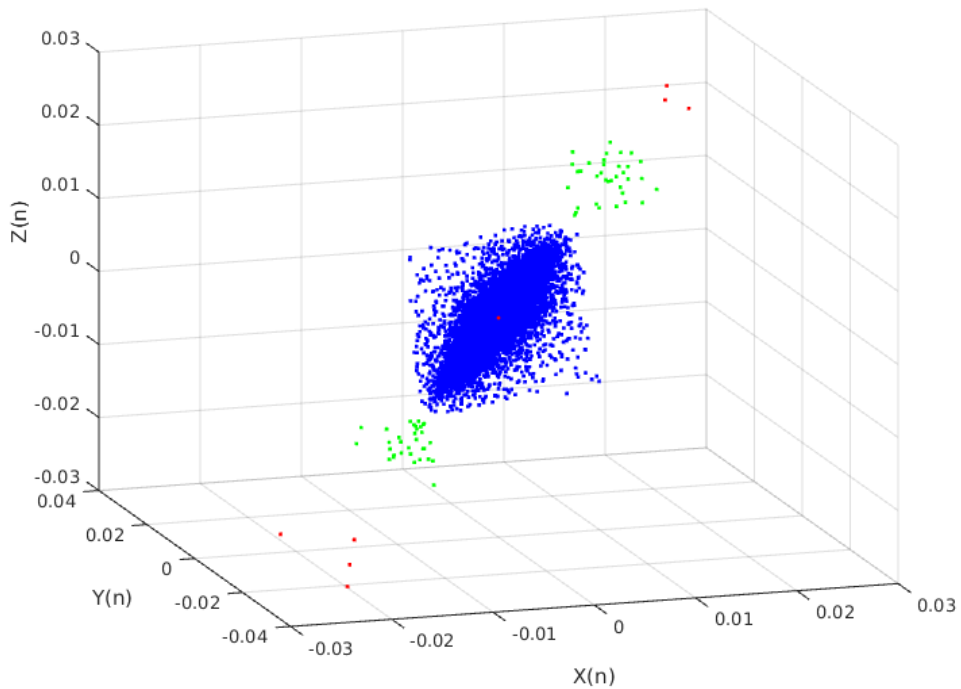


Figure 4.2. Highly responsible spaces using Cuboid polyhedrons-based 3D-SODP quantization for separation of lung sounds from different COPD severities

The outermost space for cuboid methods is consequential for diagnosis of the severities of the COPD. The high responsible segmented spaces for the SFFS are pictured in Figure 4.2 for Cuboid₅ quantization method. The achievements prove that, 3D-SODP analysis enables separation of five types of the COPD severities by applying the proposed nonlinear quantization algorithm with the DBN and Deep ELM classifiers. The Deep ELM classifier performed an extraordinary performance in the iterated ranges of classification parameters.

One of the most demanding questions for Deep Learning is “How Deep is enough?”. The depth of the classifier model is affiliated to the feature dimensionality, range of classification parameters, the learning algorithms and more. The reconstructed presentations of the input may lose its meaning and cause overfitting and mistaken classifications. The decrease in classification performances has been experienced with same iteration of neuron sizes on 3 hidden layers structure for both DBN and Deep ELM models. The best accuracy rates are 56.03% and 90.59% for the DBN and the Lu based Deep ELM, respectively.

4.5. ELM Autoencoder Kernel Impact

The proposed multi-kernel Deep ELM model consists of three ELM autoencoder kernels including traditional ELM autoencoder, Lu decomposition based ELM autoencoder, and Hessenberg decomposition based ELM autoencoder. The three ELM autoencoder techniques are performed for the same structures, and the experimental results are evaluated for the COPD severity classification using 3D-SODP features.

The contingency tables for the best classification performances using the proposed ELM autoencoder kernels are indicated in Table 4.22 and Table 4.23. The contingency tables provide assessing the separation capabilities of the proposed models between the COPD severities.

Table 4.22. Contingency table for COPD severity classification using the Deep ELM with the proposed LU decomposition based ELM autoencoder

		Predicted				
		COPD0	COPD1	COPD2	COPD3	COPD4
Actual	COPD0	54	4	2	1	1
	COPD1	4	52	2	2	1
	COPD2	1	2	78	4	0
	COPD3	1	1	1	75	2
	COPD4	0	1	1	2	200

Using the Table 4.22, the sensitivity rates and specificity rates of the proposed Deep ELM model with LU decomposition based ELM autoencoder kernel for the COPD0, COPD1, COPD2, COPD3, and COPD4 can be calculated using the equations in section 3.8. In the consequence of various numbers of the subjects from COPD severities, the weighted mean specificity and the weighted mean sensitivity can be calculated for assessing the models. The sensitivity and specificity rates of the COPD severities are given in Table 4.23.

Table 4.23. Sensitivity and specificity rates (%) for each COPD severities using the Deep ELM with the proposed LU decomposition based ELM autoencoder contingency table

Severities	Sensitivity	Specificity
COPD0	98.28	98.60
COPD1	98.07	98.14
COPD2	98.49	98.52
COPD3	98.92	97.83
COPD4	99.12	98.61

The overall accuracy rate is 93.29%, WA-SEN rate is 98.75% and WA-SPE is 98.40% for the Deep ELM model with the proposed LU decomposition based ELM autoencoder kernel.

Table 4.24. Contingency table for COPD severity classification using the Deep ELM with the proposed Hessenberg decomposition based ELM autoencoder

		Predicted				
		COPD0	COPD1	COPD2	COPD3	COPD4
Actual	COPD0	48	6	2	1	1
	COPD1	6	48	2	2	0
	COPD2	1	3	79	3	1
	COPD3	2	2	1	77	5
	COPD4	3	1	0	1	197

Using the Table 4.24, the sensitivity rates and specificity rates of the proposed Deep ELM model with Hessenberg decomposition based ELM autoencoder kernel for the COPD0, COPD1, COPD2, COPD3, and COPD4 are presented in Table 4.25.

Table 4.25. Sensitivity and specificity rates (%) for each COPD severities using the Deep ELM with the proposed Hessenberg decomposition based ELM autoencoder contingency table

Severities	Sensitivity	Specificity
COPD0	97.82	97.23
COPD1	97.82	97.23
COPD2	98.24	98.76
COPD3	97.82	98.29
COPD4	98.89	97.58

The overall accuracy rate is 91.26%, WA-SEN rate is 98.34% and WA-SPE rate is 97.32% for the Deep ELM model with the proposed Hessenberg decomposition based ELM autoencoder kernel. The Figure 4.3 indicates the sensitivity and specificity rates for COPD severities using proposed ELM autoencoder kernels

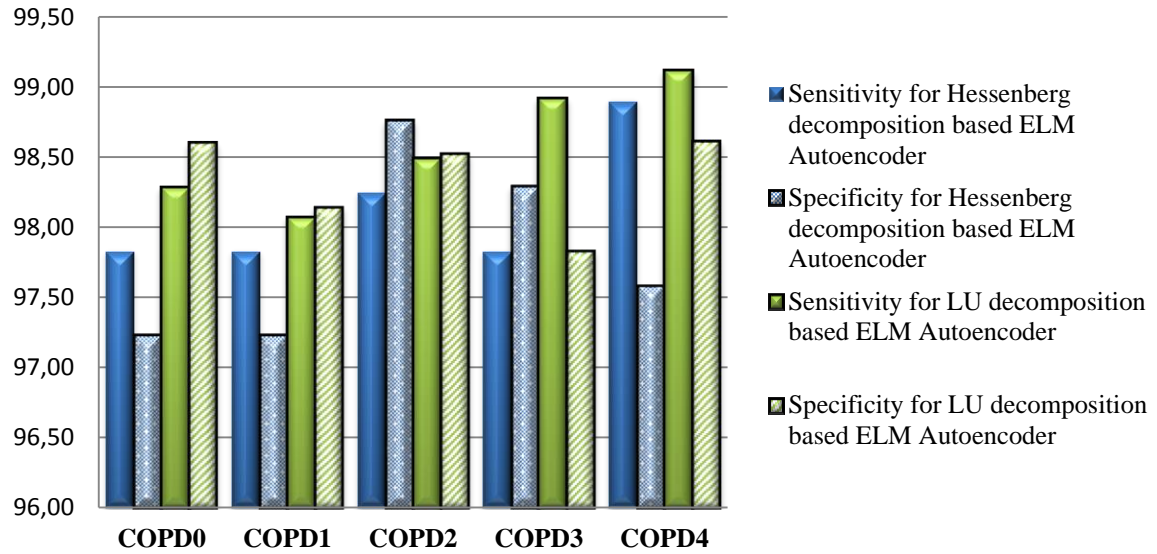


Figure 4.3. The sensitivity and specificity rates of COPD severities using Deep ELM model with proposed ELM autoencoder kernels

As it is seen in Fig 4.3, the sensitivity and specificity rates for the diagnosis of the COPD4 is the highest achievements for both proposed ELM autoencoder kernels. The sensitivity and specificity achievement increases from COPD0 to COPD4. Aforementioned characteristics of lung sounds from different COPD severities enables the separation of the COPD1, COPD2, COPD3, and COPD patients with better generalization performance. The separation of COPD0 from the severe levels of the COPD is also an embarrassing examination in real world that depends on specialist and too much clinical test and metric.

The best five classification performances including overall accuracy, weighted mean sensitivity, weighted mean specificity for the models, and time consuming are presented in Table 4.26.

Table 4.26. The classification performances (%) of the Deep ELM and DBN models for COPD severity classification using proposed and traditional ELM autoencoder kernels

	ACC	WA-SEN	WA-SPE	Time(s)
LU based ELM Autoencoder	93.29	98.75	98.40	4.21
	92.48	90.40	90.23	4.32
	92.07	89.92	89.76	3.90
	90.45	88.03	88.50	4.07
	89.84	87.65	87.14	3.98
Hessenberg ELM Autoencoder	91.26	98.34	97.82	3.04
	90.85	88.62	88.33	2.78
	90.24	88.03	87.61	2.86
	88.01	84.70	84.50	2.94
	85.77	84.02	85.46	2.96
Traditional ELM Autoencoder	86.59	84.63	85.85	5.07
	83.13	79.77	80.05	4.89
	81.71	77.93	80.13	4.13
	80.69	76.98	79.50	4.87
	80.28	76.65	79.31	3.86
DBN	74.59	69.27	69.60	9.32
	74.59	70.56	71.88	11.24
	72.56	68.85	70.90	9.38
	71.95	68.42	69.90	10.23
	71.54	68.02	69.23	10.44

The Deep Learning algorithms such as the DBN are efficient ways in machine learning approaches and have ability to analyse the input data in various depths using the hidden layer variations. The DBN model for the COPD severity classification is has performed unsuccessful separation using the SFFS. The proposed Deep ELM model has

better achievements for experimental ranges of the classification parameters compared to the DBN. The proposed ELM autoencoder models including both Hessenberg decomposition and LU triangularization based ELM autoencoder kernels have more accurate classification performances compared to the traditional ELM autoencoder.

The proposed Deep ELM kernels have faster classification time (containing training and testing time) than DBN classifier using same hidden layers, and neuron sizes. The results indicate that LU triangularization based ELM autoencoder has achieved the highest classification and generalization performances using 3D-SODP for SFFS. In the view of the fact the simplicity of the mathematical solutions on proposed decomposition techniques, the classification time is about 2x faster than the traditional ELM autoencoder, and is 3x faster than one of the fastest Deep Learning approached, DBN. The fastest ELM autoencoder kernel is noted as the Hessenberg decomposition based ELM autoencoder with close classification times to the LU triangularization based ELM autoencoder kernel.

The generalization capacity, adaptation capability to supervised algorithms, simplicity of the mathematical solutions and the fast training time of the proposed ELM autoencoder kernels generate conspicuous selection for deep analysis of the patterns.

4.6. SODP Dimension Impact

SODP is a nonlinear technique to quantify the chaos of the consecutive data points from the origin. The form and the distribution of the differences of the consecutive data points enable focusing the presence variations from the randomness. Especially abnormal pathological changes in the time series can be easily detected by the chaos of the SODP. Depending on the analysis problem, the pathological changes are the symptoms of the abnormalities in the biomedical analysis. To address the efficiency of the SODP and the proposed 3D-SODP quantization on lung sounds for COPD severity classification is evaluated for proposed multi-kernel Deep ELM model.

If the Euclidean theorem is focused on, whereas the location of data points on a line which graphically represents the real numbers at a range provides limited g number of depth for the location of the data point. The plot of data points with two-dimensional plane

(SODP) increases the depth into g^2 , the 3D-SODP allows for detailed analysis of the data points with g^3 features at different depths. If the dimension is increased the assessing capability of feature depths is possible, but the visualisation is impossible in the data space. 3D-SODP is analysed in Section 4.4. Similarly to the 3D-SODP quantization, the SODP is segmented at a range between 3 and 6 regions.

The SODP is segmented into regions; origin centred 3-6 spaces entwined circles using central tendency measure with distances-base metrics (seen in Figure 4.4). The feature set includes 20 of chaos quantization, 2 of elliptical features and 4 of sign-based quantization.

The max limit of the cuboid polyhedron size is set to the mean SD1. The same classification parameters such as neuron sizes and Deep ELM structures are utilized in the analysis of the SODP and 3D-SODP quantization. Table 4.27 present the best classification results of the proposed multi-kernel Deep ELM on SODP and the proposed 3D-SODP quantization models.

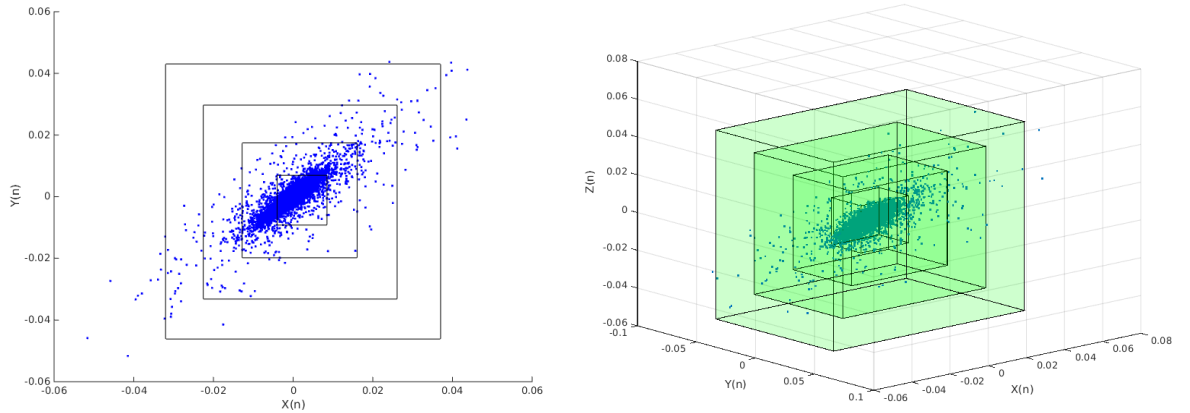


Figure 4.4. Comparison of the SODP and 3D-SODP quantization focusing on cuboid and chaos segmentation on lung sounds from a random COPD patient

Even though the same number of the feature for both 3D-SODP and SODP quantization, the 3D-SODP features have achieved more efficient classification performances than the SODP. Especially the integration of 3D-SODP quantization features and Deep ELM model with the proposed LU decomposition based ELM autoencoder has best generalization performance for the COPD severity classification.

Table 4.27. Comparison of the best classification performances (%) of the proposed multi-kernel Deep ELM, traditional ELM autoencoder and DBN model for COPD severity classification using 3D-SODP and SODP quantization

		ACC	WA-SEN	WA-SPE	Time(s)
3D-SODP	LU based ELM Autoencoder	93.29	98.75	98.40	4.21
	Hessenberg ELM Autoencoder	91.26	98.34	97.82	3.04
	Traditional ELM Autoencoder	86.59	84.63	85.85	5.07
SODP	LU based ELM Autoencoder	84.76	81.22	82.73	3.2
	Hessenberg ELM Autoencoder	79.67	76.10	78.87	2.6
	Traditional ELM Autoencoder	76.42	75.58	78.71	4.8

The results prove the efficiency of the 3D-SODP against SODP quantization. The 3D dispersion of the lung sounds enhances the depth of the assessing capability with additional Z plane. 3D-SODP is comprised of two SODP at same time. Whereas the proposed multi-kernel Deep ELM model with LU based ELM autoencoder kernel achieves an accuracy rate of 84.76% using SODP features for SFFS, the highest classification performance rates are also attained to 93.29% using the proposed multi-kernel Deep ELM model with LU based ELM autoencoder kernel on 3D-SODP quantization. The proposed multi-kernel Deep ELM model with has a better generalization performance for COPD severity classification. Especially, Hessenberg decomposition based ELM autoencoder is fastest kernel among the kernel pool.

5. CONCLUSION AND DISCUSSION

Respiratory diseases have chronic symptoms and seasonal exchange which must be faithfully monitored and must be kept under control. In this thesis, the RespiratoryDatabase@TR gathered up the multimedia data from the COPD patients with different stages, asthma patients and healthy subjects. It facilitates monitoring the changes of respiratory diseases and pulmonary-cardiac diseases within the treatment periods. RespiratoryDatabase@TR depicts a unique auscultation and multimedia diagnostic respiratory database. The including auscultation channels have ability to examine the lungs and the heart status of the subject population. It ensures the detailed examinations on the respiratory diseases including the COPD and asthma with 16-channels respiratory auscultation sounds, the PFT measurements and chest X-rays. The major advantages of the RespiratoryDatabase@TR are allowing the clinicians to easily compare changes within the each step, assigning the extent on treatment routines triumphantly, and managing improvement information for various disciplines to diagnose the degree of treatment for respiratory diseases.

In this thesis, novel extensions of traditional ELM autoencoder, Multi-kernel Deep ELM, is proposed. Experimental results with DBN and proposed Deep ELMs, on respiratory sound analysis improved in both performance measures and training pace.

The DBN can be explained as a specific structure with many hidden layers of Deep Learning. The top hidden layers of the DBN may handle more particular and descriptive information to identify the solution, whereas lower layers not. The Deep ELM has the same characteristic with the use of multiple hidden layers and fully connection between the neurons. The Deep ELM model has better advantages than the common machine learning algorithms such as performing high performance on classification solutions with small number of training sample size, and enabling transportation of the connections and model parameters between the layers in deep analysis. The structure of the Deep ELM may also inspire the improvement on effective parallel feature analysing in both supervised and unsupervised stages such classifier.

In Deep ELM model, the weights between the hidden layers are calculated by ELM autoencoder model. The first layer of the ELM autoencoder is selected from random variables and the output weights and hidden layer neurons are computed by iterative steps. The output weights are the decoder model of the autoencoder. The ELM autoencoder has ability to manage perfectly recovering more quality samples of given input from the corrupted features for each hidden layer. The resultant β^n weights of the proposed LU decomposition based autoencoder and Hessenberg decomposition based autoencoder provide reflecting the compact representations of the original data using the inner product of inputs in deep dimensions. Moreover, as the autoencoder is adopted as the building block of the proposed Hessenberg decomposition based ELM, and LU decomposition based ELM higher level feature representations can be generated by layer wise comparison.

In both Deep ELM and the DBN models, the input signal is presented with various forms in each hidden layer. The number of the hidden layers and the number of the neuron in the layers enables deep analysis and distinct representations for the input signal. Especially, increasing the number of the hidden layer in the models grants most of the feature presentations and detailed characteristics including feature learning.

The feature dimensionality is a determinative majority for supervised machine learning algorithms to prevent overfitting. It is experienced that, whereas the low dimensionality of the feature set stands out in relief in DBN models, constantly the Deep ELM models achieve better classification performances for high dimensions of features. This has led to the conclusion that new presentations in proposed multi-kernel Deep ELM perform determining dominant features by weighting the input model as PCA. In the SFFS applications, the proposed multi-kernel Deep ELM model has a better generalization capacity for the higher feature size, while the DBN structure can better classification performance for low dimensionality.

In both the DBN and Deep ELM with the same structure, obtaining classification parameters by unsupervised ways instead of randomized selection achieves more accurate results and prevents wasting time in the training in consequence of requiring less iteration for optimization. The proposed multi-kernel Deep ELM has better classification performance and generalization capacity in appreciable velocity than the DBN by force of

utilizing simple mathematical solutions and inverting solutions such as proposed LU decomposition and Hessenberg decomposition based ELM autoencoder kernels.

Increasing the training time in machine learning approaches is consequential materiality. The DBN, with the unsupervised definition of the weights, is one of the fastest machine learning approaches comparing the Deep Learning algorithms, ANN, SVM and more. The proposed multi-kernel Deep ELM model has achieved high classification performances almost 3 times faster than the DBN model with the same structure settings. The rapidness of the proposed model renders the proposed multi-kernel Deep ELM as preferable algorithm for deep analysis of the patterns.

With proposed classifiers CMI system based on RespiratoryDatabase@TR lets severely clinicians and the other medical personnel for assessing their physical experiments according to a standardized rules and manners easily and effectively on the auscultation sounds by visualization of the auscultation sounds. The proposed CMI holds controlling capability on chest X-rays, the PFT measurements.

The auscultation areas are specified as the clearest hearing of the both pathological and healthy inner body sounds by the pulmonologist clinicians and the internal medicine specialist in experimental scenarios. They especially noted that investigating different versions of displaced auscultation areas may result in various pulmonary disorders, but the RespiratoryDatabase@TR auscultation areas are common and are the most diagnostic for the COPD and chronic respiratory diseases.

The proposed multi-kernel Deep ELM model has ability to speed up training process in other classification with unsupervised learning. The proposed high performance and rapid ELM autoencoder kernels enable adaptation of various supervised algorithms for unsupervised optimization of model weights in the deep analysis.

The results show that proposed 3D-SODP and multi-kernel Deep ELM model has capability to diagnosis of asthma, COPD and severities of the COPD better than Deep Learning approaches. One of the biggest deficiencies of the machine learning, training time has been overcome in very short time. This work can inspire researches, pulmonologists to advance control applications for wide range of clinical problems using proposed techniques.

FUTURE WORK

With the ongoing analysis of COPD which is a significant problem continuing day by day, the enhancing of computer-aided diagnostic systems and the provision of early diagnosis are necessary steps. Analyses in this study show that, whereas the separation of COPD1, COPD2, COPD3, and COPD4 patients from healthy subjects has been highly accurate using lung sounds from RespiratoryDatabase@TR, the separation of COPD0 from healthy subjects is a demanding process. The researchers who will perform COPD severity analysis and early diagnosis of the COPD need to focus on extracting significant characteristics of the lung sounds with COPD0 against healthy lung sounds.

The proposed unsupervised Autoencoder kernels, Lower-upper decomposition and Hessenberg decomposition based ELM autoencoder, may be adapted to Deep Learning approaches to enable feature mapping and detailed analysis for performing machine learning training with high generalization capacity in a short time.

BIBLIOGRAPHY

- Abdel-Zaher, A.M., Eldeib, A.M., 2016. Breast cancer classification using deep belief networks, **Expert Systems with Applications**, Volume 46, p.139-144, ISSN 0957-4174, <https://doi.org/10.1016/j.eswa.2015.10.015>.
- Adeli, H., Zhou, Z., Dadmehr, N., 2000. Analysis of EEG Records in an Epileptic Patient using Wavelet Transform, **Journal of Neuroscience Methods**, 123, .69-7.
- Aizenberg, I., Aizenberg, N.N., Vandewalle, J.P.L., 2000. Multi-Valued and Universal Binary Neurons: Theory, Learning and Applications. **Springer Science & Business Media**.
- Altan, G., Kutlu, Y., 2015. ECG based Human identification using Logspace Grid Analysis of Second Order Difference Plot, **Signal Processing and Communications Applications Conference (SIU)** p.1288–1291
- Altan, G, Kutlu, Y., Allahverdi, N., 2016. A new approach to early diagnosis of congestive heart failure disease by using Hilbert–Huang transform, **Computer Methods and Programs in Biomedicine**, Volume 137, 2016, p.23-34, ISSN:0169-2607, <https://doi.org/10.1016/j.cmpb.2016.09.003>
- Altan, G, Kutlu, Y., Allahverdi, N., 2016. A Multistage Deep Belief Networks Application on Arrhythmia Classification, **International Journal of Intelligent Systems and Applications in Engineering**, Volume 4, Special Issue 1, p.23-34, ISSN 2147-6799, DOI: 10.18201/ijisae.270367
- Altan, G, Kutlu, Y., Allahverdi, N., 2016. Deep Belief Networks Based Brain Activity Classification Using EEG from Slow Cortical Potentials in Stroke, **International Journal of Applied Mathematics, Electronics and Computers**, Volume 4, Special Issue 1, p.205-210, ISSN 2147-8228, <http://dx.doi.org/10.18100/ijamec.270307>
- Altan, G, Allahverdi, N., Kutlu, Y., 2017. Diagnosis of Coronary Artery Disease Using Deep Belief Networks, **European Journal of Engineering and Natural Sciences** Vol:2 Issue(1), ISSN:2458-8156, p.29-36
- Altan, G, Kutlu, Y., Garbi, Y., Pekmezci A.O and Nural, S., 2017. Multimedia Respiratory Database (RespiratoryDatabase@TR): Auscultation Sounds and Chest X-rays. **Natural and Engineering Sciences**, Vol:2 Issue (3), p.59-72
- Amaral, J. L. M., Faria, A. C. D., Lopes, A. J., Jansen, J. M. and Melo, P. L., 2010. Automatic identification of Chronic Obstructive Pulmonary Disease Based on forced oscillation measurements and artificial neural networks, **Annual International Conference of the IEEE Engineering in Medicine and Biology**, Buenos Aires, pp. 1394-1397. doi: 10.1109/IEMBS.2010.5626727
- Attoh-Okine, N., Barner, K., Bentil, D., & Zhang, R., 2008. The empirical mode decomposition and the hilbert-huang transform. **Springer**, ISSN=1687-6180, pp.2515-18, doi=<https://doi.org/10.1155/2008/251518>
- Bahoura, M. and Pelletier, C., 2004. Respiratory sounds classification using Gaussian mixture models, **Canadian Conference on Electrical and Computer Engineering** (IEEE Cat. No.04CH37513), Vol.3, pp. 1309-1312. doi: 10.1109/CCECE.2004.1349639
- Bahoura, M. and Pelletier, C., 2004. Respiratory sounds classification using cepstral analysis

- and Gaussian mixture models., **Conf. Proc. IEEE Eng. Med. Biol. Soc.**, vol. 1, no. 2, pp. 9–12
- Bateman, E. D., Hurd, S. S., Barnes, P. J., Bousquet, J., Drazen, J. M., FitzGerald, M., Gibson, P., Ohta, K., O'Byrne, P., Pedersen, S. E., Pizzichini, E., Sullivan, S. D., Wenzel, S. E., Zar, H. J., 2008. Global strategy for asthma management and prevention: GINA executive summary, **European Respiratory Journal** Vol.31: pp.143-178; DOI: 10.1183/09031936.00138707
- Bengio, Y., Lamblin, P., Popovici, D., Larochelle, H., 2007. Greedy Layer-Wise Training of Deep Networks. **Adv Neural Inf Process Syst** vol.19: pp.153. doi:citeulike-article-id:4640046.
- Bengio Y., and Delalleau O., 2009. Justifying and generalizing contrastive divergence. **Neural Comput** vol.21: pp.1601–21. doi:10.1162/neco.2008.11-07-647.
- Bezak, P., Bozek, P., Nikitin, Y., 2014. Advanced Robotic Grasping System Using Deep Learning, **Procedia Engineering**, Volume 96, pp.10-20, ISSN 1877-7058, <https://doi.org/10.1016/j.proeng.2014.12.092>.
- Buist S. A., Introduction, 2008. **Proceedings of the American Thoracic Society**, Vol. 5, No. 8
- Bunch, J. R. and Hopcroft, J. E., 1974. Triangular factorization and inversion by fast matrix multiplication. **Mathematics of Computation**, 28(125), p.231–236.
- Celli, B. R., MacNee, W., Agustí, A., Anzueto, A., Berg, B., Buist, A. S., ZuWallack, R., 2004. Standards for the diagnosis and treatment of patients with COPD: A summary of the ATS/ERS position paper. **European Respiratory Journal**. Vol.23, pp.932-946 <https://doi.org/10.1183/09031936.04.00014304>
- Chacko, B., Krishnan, V., Raju, G. and Anto, P., 2012. Handwritten character recognition using wavelet energy and extreme learning machine. **International Journal of Machine Learning and Cybernetics**, 3(2), p.149-161.
- Charleston-Villalobos, S., Martinez-Hernandez, G., Gonzalez-Camarena, R., Chi-Lem, G., Carrillo, J.G., Aljama-Corrales, T., 2011. Assessment of multichannel lung sounds parameterization for two-class classification in interstitial lung disease patients, **Computers in Biology and Medicine**, 41(7), pp. 473-482, ISSN:0010-4825, <https://doi.org/10.1016/j.compbiomed.2011.04.009>.
- Chen F. S., 1998. Wavelet transform in signal processing theory and applications. **National Defense Publication of China**, ISBN-10: 0201634635
- Cheplygina, V., Sørensen, L., Tax, D. M. J., Pedersen, J. H., Loog, M. and Bruijne, M. d., 2014. Classification of COPD with Multiple Instance Learning, **22nd International Conference on Pattern Recognition, Stockholm**, pp.1508-1513. doi: 10.1109/ICPR.2014.268
- COSMED, Spirometry Test. <http://international.cosmed-store.com/> 26.01.2018.
- Daubechies, I., 1986. The Wavelet Transform, Time-Frequency Localization and Signal Analysis, **IEEE Transactions on Information Theory**, 36(5), pp.961-1005.
- Dechter R., 1986. Learning while searching in constraint-satisfaction problems. University of California, Computer Science Department, **Proceedings of the 5th National Conference on Artificial Intelligence**, Vol1. Pp.178-183
- Decramer, M., Janssens, W., & Miravittles, M., 2012. Chronic obstructive pulmonary disease. **Lancet**, 379(9823), pp.1341–51. <https://doi.org/10.1016/S0140->

6736(11)60968-9

- Ding, S., Zhang, N., Xu, X., Guo, L., and Zhang, J., 2015. Deep Extreme Learning Machine and Its Application in EEG Classification, **Mathematical Problems in Engineering**, vol. 2015, Article ID 129021, 11 pages, 2015. doi:10.1155/2015/129021
- Dokur, Z., 2009. Respiratory sound classification by using an incremental supervised neural network. **Pattern Analysis and Applications**, 12(4), pp.309–319. <https://doi.org/10.1007/s10044-008-0125-y>
- Drotár, P., Gazda, J., Smékal, Z., 2015. An experimental comparison of feature selection methods on two-class biomedical datasets, **Computers in Biology and Medicine**, Volume 66, pp.1-10, ISSN:0010-4825, <https://doi.org/10.1016/j.compbimed.2015.08.010>.
- Duda, R., Hart, P. and Stork, D.G., 2012. **Pattern Classification**. John Wiley & Sons
- Duman, F., Özdemir, N. and Yildirim, E., 2012. Patient specific seizure prediction algorithm using Hilbert-Huang Transform, **Proceedings of 2012 IEEE-EMBS International Conference on Biomedical and Health Informatics**, Hong Kong, pp. 705-708. doi: 10.1109/BHI.2012.6211680
- Flandrin, P., Rilling, G. and Gonçalves, P., 2003. Empirical mode decomposition as a filterbank. **IEEE Signal Proc Lett.** 11 (2): pp.112-114.
- Fletcher C., Petro R., 1977. The natural history of chronic airway obstruction. **BMJ**, pp.1-1645-8
- Friis, B., Eiken, M., Hornsleth, A., & Jensen, A., 1990. Chest X-ray appearances in pneumonia and bronchiolitis. Correlation to virological diagnosis and secretory bacterial findings. **Acta Paediatrica Scandinavica**, 79(2), pp.219–25.
- Jané, R., Cortés, S., Fiz, J. A., and Morera, J., 2004. Analysis of wheezes in asthmatic patients during spontaneous respiration., **Annu. Int. Conf. IEEE Eng. Med. Biol. Soc.**, vol. 5, pp. 3836–9.
- Johnson, W. and Lindenstrauss, J., 1984. Extensions of Lipschitz mappings into a Hilbert space, **Conference in modern analysis and probability**, vol. 26, pp. 189–206.
- GBD 2015, Disease and Injury Incidence and Prevalence Collaborators, G. 2015 D. and I. I. and P., 2016. Global, regional, and national incidence, prevalence, and years lived with disability for 310 diseases and injuries, 1990-2015: a systematic analysis for the Global Burden of Disease Study 2015. **Lancet** (London, England), 388(10053), pp.1545–1602. [https://doi.org/10.1016/S0140-6736\(16\)31678-6](https://doi.org/10.1016/S0140-6736(16)31678-6)
- Golub, G. H. and Van Loan, C. F., 1996. The Hessenberg and Real Schur Forms. 7.4 in **Matrix Computations**, 3rd ed. Baltimore, MD: **Johns Hopkins University Press**, pp. 361-372
- Golub, G. H. and Van Loan, C. F., 2012. **Matrix Computations**. JHU Press.
- Graps, A., An Introduction to Wavelets. 1995. **IEEE Computational Sciences and Engineering**, Volume 2, Number 2, pp.50-61
- Gross, V., Hadjileontiadis, L. J., Penzel, T., Koehler, U. and Vogelmeier, C., 2003. Multimedia database "Marburg Respiratory Sounds (MARS)", **Proceedings of the 25th Annual International Conference of the IEEE Engineering in Medicine and Biology Society (IEEE Cat. No.03CH37439)**, pp. 456-457 Vol.1.doi: 10.1109/IEMBS.2003.1279717

- Guo, X., Pang, Y., Yan, G. and Qiao, T., 2017. Time series forecasting based on deep extreme learning machine, **29th Chinese Control And Decision Conference (CCDC)**, Chongqing, pp. 6151-6156. doi: 10.1109/CCDC.2017.7978277
- Gunen, H., Hacıevliyagil S.S., Yetkin, O., Gulbas, G., Mutlu, L.C., Pehlivan, E., 2008. Prevalence of COPD: First epidemiological study of a large region in Turkey, **Eur J Intern Med.**, Volume 19, Issue 7, pp.499–504, doi: 10.1016/j.ejim.2007.06.028
- Guntupalli, K. K., Alapat, P. M., Bandi, V. D., and Kushnir, I., 2008. Validation of automatic wheeze detection in patients with obstructed airways and in healthy subjects., **J. Asthma**, vol. 45, no. 10, pp. 903–907
- Gülesen, Ö., 2003. **Epidemolojiye Giriş. Epidemoloji Ankara**: Ayyıldız Matbaa, pp.1-4
- Hederos, C.-A., Janson, S., Andersson, H., & Hedlin, G. 2004. Chest X-ray investigation in newly discovered asthma. **Pediatric Allergy and Immunology: Official Publication of the European Society of Pediatric Allergy and Immunology**, 15(2), pp.163–5. <https://doi.org/10.1046/j.1399-3038.2003.00098.x>
- Himeshima, M., Yamashita, M., Matsunaga, S., & Miyahara, S., 2012. Detection of abnormal lung sounds taking into account duration distribution for adventitious sounds. **European Signal Processing Conference**, pp. 1821–1825.
- Hinton, G., Hinton, G., Sejnowski, T., Sejnowski T., 1986. Learning and relearning in Boltzmann machines. **Parallel distributed processing: explorations in the microstructure of cognition**, vol. 1, MIT Press Cambridge, MA, USA, pp. 282-317
- Hinton G., 2002. Training products of experts by minimizing contrastive divergence. **Neural computation**. Vol.14 pp.1771–1800. [PubMed: 12180402]
- Hinton, G. E.; Osindero, S. and Teh, Y. W., 2006. A Fast Learning Algorithm for Deep Belief Nets. **Neural Computation**. 18 (7) pp.1527–1554. doi:10.1162/neco.2006.18.7.1527. PMID 16764513.
- Homs-Corbera, A., Fiz, J. A., Morera, J., & Jané, R., 2004. Time-Frequency Detection and Analysis of Wheezes during Forced Exhalation. **IEEE Transactions on Biomedical Engineering**, 51(1), pp.182–186. <https://doi.org/10.1109/TBME.2003.820359>
- Hossain, I. and Moussavi, Z., 2004. Finding the lung sound-flow relationship in normal and asthmatic subjects., **Conf. Proc. IEEE Eng. Med. Biol. Soc.**, vol. 5, pp. 3852–5.
- Hosseini, M. P., Soltanian-Zadeh, H. and Akhlaghpour, S., 2011. A novel method for identification of COPD in inspiratory and expiratory states of CT images, **1st Middle East Conference on Biomedical Engineering**, Sharjah, pp.235-238. doi: 10.1109/MECBME.2011.5752109
- Huang, G-B., Zhu, Q-Y. and Siew, C-K., 2004. Extreme learning machine: a new learning scheme of feedforward neural networks, **IEEE International Joint Conference on Neural Networks (IEEE Cat. No.04CH37541)**, pp.985-990, vol.2. doi: 10.1109/IJCNN.2004.1380068
- Huang, G-B, Chen, L., 2008. Enhanced random search based incremental extreme learning machine. **Neurocomputing**, vol.71 pp.3460–8.
- Huang, G-B, Chen, L, Siew, C-K. 2006. Universal approximation using incremental constructive feedforward networks with random hidden nodes. **IEEE Trans Neural Netw.**, 17(4):pp.879–92.

- Huang, G-B, Chen, L. 2007. Convex incremental extreme learning machine. **Neurocomputing**. 70, pp.3056–62.
- Huang, G-B., 2014. An insight into extreme learning machines: random neurons, random features and kernels. **Cogn Comput.**, 6(3), pp.376–90
- Huang, G-B, Zhou, H, Ding, X, Zhang, R., 2012. Extreme learning machine for regression and multiclass classification. **IEEE Trans Syst Man Cybern B**. 42(2), pp.513–29.
- Huang, N. E., Shen, Z., Long, S. R., et al., 1998. The Empirical Mode Decomposition and The Hilbert Spectrum for Nonlinear and non-stationary time series analysis, **Proc R. Soc. Lond A**, vol.454, pp.903-995..
- Huang, N. E, Shen, S. S. P., 2005. Hilbert-Huang Transform and Its Application, **World Scientific**, ISBN: 978-981-256-376-7.
- Isler, Y., Kuntalp, M., 2007. Combining classical HRV indices with wavelet entropy measures improves to performance in diagnosing congestive heart failure, **Computers in Biology and Medicine** 37, pp.1502–1510
- Işık, Ü., Güven, A. and Büyükoğlu, H., 2015. Chronic Obstructive Pulmonary Disease classification with Artificial Neural Networks, **Medical Technologies National Conference (TIPTEKNO)**, Bodrum, pp. 1-4. doi: 10.1109/TIPTEKNO.2015.7374589
- Kandaswamy, A., Sathish Kumar, C., Ramanathan, Rm.Pl., Jayaraman, S., Malmurugan, N., 2004. Neural classification of lung sounds using wavelet coefficients, **Computers in Biology and Medicine**, 34(6), pp.523-537, ISSN 0010-4825, [https://doi.org/10.1016/S0010-4825\(03\)00092-1](https://doi.org/10.1016/S0010-4825(03)00092-1).
- Kasun, L. L. C., Zhou, H., Huang, G. B., and Vong, C. M., 2013. Representational learning with ELMs for big data. **IEEE Intelligent Systems**, vol=28, pp:31-34
- Kaya, A., Karadağ, M., Metintaş, M., Özlü, T., 2010. **Solunum Sistemi ve Hastalıkları**, ISBN: 9789944211871, İstanbul Tıp Kitabevi
- Kim, J., Shin, H., Shin, K. and Lee, M., 2009. Robust algorithm for arrhythmia classification in ECG using extreme learning machine. **Biomedical Engineering Online**, 8(1), p.31
- Kraman, S. S., 1993. Lung Sounds: An Introduction to the Interpretation of the Auscultatory Finding. Northbrook, IL: **Amer. College Chest Phys.** (audio tape).
- Kumar, B. H., 2007, A fuzzy expert system design for analysis of body sounds and design of an unique electronic stethoscope (development of HILSA kit), **Biosensors and Bioelectronics**, 22(6), pp.1121-1125, ISSN:0956-5663, <https://doi.org/10.1016/j.bios.2006.04.012>.
- Kumar, N. K., Savith, R., Mamun A.A., 2017. Ocean wave height prediction using ensemble of Extreme Learning Machine, **Neurocomputing**, ISSN:0925-2312, <https://doi.org/10.1016/j.neucom.2017.03.092>.
- Kuremoto, T., Kimura, S., Kobayashi, K., Obayashi, M., 2014. Time series forecasting using a deep belief network with restricted Boltzmann machines, **Neurocomputing**, Vol.137, pp.47-56, ISSN:0925-2312, <https://doi.org/10.1016/j.neucom.2013.03.047>.
- Kutlu, Y., Altan, G., İşçimen, B., Doğdu, S. A., and Turan, C., 2017. Recognition of species of Triglidae Family using Deep Learning. **Journal of the Black Sea/Mediterranean Environment**, 23(1), pp.56-65.

- Kutlu, Y., Yayik, A., Yildirim, E. et al., 2017. LU triangularization extreme learning machine in EEG cognitive task classification, **Neural Comput & Applic.**, Issn:1433-3058, pp.1-10 <https://doi.org/10.1007/s00521-017-3142-1>
- Kutlu, Y., Yayik, A., Yildirim, E., & Yildirim, S., 2015. Orthogonal Extreme Learning Machine Based P300 Visual Event-Related BCI. **International Conference on Neural Information Processing**. Springer, Cham pp. 284-291
- Lehrer, S., 1993. **Understanding Lung Sounds**. Philadelphia, PA: Saunders (audio tape).
- Leontios J. H., Stavros M. P., 1998. A wavelet-based reduction of heart sound noise from lung sounds, **International Journal of Medical Informatics**, 52(1-3), pp.183-190, ISSN 1386-5056, [https://doi.org/10.1016/S1386-5056\(98\)00137-3](https://doi.org/10.1016/S1386-5056(98)00137-3).
- Liou, C.-Y., Huang, J.-C. and Yang, W.-C., 2008. Modeling word perception using the Elman network, **Neurocomputing**, vol.71, pp.3150-3157, doi:10.1016/j.neucom.2008.04.030
- Liou, C.-Y., Cheng, C.-W., Liou, J.-W., and Liou, D.-R., 2014. Autoencoder for Words, **Neurocomputing**, vol.139, pp.84-96 (2014), doi:10.1016/j.neucom.2013.09.055
- Loudon, R. and Murph, R. L., 1984. Lung sounds., **Am. Rev. Respir. Dis.**, 130(4), pp. 663-73.
- Mangiore, S., 2000. **Secrets Heart & Lung Sounds Workshops: Audio CD** Philadelphia, PA: Hanley & Belfus, (CD-ROM)
- Mastorocostas, P. A., 2006. A recurrent fuzzy filter for the analysis of lung sounds, **Fuzzy Sets and Systems**, 157(4), pp.578-594, ISSN:0165-0114, <https://doi.org/10.1016/j.fss.2005.06.020>.
- Matsutake, S., Yamashita, M., & Matsunaga, S., 2015. Abnormal-respiration detection by considering correlation of observation of adventitious sounds. **23rd European Signal Processing Conference, EUSIPCO**, pp.634-638. <https://doi.org/10.1109/EUSIPCO.2015.7362460>
- McLachlan, G. J., Do, K.-A., Ambrose, C., 2004. **Analyzing microarray gene expression data**. Wiley. Print ISBN: 9780471226161, DOI: 10.1002/047172842X
- McGee, S., 2012. Chapter 28--Auscultation of the lungs, **Evidence-based Phys. diagnosis (third Ed.)**, Philadelphia WB Saunders, pp. 251-266.
- Melbye, H., 2001. Auscultation of the lungs--still a useful examination?, **Tidsskr. den Nor. lægeforening Tidsskr. Prakt. Med. ny række**, 121 (4), pp. 451-4.
- Misiti M., Misiti, Y., Oppenheim, G., Poggi, J., 2004. User Guide Wavelet Toolbox For Use with MATLAB.
- Mitchell, T. M., 1997. Machine Learning. **WCB**, McGraw-Hill, Inc. New York, NY, USA, ISBN:0070428077 9780070428072 .
- Mohammed, A., Minhas, R., Wu, Q. and Sid-Ahmed, M., 2011. Human face recognition based on multidimensional PCA and extreme learning machine. **Pattern Recognition**, 44(10), pp.2588-2597.
- Mondal, A., Bhattacharya, P., Saha, G., 2014. Detection of Lungs Status Using Morphological Complexities of Respiratory Sounds. **The Scientific World Journal**. Vol.2014 Article ID:182938. doi:10.1155/2014/182938.
- Morillo, D.S, León Jiménez, A., & Moreno, S. A., 2013. Computer-aided diagnosis of pneumonia in patients with chronic obstructive pulmonary disease. **Journal of the American Medical Informatics Association : JAMIA**, 20(e1),pp.e111-e117.

- <http://doi.org/10.1136/amiajnl-2012-001171>
- Nakamura, N., Yamashita, M., & Matsunaga, S., 2016. Detection of patients considering observation frequency of continuous and discontinuous adventitious sounds in lung sounds. **38th Annual International Conference of the IEEE Engineering in Medicine and Biology Society (EMBC)**, pp. 3457-3460, <https://doi.org/10.1109/EMBC.2016.7591472>
- Naves, R., Barbosa, B.H.G., Ferreira, D. D., 2016. Classification of lung sounds using higher-order statistics: A divide-and-conquer approach, **Computer Methods and Programs in Biomedicine**, Vol.129, pp.12-20, ISSN:0169-2607, <https://doi.org/10.1016/j.cmpb.2016.02.013>.
- Newandee, D. A., Reisman, S. S., Bartels, A. N. and Meersman, R. E. De, 2003. COPD severity classification using principal component and cluster analysis on HRV parameters, **IEEE 29th Annual Proceedings of Bioengineering Conference**, pp.134-135. doi: 10.1109/NEBC.2003.1216028
- Pachori, R. B., Patidar, S., 2014. Epileptic seizure classification in EEG signals using second-order difference plot of intrinsic mode functions, **Computer Methods and Programs in Biomedicine** 113 (2014), pp.494–502
- Palaniappan, R., Sundaraj, K., Sundaraj, S., 2014. A comparative study of the svm and k-nn machine learning algorithms for the diagnosis of respiratory pathologies using pulmonary acoustic signals. **BMC Bioinformatics**.vol.15, pp.223. doi:10.1186/1471-2105-15-223.
- Parkhi, A. and Pawar, M., 2011. Analysis of deformities in lung using short time Fourier transform spectrogram analysis on lung sound, **International Conference on Computational Intelligence and Communication Systems, CICN 2011**, pp. 177–181.
- Pasterkamp, H., Kraman, S. S., and Wodicka, G. R., 1997. Respiratory sounds: Advances beyond the stethoscope, **American Journal of Respiratory and Critical Care Medicine**,156(3I). pp. 974–987.
- Press, W.H.; Flannery, B.P.; Teukolsky, S.A.; and Vetterling, W.T., 1992. LU Decomposition and Its Applications. **2.3 in Numerical Recipes in FORTRAN: The Art of Scientific Computing, 2nd ed.** Cambridge, England: Cambridge University Press, pp.34-42.
- R.A.L.E., 2005. Lung Sounds 3.1. **Respiratory Care**, vol.50 pp.1385
- Reichert, S., Gass, R., Hajjam, A., Brandt, C., Nguyen, E., Baldassari, K., and Andrès, E., 2009. The ASAP project: A first step to an auscultation's school creation, **Respir. Med. CME**, 2 (1), pp. 7–14.
- Reunanen, J., 2006. Search Strategies, Feature Extraction Foundations and Applications Studies , **Fuzzy and Soft computing**, Springer, pp.119–136
- Riella, R.J., Nohama, P., & Maia, J.M., 2009. Method for automatic detection of wheezing in lung sounds. **Brazilian Journal of Medical and Biological Research**, 42(7), pp.674-684. <https://dx.doi.org/10.1590/S0100-879X2009000700013>
- Rioul, O., Vetterli, M., 1991. Wavelets and Signal Processing. **Signal Processing Magazine IEEE**, 8 (4), pp.14–38.
- Roisin RR., 2016. Chronic Obstructive Pulmonary Disease Updated 2010 Global Initiative for Chronic Obstructive Lung Disease. **Global Initiative for Chronic Obstructive**

- Lung Disease.** Inc, pp.1–94. <https://doi.org/10.1097/00008483-200207000-00004>
- Rosenberg, S. R., and Kalhan, R., 2011. Dying from, and with, Chronic Obstructive Pulmonary Disease, **Proceedings of the American Thoracic Society**, 183 (8), pp:960-962.
- Rückstieß T., Osendorfer C., Van der Smagt P., 2011. Sequential Feature Selection for Classification. **Wang D., Reynolds M. (eds) AI: Advances in Artificial Intelligence. Lecture Notes in Computer Science**, vol.7106. Springer, Berlin, Heidelberg, https://doi.org/10.1007/978-3-642-25832-9_14
- Salvi, S. S., & Barnes, P. J., 2009. Chronic obstructive pulmonary disease in non-smokers. **The Lancet**. [https://doi.org/10.1016/S0140-6736\(09\)61303-9](https://doi.org/10.1016/S0140-6736(09)61303-9)
- Shen, F., Chao, J., Zhao, J., 2015. Forecasting exchange rate using deep belief networks and conjugate gradient method, **Neurocomputing**, vol.167, pp.243-253, ISSN 0925-2312, <https://doi.org/10.1016/j.neucom.2015.04.071>.
- Shukla, S., Mishra, S., Singh, B., 2009. Emprical-Mode Decomposition with Hilbert Transform for Power Quality Assessment, **IEEE Transactions on Power Delivery**, vol. 24, pp.2159-1165.
- Song, Y. and Liò, P., 2010. A new approach for epileptic seizure detection: sample entropy based feature extraction and extreme learning machine. **Journal of Biomedical Science and Engineering**, 3(6), pp.556-567, doi: <http://dx.doi.org/10.4236/jbise.2010.36078>
- Sovijärvi, A. R. A., Vanderschoot, J., & Earis, J. E., 2000. Standardization of computerized respiratory sound analysis. **Eur Respir Rev**, 10, pp.77–585
- Sun, K., Zhang, J., Zhang, C., Hu, J., 2017. Generalized extreme learning machine autoencoder and a new deep neural network, **Neurocomputing**, vol.230, pp.374-381, ISSN 0925-2312, <https://doi.org/10.1016/j.neucom.2016.12.027>.
- Sun, Z., Choi, T., Au, K. and Yu, Y., 2008. Sales forecasting using extreme learning machine with applications in fashion retailing. **Decision Support Systems**. 46(1), pp.411-419.
- Tamilselvan, P., Wang, P., 2013. Failure diagnosis using deep belief learning based health state classification, **Reliability Engineering & System Safety**, vol.115, pp.124-135, ISSN 0951-8320, <https://doi.org/10.1016/j.ress.2013.02.022>.
- Tang, J., Den, C. and Huang, G-B., 2016. Extreme Learning Machine for Multilayer Perceptron, **IEEE Transactions on Neural Networks and Learning Systems**, 27 (4), pp. 809-821. doi: 10.1109/TNNLS.2015.2424995
- Thuraisingham, R. A., 2009. A Classification System to Detect Congestive Heart Failure Using Second-Order Difference Plot of RR Intervals, **Cardiology Research and Practice** pp.1–7
- Tilikian, A. G. and Conover, M. B., 1993. **Understanding Heart Sounds and Murmurs With an Introduction to Lung Sounds** . Philadelphia, PA: Saunders (audio tape).
- Tocchetto, M.A., Bazanella, A.S., Guimaraes, L., Fragoso, J.L., Parraga, A., 2014. An Embedded Classifier of Lung Sounds based on the Wavelet Packet Transform and ANN, **IFAC Proceedings Volumes**, 47 (3), pp.2975-2980, ISSN 1474-6670, ISBN 9783902823625, <https://doi.org/10.3182/20140824-6-ZA-1003.01638>.
- Troosters, T., Casaburi, R., Gosselink, R., & Decramer, M., 2005. Pulmonary rehabilitation in chronic obstructive pulmonary disease. **American Journal of Respiratory and**

- Critical Care Medicine**, 172 (1), pp.19-38. <https://doi.org/10.1164/rccm.200408-1109SO>
- Ulukaya, S., Serbes, G., Sen, I., and Kahya, Y. P., 2016. A lung sound classification system based on the rational dilation wavelet transform, **Proceedings of the Annual International Conference of the IEEE Engineering in Medicine and Biology Society, EMBS**, vol. 2016–Octob, pp. 3745–3748.
- Umeki, S., Yamashita, M., & Matsunaga, S., 2015. Classification between normal and abnormal lung sounds using unsupervised subject-adaptation. **Asia-Pacific Signal and Information Processing Association Annual Summit and Conference (APSIPA)**, pp. 213-216. <https://doi.org/10.1109/APSIPA.2015.7415506>
- Uysal, S., Uysal, H., Bolat, B. and Yıldırım, T., 2014. Classification of normal and abnormal lung sounds using wavelet coefficients, **22nd Signal Processing and Communications Applications Conference (SIU)**, Trabzon, pp.2138-2141.doi: 10.1109/SIU.2014.6830685
- Xie, W., Li, Y., Ma, Y., 2016. Breast mass classification in digital mammography based on extreme learning machine, **Neurocomputing**, 173 (3), pp.930-941, ISSN 0925-2312, <https://doi.org/10.1016/j.neucom.2015.08.048>.
- Vannuccini, L., Earis, J. E., Helisto, P., Cheetham, B. M. G., Rossi, M., Sovijarvi, A. R. A., and Vanderschoot, J., 2000. Capturing and preprocessing of respiratory sounds, **Eur. Respir. Rev.**, 10 (77), pp. 616–620.
- Vaz Fragoso, C. A., Concato, J., McAvay, G., Van Ness, P. H., Rochester, C. L., Yaggi, H. K., & Gill, T. M., 2010. The ratio of FEV1 to FVC as a basis for establishing chronic obstructive pulmonary disease. **American Journal of Respiratory and Critical Care Medicine**, 181(5), pp.446–451. <https://doi.org/10.1164/rccm.200909-1366OC>
- Vincent, P., Larochelle, H., Lajoie, I., Bengio, Y., Manzagol, P-A 2010. Stacked Denoising Autoencoders: Learning Useful Representations in a Deep Network with a Local Denoising Criterion. **The Journal of Machine Learning Research**. Vol.11, pp.3371–3408.
- Vogelmeier, C. F., Criner, G. J., Martinez, F. J., Anzueto, A., Barnes, P. J., Bourbeau, J., and Frith, P., 2017. Global Strategy for the Diagnosis, Management and Prevention of Chronic Obstructive Lung Disease 2017 Report. **Respirology**, 22(3), pp.575-601.
- Vyshedskiy, A., Alhashem, R. M., Paciej, R., Ebril, M., Rudman, I., Fredberg, J. J., and Murphy, R., 2009. Mechanism of inspiratory and expiratory crackles, **Chest**, 135 (1), pp. 156–164.
- Waitman, L. R., Clarkson, K. P., Barwise, J. A., & King, P. H., 2000. Representation and classification of breath sounds recorded in an intensive care setting using neural networks. **Journal of Clinical Monitoring and Computing**, 16(2), pp.95–105. <https://doi.org/10.1023/A:1009934112185>
- Wang, J., Gu, Z., Yu, Z., Li, Y., 2017. An online semi-supervised P300 speller based on extreme learning machine, **Neurocomputing**, vol.269, pp.148-151, ISSN 0925-2312, <https://doi.org/10.1016/j.neucom.2016.12.098>.
- Wang, Y., Cao, F. and Yuan, Y., 2011. A study on effectiveness of extreme learning machine. **Neurocomputing**, 74(16), p.2483–2490.

- WHO. (n.d.). 2017. The top 10 causes of death. Retrieved December 23, 2017, from <http://www.who.int/mediacentre/factsheets/fs310/en/>
- Wiśniewski, M. and Zieliński, T., 2010. Digital analysis methods of wheezes in asthma, **ICSES 2010 International Conference on Signals and Electronic Circuits**. pp. 69–72, 2010.
- Wu, Z. and Huang, N. E., 2009. Ensemble Empirical Mode Decomposition: A Noise-assisted data analysis method, **Adv. Adapt. Data Anal.** 1(1), pp.1-41. <https://doi.org/10.1142/S1793536909000047>
- Yamashita, M., Matsunaga, S. and Miyahara, S., 2011. Discrimination between healthy subjects and patients with pulmonary emphysema by detection of abnormal respiration, **IEEE International Conference on Acoustics, Speech and Signal Processing (ICASSP)**, Prague, pp. 693-696. doi: 10.1109/ICASSP.2011.5946498
- Yazgan, E. and Korürek, M., 1996. **Tip Elektronik**, İTÜ Matbaası, 220s.
- Ying, J. et al., 2016. Gold classification of COPD Gene cohort based on deep learning, **IEEE International Conference on Acoustics, Speech and Signal Processing (ICASSP)**, Shanghai, pp. 2474-2478. doi: 10.1109/ICASSP.2016.7472122
- Zong, W. and Huang, G-B., 2011. Face recognition based on extreme learning machine. **Neurocomputing**, 74(16), p.2541-2551.
- Zong, W., Huang, G.-B. and Chen, Y., 2013. Weighted extreme learning machine for imbalance learning. **Neurocomputing**, 101, p.229–242.

VITA

Gokhan ALTAN was born in Payas, Hatay, Turkey, on October 8, 1986. In 2004 he was graduated from Süleyman Demirel Anatolian High School, in Hatay, Turkey. In 2008 he received his B.S. in Computer Teacher from Selcuk University, Konya, Turkey. In 2011 he received his M.S. degree in Computer and Electronics Department of Selcuk University, Konya, Turkey. He has published 7 research articles in peer-review international journals, one of which has science citation index (SCI) index and has presented 10 oral proceedings in several international conferences.

Academic publications (1 article, and 4 oral proceedings) derived from this doctorate dissertation are listed below.

- G. ALTAN, Y. KUTLU, Y. GARBI, A. Ö. PEKMEZCİ & S. NURAL**, Multimedia Respiratory Database (RespiratoryDatabase@TR): Auscultation Sounds And Chest X-rays, Natural and Engineering Sciences, 2017, 2458-8989, 2, 3, pp.59--72.
- G. ALTAN, Y. KUTLU, Y. GARBI, A. Ö. PEKMEZCİ & S. NURAL**, Efficiency Of Three-dimensional Second Order Difference Plot And Deep Learning On Respiratory Sounds, Abstract, International Conference On Mathematics And Engineering, 10 May 2017, 12 May 2017, p. 328
- G. ALTAN & Y. KUTLU**, A review on respiratory sound analysis using machine learning, 20th National Biomedical Engineering Meeting (BIYOMUT), 03 November 2016, 05 November 2016, 1 - 4.
- G. ALTAN, Y. KUTLU, A. Ö. PEKMEZCİ & S. NURAL**, The Diagnosis of Asthma using Hilbert-Huang Transform and Deep Learning on Lung Sounds, Akıllı Sistemlerde Yenilikler ve Uygulamaları Konferansı (ASYU), 5-7 Oct. 2017, pp.82
- G. ALTAN, Y. KUTLU, A. Ö. PEKMEZCİ, S. NURAL, Y. GARBI & E. ARSLAN**, Diagnosis of Chronic Obstructive Pulmonary Disease using Wavelet Transform Analysis from Auscultation Sounds, 4th International Conference on Pure and Applied Sciences (Renewable Energy) (ICPAS), 23-25 Nov. 2017, Abstract

- Y. KUTLU, G. ALTAN, B. İŞÇİMEN, S. A. DOĞDU, & C.TURAN, Recognition of species of Triglidae Family using Deep Learning. Journal of the Black Sea/Mediterranean Environment, 23(1), 2017
- G. ALTAN, Y. KUTLU, N. ALLAHVERDI, A new approach to early diagnosis of congestive heart failure disease by using Hilbert–Huang transform. Computer Methods and Programs in biomedicine, 2016, 137: 23-34. (SCI)
- G. ALTAN, Y. KUTLU, ECG based human identification using logspace grid analysis of second order difference plot. In: Signal Processing and Communications Applications Conference (SIU), 2015 23th. IEEE, 2015. p. 1288-1291.
- G. ALTAN, N. ALLAHVERDI, Y. KUTLU, Diagnosis of Coronary Artery Disease Using Deep Belief Networks, European Journal of Engineering and Natural Sciences Vol:2 Issue(1), ISSN:2458-8156, March 2017, Pages 29-36
- G. ALTAN, Y. KUTLU, N. ALLAHVERDI, A Multistage Deep Belief Networks Application on Arrhythmia Classification, International Journal of Intelligent Systems and Applications in Engineering, Volume 4, Special Issue 1, December 2016, Pages 23-34, ISSN 2147-6799, DOI: 10.18201/ijisae.270367
- G. ALTAN, Y. KUTLU, N. ALLAHVERDI, Deep Belief Networks Based Brain Activity Classification Using EEG from Slow Cortical Potentials in Stroke, International Journal of Applied Mathematics, Electronics and Computers, Volume 4, Special Issue I, December 2016, Pages 205-210, ISSN 2147-8228, <http://dx.doi.org/10.18100/ijamec.270307>
- G. ALTAN, A. YAYIK, Y. KUTLU, S. YILDIRIM, E. YILDIRIM, Konjestif Kalp Yetmezliğinin Hilbert-Huang Dönüşüm ile Analizi (Analyse of Congestive Heart Failure Using Hilbert- Huang Transform), DEU J. Sci. Eng. 16 (2014) 94-103. ISSN: 1302-9304
- A. YAYIK, G. ALTAN, Y. KUTLU, S. YILDIRIM, E. YILDIRIM, Görgül Mod Fonksiyonların Eliptik Analizi ile Kongestif Kalp Yetmezliği Teşhisi (Elliptic Analysis of Instinct Mode Functions based CHF Detection), Elektrik, Elektronik, Bilgisayar ve Biyomedikal Mühendisliği Sempozyumu , ELECO 2014

APPENDIX 1



Medicine, Biomedical Sciences, Health and Social Care Sciences

1 February 2017

Cranmer Terrace
London SW17 0RE
Switchboard
+44 (0)20 8672 9944
www.sgul.ac.uk

To Whom It May Concern:

This is to confirm that St George's, University of London (St George's Hospital Medical School) has given permission for Gokhan Altan, Iskenderun Technical University, Turkey to use the SGRQ-C for research purposes.

Professor Paul Jones, PhD FRCP
Professor of Respiratory Medicine

APPENDIX 2

ST. GEORGE'S RESPIRATORY QUESTIONNAIRE for COPD patients

(SGRQ-C)

*This questionnaire is designed to help us learn much more about how your breathing is troubling you and how it affects your life.
We are using it to find out which aspects of your illness cause you most problems, rather than what the doctors and nurses think your problems are.*

Please read the instructions carefully and ask if you do not understand anything. Do not spend too long deciding about your answers.

ID: _____

Date: ____/____/____ (dd/mm/yy)

Before completing the rest of the questionnaire:

Please select one box to show how you describe your current health:

Very good

☐

Good

☐

Fair

☐

Poor

☐

Very poor

☐

Version: 1st Sept 2005

Copyright reserved

P.W. Jones, PhD FRCP
Professor of Respiratory Medicine,
St. George's University of London,
Cranmer Terrace
London SW17 0RE, UK.

Tel. +44 (0) 20 8725 5371
Fax +44 (0) 20 8725 5955

St. George's Respiratory Questionnaire PART 1

Questions about how much chest trouble you have.

Please select **ONE** box for each question:

Question 1. I cough:

- most days a week..... ☐ a
several days a week ☐ b
only with chest infections ☐ c
not at all..... ☐ d

Question 2. I bring up phlegm (sputum):

- most days a week..... ☐ a
several days a week ☐ b
only with chest infections ☐ c
not at all..... ☐ d

Question 3. I have shortness of breath:

- most days a week..... ☐ a
several days a week ☐ b
not at all..... ☐ c

Question 4. I have attacks of wheezing:

- most days a week..... ☐ a
several days a week ☐ b
a few days a month..... ☐ c
only with chest infections ☐ d
not at all..... ☐ e

Question 5. How many attacks of chest trouble did you have during the last year?

3 or more attacks ☐ a

1 or 2 attacks..... ☐ b

none ☐ c

Question 6. How often do you have good days (with little chest trouble)?

no good days..... ☐ a

a few good days..... ☐ b

most days are good ☐ c

every day is good..... ☐ d

Question 7. If you have a wheeze, is it worse in the morning?

no ☐

yes..... ☐

St. George's Respiratory Questionnaire PART 2

8. *How would you describe your chest condition?*

Please select **ONE**:

Causes me a lot of problems or is the most important problem I have ☐ a

Causes me a few problems ☐ b

Causes no problem ☐ c

9. *Questions about what activities usually make you feel breathless.*

For each statement please select *the box* that applies to you **these days**:

	True	False	
Getting washed or dressed.....	<input type="checkbox"/>	<input type="checkbox"/>	a
Walking around the home.....	<input type="checkbox"/>	<input type="checkbox"/>	b
Walking outside on the level.....	<input type="checkbox"/>	<input type="checkbox"/>	c
Walking up a flight of stairs.....	<input type="checkbox"/>	<input type="checkbox"/>	d
Walking up hills.....	<input type="checkbox"/>	<input type="checkbox"/>	e

St. George's Respiratory Questionnaire PART 2

10. Some more questions about your cough and breathlessness.

For each statement please select *the box* that applies to you **these days**:

	True	False	
My cough hurts	<input type="checkbox"/>	<input type="checkbox"/>	a
My cough makes me tired	<input type="checkbox"/>	<input type="checkbox"/>	b
I am breathless when I talk	<input type="checkbox"/>	<input type="checkbox"/>	c
I am breathless when I bend over	<input type="checkbox"/>	<input type="checkbox"/>	d
My cough or breathing disturbs my sleep.....	<input type="checkbox"/>	<input type="checkbox"/>	e
I get exhausted easily	<input type="checkbox"/>	<input type="checkbox"/>	f

11. Questions about other effects that your chest trouble may have on you.

For each statement please select *the box* that applies to you **these days**:

	True	False	
My cough or breathing is embarrassing in public	<input type="checkbox"/>	<input type="checkbox"/>	a
My chest trouble is a nuisance to my family, friends or neighbours	<input type="checkbox"/>	<input type="checkbox"/>	b
I get afraid or panic when I cannot get my breath	<input type="checkbox"/>	<input type="checkbox"/>	c
I feel that I am not in control of my chest problem.....	<input type="checkbox"/>	<input type="checkbox"/>	d
I have become frail or an invalid because of my chest.....	<input type="checkbox"/>	<input type="checkbox"/>	e
Exercise is not safe for me	<input type="checkbox"/>	<input type="checkbox"/>	f
Everything seems too much of an effort.....	<input type="checkbox"/>	<input type="checkbox"/>	g

St. George's Respiratory Questionnaire PART 2

12. These are questions about how your activities might be affected by your breathing.

For each statement please select *the box* that applies to you **because of your breathing**:

	True	False
I take a long time to get washed or dressed.....	<input type="checkbox"/>	<input type="checkbox"/> a
I cannot take a bath or shower, or I take a long time	<input type="checkbox"/>	<input type="checkbox"/> b
I walk slower than other people, or I stop for rests.....	<input type="checkbox"/>	<input type="checkbox"/> c
Jobs such as housework take a long time, or I have to stop for rests....	<input type="checkbox"/>	<input type="checkbox"/> d
If I walk up one flight of stairs, I have to go slowly or stop	<input type="checkbox"/>	<input type="checkbox"/> e
If I hurry or walk fast, I have to stop or slow down	<input type="checkbox"/>	<input type="checkbox"/> f
My breathing makes it difficult to do things such as walk up hills, carrying things up stairs, light gardening such as weeding, dance, play bowls or play golf	<input type="checkbox"/>	<input type="checkbox"/> g
My breathing makes it difficult to do things such as carry heavy loads, dig the garden or shovel snow, jog or walk at 5 miles per hour, play tennis or swim.....	<input type="checkbox"/>	<input type="checkbox"/> h

13. We would like to know how your chest trouble usually affects your daily life.

For each statement please select *the box* that applies to you **because of your breathing**:

	True	False
I cannot play sports or games	<input type="checkbox"/>	<input type="checkbox"/> a
I cannot go out for entertainment or recreation	<input type="checkbox"/>	<input type="checkbox"/> b
I cannot go out of the house to do the shopping	<input type="checkbox"/>	<input type="checkbox"/> c
I cannot do housework	<input type="checkbox"/>	<input type="checkbox"/> d
I cannot move far from my bed or chair.....	<input type="checkbox"/>	<input type="checkbox"/> e

St. George's Respiratory Questionnaire

14. *How does your chest trouble affect you?*

Please select *ONE*:

It does not stop me doing anything I would like to do ☐ a

It stops me doing one or two things I would like to do..... ☐ b

It stops me doing most of the things I would like to do..... ☐ c

It stops me doing everything I would like to do..... ☐ d

Thank you for filling in this questionnaire.

Before you finish, would you please check to see that you have answered all the questions.

APPENDIX 3

BİLGİLENDİRİLMİŞ GÖNÜLLÜ OLUR FORMU

Bu katıldığınız çalışma bilimsel bir araştırma olup, araştırmanın adı “**Oskültasyon Seslerindeki Anormalliklerin Tanısı**” araştırmasıdır.

Bu araştırmanın amacı, öncelikli olarak KOAH olmak üzere bazı Akciğer rahatsızlıklarının tanısı konmuş hastalarda solunum seslerinin ve kalp seslerinin analizini yaparak KOAH tanısı ve derecelerinin belirlenmesi üzerine bir oskültasyon sesi analizi yapmaktır. Bu çalışmada tarafınıza herhangi bir kan alımı, cerrahi müdahale, enjeksiyon uygulaması veya bir ilaç denetilmesi söz konusu olmayacaktır. Yalnızca klasik klinik oskültasyon işlemi yapılacak ve herhangi bir ek süreye ihtiyaç duyulmadan bu sesler kaydedilecektir. Bu çalışmada yer almanız öngörülen süre sadece klinik teşhis sırasında oskültasyon süresiyle sınırlı olup, çalışmada yer alacak gönüllülerin sayısı en az 100 kişi civarındadır.

Bu çalışmada sizin için herhangi bir risk veya rahatsızlık söz konusu değildir; ancak sizin için beklenen yararlar çalışma sonucunda belirlenen KOAH ve diğer akciğer rahatsızlıkların saptanması, hastalık ilerlemeden kontrole daha sık çağırılmanız ve gereken müdahalelerin yapılması sağlanacaktır.

Araştırmaya bağlı bir zarar söz konusu değildir. Gönüllüye herhangi bir iğne yapılması, ilaç verilmesi, kan alınması, cerrahi müdahale yapılması söz konusu değildir. Araştırma sırasında hastalığınız hakkında edinilecek bilgiler size veya yasal temsilcinize derhal bildirilecektir. Araştırma hakkında ek bilgiler almak için ya da çalışma ile ilgili herhangi bir sorun için 0544 254 4389 no.lu telefondan Doktora Öğrencisi Gökhan ALTAN’ a başvurabilirsiniz.

Bu çalışmada yer almanız nedeniyle size hiçbir ödeme yapılmayacaktır. Ayrıca, bu araştırma kapsamındaki size fazladan yapılan tetkik ve tıbbi bakım hizmetleri için sizden veya bağlı bulunduğunuz sosyal güvenlik kuruluşundan hiçbir ücret istenmeyecektir.

Bu çalışmada yer almak tamamen sizin isteğinize bağlıdır. Araştırmada yer almayı reddedebilirsiniz ya da herhangi bir aşamada çalışmadan ayrılabilirsiniz; bu durum herhangi bir cezaya ya da sizin yararlarınıza engel duruma yol açmayacaktır. Araştırmacı bilginiz dâhilinde veya isteğiniz dışında, uygulanan tedavi şemasının gereklerini yerine getirmemeniz, çalışma programını aksatmanız veya tedavinin etkinliğini artırmak vb. nedenlerle sizi çalışmadan çıkarabilir. Araştırmanın sonuçları bilimsel amaçla kullanılacaktır; çalışmadan çekilmeniz ya da araştırmacı tarafından çıkarılmanız durumunda, sizinle ilgili tıbbi veriler de gerekirse bilimsel amaçla kullanılabilir.

Size ait tüm tıbbi ve kimlik bilgileriniz gizli tutulacaktır ve araştırma yayınlsa bile kimlik bilgileriniz verilmeyecektir, ancak araştırmanın izleyicileri, yoklama yapanlar, etik kurullar ve resmi makamlar gerektiğinde tıbbi bilgilerinize ulaşabilir. Siz de istediğinizde kendinize ait tıbbi bilgilere ulaşabilirsiniz (tedavinin gizli olması durumunda, gönüllüye kendine ait tıbbi bilgilere ancak verilerin analizinden sonra ulaşabileceği bildirilmelidir).

Çalışmadan elde edilecek ürünlerden daha sonra planlanacak çalışmalarda da faydalanılacaktır.

Çalışmaya Katılma Onayı:

Yukarıda yer alan ve araştırmaya başlanmadan önce gönüllüye verilmesi gereken bilgileri okudum ve sözlü olarak dinledim. Aklıma gelen tüm soruları araştırmacıya sordum, yazılı ve sözlü olarak bana yapılan tüm açıklamaları ayrıntılarıyla anlamış bulunmaktayım. Çalışmaya katılmayı isteyip istemediğime karar vermem için bana yeterli zaman tanındı. Bu koşullar altında, bana ait tıbbi bilgilerin gözden geçirilmesi, transfer edilmesi ve işlenmesi konusunda araştırma

yürütücüsüne yetki veriyor ve söz konusu araştırmaya ilişkin bana yapılan katılım davetini hiçbir zorlama ve baskı olmaksızın büyük bir gönüllülük içerisinde kabul ediyorum.

Bu formun imzalı bir kopyası bana verilecektir.

Gönüllünün,

Adı-Soyadı:

Adresi:

Tel.-Faks:

Tarih ve İmza:

Velayet veya vesayet altında bulunanlar için veli veya vasinin,

Adı-Soyadı:

Adresi:

Tel.-Faks:

Tarih ve İmza:

Açıklamaları yapan araştırmacının,

Adı-Soyadı: Gökhan ALTAN

Görevi: Doktora Öğrencisi

Adresi: İskenderun Teknik Üniversitesi Mühendislik Fakültesi

Tel.-Faks: 0544 254 4389

Tarih ve İmza:

Olur alma işlemine başından sonuna kadar tanıklık eden kuruluş görevlisinin/görüşme tanığının,

Adı-Soyadı: Adnan Özhan PEKMEZCİ

Görevi: Doktor

Adresi: Hatay Antakya Devlet Hastanesi Dâhiliye Birimi

Tel.-Faks: 0 (326) 219 40 00

Tarih ve İmza: